Climate Variability and Change Over Eastern South Africa

Master of Science Degree

Bongani Blessing Sithole

May, 2025

CLIMATE VARIABILITY AND CHANGE OVER EASTERN SOUTH AFRICA

Ву

Bongani Blessing Sithole

Submitted in fulfilment of the requirements for the degree of Master of Science to be awarded at the University of Mpumalanga

May 2025

Supervisor: Prof Wisemen Chingombe (University of Mpumalanga, South Africa) Co-supervisor: Prof Hector Chikoore (University of Limpopo, South Africa)

DECLARATION

I, *Bongani Blessing Sithole & 201935848*, hereby declare that the *dissertation for Master of Science Degree* to be awarded is my own work and that it has not previously been submitted for assessment or completion of any postgraduate qualification to another University or for another qualification.

Students' signature

Bongani Blessing Sithole

ACKNOWLEDGEMENTS

Firstly, I would like to thank God for all the knowledge I acquired from this research and for making this research possible. I acknowledge my supervisors; Prof Wisemen Chingombe and Prof Hector Chikoore for their great supervision, patience, guidance, and encouragement. I would also like to acknowledge Tumelo Mohomi, Mukovhe Singo, and Percy Muofhe, who played a vital role in the data analysis of this study. I extend my gratitude to my mother for her prayers and support. Lastly, I thank the National Research Foundation (NRF) for funding this degree to its completion.



SUPERVISOR'S APPROVAL TO SUBMIT MSC80C FINAL RESEARCH REPORT

This is to certify that (Student name) Bongani B. Sithole with student number 201935848 and project title

Climate variability and change over eastern South Africa

executed his MSc project under my supervision and is hereby permitted to submit his/her final research report for assessment.

Date: 15/04/2025

Date: 03/04/2025

Supervisor's Name & Signature:

Prof Wisemen Chingombe

Co-supervisor's Name & Signature:

Prof Hector Chikoore

Heck.

٧

DEDICATION

I dedicate this dissertation to God the Creator of the heavens and the Earth, and my mother (Mrs N.S Sithole) who has been my support system from the beginning to the completion of this dissertation.

ABSTRACT

South Africa is increasingly vulnerable to extreme weather events, including rising temperatures, droughts, and floods, particularly along the east coast. These phenomena have historically caused fatalities, infrastructure damage, and agricultural disruption. This study explores the historical and projected climate variability and changes over eastern South Africa, focusing on the near-future (2021-2050) and far-future (2070-2099) under high and low mitigation scenarios. The research was conducted in KwaZulu-Natal (KZN) and Mpumalanga (MP) provinces using observational and climate projection data from Copernicus Climate Change Service (C3S), managed by the European Centre for Medium-Range Weather Forecasts (ECMWF), and Coupled Model Intercomparison Project Phase 6 (CMIP6) models for future projections. Statistical and visual methods verified the CMIP6 models' performance. Trend analyses of historical data from 1961-2020 were conducted using ERA5 reanalysis. Temperature indices (TX10P and TX90P) and rainfall indices (R10mm and R50mm) were calculated using RClimDex. Tools like Grid Analysis and Display System (GrADS), climate data operators (CDO), R and R Studio were used for data analysis. Results showed persistent cool days in 1968 for 29 days and more than 35 days in Kruger Mpumalanga International Airport and Durban respectively and an increasing trend in hot days and decreasing trend in heavy rainfall days at both locations. Furthermore, the frequency of rainfall exceeding 50mm/day trends varied by location. Statistical verification for Surface Air Temperature (SAT) showed a high correlation (≥0.9) and low Root Mean Square Error (RMSE) with ERA5 data, while rainfall model verification had a moderate correlation (0.5-0.7) and least RMSE, indicating higher uncertainty in precipitation modelling. The CMIP6 models performed well in projecting temperature and rainfall trends, with the highest temperatures and rainfall projected for KZN, while MP showed lower values. These findings align with previous studies on South African climate trends and they highlight the need for enhanced climate monitoring, continued high-resolution modelling, and improved climate projections at regional scales.

Key-words: Climate change, Climate variability, Climate models, KwaZulu Natal, Mpumalanga, Projection, Shared Socioeconomic Pathways

TABLE OF CONTENTS

DECLARATION	iii
ACKNOWLEDGEMENTS	iv
SUPERVISOR'S APPROVAL TO SUBMIT MSC80C FINAL RESEARCH REPORT	V
DEDICATION.	vi
ABSTRACT	vii
LIST OF FIGURES	xii
LIST OF TABLES	XV
LIST OF ABBREVIATIONS	
CHAPTER 1: INTRODUCTION	1
1.0 Background	1
1.1 Climate change and variability	1
1.1.1 Anthropogenic climate change	1
1.2 Problem statement	2
1.3 Research questions	5
1.4 Research aim	5
1.5 The specific objectives of the study	5
1.6 Chapter outline	5
CHAPTER 2: LITERATURE REVIEW	6
2.0 Introduction	6
2.1 Climate of South(ern) Africa	6
2.1.1 Dominant weather systems	6
2.1.2 Rainfall climatology	9
2.1.3 Temperature variability	
2.1.4 Impacts of the ENSO	
2.2 Climate trends and change in South Africa	
2.3 Climate models and climate modelling	13

2.3.1 Regional climate models (RCM) and Global climate models (GCM)	13
2.3.2 Shared Socioeconomic Pathways (SSP)	14
2.3.3 Verification/validation of climate models	16
2.3.4 CMIP6 models and the IPCC Sixth Assessment Report (AR6)	17
2.4 Future climate projections over South Africa	
2.5 Impacts, vulnerability, and adaptation to climate change	19
2.5.1 Impacts of climate change	19
2.5.2 Vulnerability to climate change impact	20
2.5.3 Adaptation	20
2.6 Summary	21
CHAPTER 3: DATA AND METHODOLOGY	22
3.0 Introduction	22
3.1 Study area	22
3.2 Observed data	23
3.3 Climate models	23
3.4 Model verification	26
3.4.1 Visual verification	27
3.4.2 Statistical verification	27
3.5 Trends analysis	28
3.6 Future projections	29
3.7 Data Display	29
3.7.1 Grid Analysis and Display System (GrADs)	29
3.7.2 Climate Data Operator (CDO)	30
3.7.3 R and R Studio	30
3.8 Summary	30
CHAPTER 4: HISTORICAL TRENDS AND MODEL VERIFICATION	31
4.0 Introduction	31

4.1 Historical trends	31
4.1.1 Trends in SATs	31
4.1.2 Trends in rainfall	37
4.2 Model verification	42
4.2.1 Statistical verification	42
4.2.2 Visual verification	44
4.2.2.1 SAT seasonal means	44
4.2.2.2 Rainfall seasonal means	45
4.3 Summary	55
CHAPTER 5: FUTURE PROJECTIONS OVER EASTERN SOUTH AFRICA	56
5.0 Introduction	56
5.1 Future projections of SATs	56
5.1.1 Near-future (2021-2050)	56
5.1.2 Far-future (2070-2099)	68
5.2 Future projections of rainfall over the study area	80
5.2.1 Near-future (2021-2050)	80
5.2.2 Far-future (2070-2099)	92
5.3 Summary	103
CHAPTER 6: CONCLUSION AND RECOMMENDATIONS	104
6.0 Introduction	104
6.1 Discussions of key findings	104
6.1.1 Historical trends	104
6.1.2 Model verification	106
6.1.3 Future climate change projections (2021-2099)	1077
6.2 Implications and recommendations	108
6.3 Conclusion	108

REFERENCES	110
REFERENCES	110

LIST OF FIGURES

Figure 2.1 The	tive SSP	tamilies and	l their scenai	10S				15
Figure 2.2 Tre	nds for fo	ur RCPs froi	m 2000 until 2	2100				16
Figure 3.1 Map	of the stu	udy area, KZ	N, and MP					22
Figure 4.1 This for the period over this perion	1961-2020). The trend	line indicate	s a significan	t decrease in	the numb	er of cool	days
Figure 4.2 Thi	s figure s	hows the co	ool days' ind	ex (TX10P) in	Durban for t	he period	1961-2020	. The
trend line i		•					•	
Figure 4.3 This	s figure sh	ows the hot	days' index	(TX90P) in Kru	ıger Mpumal	anga Inter	national Ai	irport
for the period over this perio								•
Figure 4.4 Thi	is figure s	hows the h	ot days' inde	ex (TX90P) in	Durban for t	he period	1961-2020	. The
trend line i period		•					•	
Figure 4.5 Th	nis figure	shows the	heavy rain	fall days' ind	ex (R10mm)	in Kruge	r Mpumal	anga
International A	Airport for	the period 1	961-2020. Th	e trend line inc	dicates a slig	ht decreas	e in the nu	mber
of	heavy		rainfall	day	s	over		this
period								40
Figure 4.6 Thi	s figure sl	hows the he	avy rainfall (days' index (R	10mm) in Du	ırban for tl	he period	1961-
2020. The tre	•		•	,	•		•	
period			J			•	•	
Figure 4.7 This								-
•	•					•	•	•
Mpumalanga I		•	-				o cnange i	
frequency	of	rainfall	days	exceeding	50mm/	day	over	this
period								41
Figure 4.8 This	s figure sh	ows the free	quency of rai	nfall exceedin	g 50mm/day	index (R50)mm) in Dເ	ırban
for the period	1961-2020	. The trend I	ine indicates	an increase in	the number	of rainfall	days exce	eding
50mm/day ove	er this peri	od						41
Figure 4.9 Tay	lor diagra	m showing \$	SAT model v	erification				43
Figure 4.10 Ta	ylor diagra	am showing	rainfall mod	el verification.				43
Figure 4.11 DJ	IF seasona	al mean SA1	for the 1961	-1990 period				47

Figure 4.13 JJA seasonal mean SAT for the 1961-1990 period	Figure 4	1.12 MAM seasonal mean SAT for the 1961-1990 period4	8
Figure 4.15 DJF seasonal mean rainfall for the 1961-1990 period	Figure 4	.13 JJA seasonal mean SAT for the 1961-1990 period4	Ģ
Figure 4.16 MAM seasonal mean rainfall for the 1961-1990 period	Figure 4	.14 SON seasonal mean SAT for the 1961-1990 period5	j(
Figure 4.17 JJA seasonal mean rainfall for the 1961-1990 period	Figure 4	.15 DJF seasonal mean rainfall for the 1961-1990 period5	1
Figure 5.1 DJF seasonal mean sAT for SSP2-4.5 during the 2021-2050 period	Figure 4	.16 MAM seasonal mean rainfall for the 1961-1990 period5	2
Figure 5.1 DJF seasonal mean SAT for SSP2-4.5 during the 2021-2050 period	Figure 4	.17 JJA seasonal mean rainfall for the 1961-1990 period) (
Figure 5.2 MAM seasonal mean SAT for SSP2-4.5 during the 2021-2050 period	Figure 4	.18 SON seasonal mean rainfall for the 1961-1990 period5	į
Figure 5.3 JJA seasonal mean SAT for SSP2-4.5 during the 2021-2050 period	Figure 5	i.1 DJF seasonal mean SAT for SSP2-4.5 during the 2021-2050 period5	į
Figure 5.4 SON seasonal mean SAT for SSP2-4.5 during the 2021-2050 period	Figure 5	5.2 MAM seasonal mean SAT for SSP2-4.5 during the 2021-2050 period6	(
Figure 5.5 DJF seasonal mean SAT for SSP5-8.5 during the 2021-2050 period	Figure 5	3.3 JJA seasonal mean SAT for SSP2-4.5 during the 2021-2050 period6	;1
Figure 5.6 MAM seasonal mean SAT for SSP5-8.5 during the 2021-2050 period	Figure 5	i.4 SON seasonal mean SAT for SSP2-4.5 during the 2021-2050 period6	1
Figure 5.7 JJA seasonal mean SAT for SSP5-8.5 during the 2021-2050 period	Figure 5	i.5 DJF seasonal mean SAT for SSP5-8.5 during the 2021-2050 period6	;
Figure 5.8 SON seasonal mean SAT for SSP5-8.5 during the 2021-2050 period	Figure 5	6.6 MAM seasonal mean SAT for SSP5-8.5 during the 2021-2050 period6	į
Figure 5.9 Seasonal changes in SAT for SSP2-4.5 between reference climate (1961-1990) and near future (2021-2050) periods	Figure 5	i.7 JJA seasonal mean SAT for SSP5-8.5 during the 2021-2050 period6	;
future (2021-2050) periods	Figure 5	i.8 SON seasonal mean SAT for SSP5-8.5 during the 2021-2050 period6	(
Figure 5.10 Seasonal changes in SAT for SSP5.8-5 between reference climate (1961-1990) and near future (2021-2050) periods	Figure 5	5.9 Seasonal changes in SAT for SSP2-4.5 between reference climate (1961-1990) and nea	r
future (2021-2050) periods	future (2	2021-2050) periods6	7
Figure 5.11 DJF seasonal mean SAT for SSP2-4.5 during the 2070-2099 period	Figure 5	i.10 Seasonal changes in SAT for SSP5.8-5 between reference climate (1961-1990) and nea	r
Figure 5.12 MAM seasonal mean SAT for SSP2-4.5 during the 2070-2099 period	future (2	2021-2050) periods6	į
Figure 5.13 JJA seasonal mean SAT for SSP2-4.5 during the 2070-2099 period	Figure 5	5.11 DJF seasonal mean SAT for SSP2-4.5 during the 2070-2099 period7	1
Figure 5.14 SON seasonal mean SAT for SSP2-4.5 during the 2070-2099 period	Figure 5	5.12 MAM seasonal mean SAT for SSP2-4.5 during the 2070-2099 period7	2
Figure 5.15 DJF seasonal mean SAT for SSP5-8.5 during the 2070-2099 period	Figure 5	5.13 JJA seasonal mean SAT for SSP2-4.5 during the 2070-2099 period7	1
Figure 5.16 MAM seasonal mean SAT for SSP5-8.5 during the 2070-2099 period	Figure 5	5.14 SON seasonal mean SAT for SSP2-4.5 during the 2070-2099 period7	′2
Figure 5.17 JJA seasonal mean SAT for SSP5-8.5 during the 2070-2099 period	Figure 5	.15 DJF seasonal mean SAT for SSP5-8.5 during the 2070-2099 period7	ļ
Figure 5.18 SON seasonal mean SAT for SSP5-8.5 during the 2070-2099 period	Figure 5	5.16 MAM seasonal mean SAT for SSP5-8.5 during the 2070-2099 period7	'(
Figure 5.19 Seasonal changes in SAT for SSP2-4.5 between reference climate (1961-1990) and far future (2070-2099) periods	Figure 5	5.17 JJA seasonal mean SAT for SSP5-8.5 during the 2070-2099 period7	7
future (2070-2099) periods	Figure 5	5.18 SON seasonal mean SAT for SSP5-8.5 during the 2070-2099 period7	'{
Figure 5.20 Seasonal changes in SAT for SSP5-8.5 between reference climate (1961-1990) and far future (2070-2099) periods	Figure :	5.19 Seasonal changes in SAT for SSP2-4.5 between reference climate (1961-1990) and fa	r
future (2070-2099) periods	future (2	2070-2099) periods7	9
Figure 5.21 DJF seasonal mean rainfall for SSP2-4.5 during the 2021-2050 period	Figure :	5.20 Seasonal changes in SAT for SSP5-8.5 between reference climate (1961-1990) and fa	r
Figure 5.22 MAM seasonal mean rainfall for SSP2-4.5 during the 2021-2050 period	future (2	2070-2099) periods7	į
Figure 5.23 JJA seasonal mean rainfall for SSP2-4.5 during the 2021-2050 period	Figure 5	5.21 DJF seasonal mean rainfall for SSP2-4.5 during the 2021-2050 period	3
Figure 5.24 SON seasonal mean rainfall for SSP2-4.5 during the 2021-2050 period	Figure 5	5.22 MAM seasonal mean rainfall for SSP2-4.5 during the 2021-2050 period	32
Figure 5.25 DJF seasonal mean rainfall for SSP5-8.5 during the 2021-2050 period Figure 5.26 MAM seasonal mean rainfall for SSP5-8.5 during the 2021-2050 period Figure 5.27 JJA seasonal mean rainfall for SSP5-8.5 during the 2021-2050 period	Figure 5	5.23 JJA seasonal mean rainfall for SSP2-4.5 during the 2021-2050 period	Ę
Figure 5.26 MAM seasonal mean rainfall for SSP5-8.5 during the 2021-2050 period89 Figure 5.27 JJA seasonal mean rainfall for SSP5-8.5 during the 2021-2050 period	Figure 5	5.24 SON seasonal mean rainfall for SSP2-4.5 during the 2021-2050 period	(
Figure 5.27 JJA seasonal mean rainfall for SSP5-8.5 during the 2021-2050 period89	Figure 5	i.25 DJF seasonal mean rainfall for SSP5-8.5 during the 2021-2050 period	37
· · · · · · · · · · · · · · · · · · ·	Figure 5	5.26 MAM seasonal mean rainfall for SSP5-8.5 during the 2021-2050 period	3
Figure 5.28 SON seasonal mean rainfall for SSP5-8.5 during the 2021-2050 period90	Figure 5	5.27 JJA seasonal mean rainfall for SSP5-8.5 during the 2021-2050 period	Ç
	Figure 5	i.28 SON seasonal mean rainfall for SSP5-8.5 during the 2021-2050 period9)(

Figure 5.29 Seasonal changes in rainfall for SSP2-4.5 between reference climate (1961-1990) and
near-future (2021-2050) periods	91
Figure 5.30 Seasonal changes in rainfall for SSP5-8.5 between reference climate (1961-1990) and
near-future (2021-2050) periods	91
Figure 5.31 DJF seasonal mean rainfall for SSP2-4.5 during the 2070-2099 period	94
Figure 5.32 MAM seasonal mean rainfall for SSP2-4.5 during the 2070-2099 period	95
Figure 5.33 JJA seasonal mean rainfall for SSP2-4.5 during the 2070-2099 period	96
Figure 5.34 SON seasonal mean rainfall for SSP2-4.5 during the 2070-2099 period	97
Figure 5.35 DJF seasonal mean rainfall for SSP5-8.5 during the 2070-2099 period	98
Figure 5.36 MAM seasonal mean rainfall for SSP5.8-5 during the 2070-2099 period	99
Figure 5.37 JJA seasonal mean rainfall for SSP5-8.5 during the 2070-2099 period	100
Figure 5.38 SON seasonal mean rainfall for SSP5-8.5 during the 2070-2099 period	101
Figure 5.39 Seasonal changes in rainfall for SSP2-4.5 between reference climate (1961	I-1990) and far-
future (2070-2099) periods	102
Figure 5.40 Seasonal changes in rainfall for SSP5-8.5 between reference climate (1961	1-1990) and far-
future (2070-2099) periods	102

LIST OF TABLES

Table 3.1 The CMIP6 models used for projected future climate change study	23
Table 4.1 The indices used for SAT and rainfall in Kruger Mpumalanga International Ai	
Durban	•

LIST OF ABBREVIATIONS

AWI-CM-1-1-MR Alfred Wegener Institute Climate Model Medium Resolution version 1.1

AR5 Fifth Assessment Report

AR6 Sixth Assessment Report

AM4.0 Atmosphere Model Version 4

AOGCM Atmosphere-Ocean General Circulation Model

ACCESS-CM2 Australian Community Climate and Earth System Simulator Coupled Model version

2

BCC-AGCM Beijing Climate Center Atmospheric General Circulation Model

BCC-CSM2-MR Beijing Climate Center Climate System Model Medium Resolution version 2

CO2 Carbon dioxide

CSIRO-BOM Commonwealth Scientific and Industrial Research Organisation

C3S Copernicus Climate Change Service

CMIP5 Coupled Model Intercomparison Project Phase 5

CMIP6 Coupled Model Intercomparison Project Phase 6

CDO Climate Data Operators

COL Cut-Off Lows

DJF December-January-February

EC Eastern Cape

ESM Earth System Model

ENSO El Niño Southern Oscillation

ENSEMEAN Ensemble mean

ECS Equilibrium Climate Sensitivity

ECMWF European Centre for Medium-Range Weather Forecasts

ETCCDI Expert Team on Climate Change Detection Indice

ELT Extreme Low Temperature

FESOM Finite Element Sea Ice-Ocean Model

GFDL-ESM4 Geophysical Fluid Dynamics Laboratory Earth System Model version 4

GCM Global Climate Models

GSAT Global Surface Air Temperature

GHG Greenhouse gas

GrADs Grid Analysis and Display System

GDP Gross Domestic Product

hPa Hectopascal

IPSL-CM6A-LR Institut Pierre Simon Laplace Climate Model Low-Resolution version 6A

IPCC Intergovernmental Panel on Climate Change

ITCZ Intertropical Convergence Zone

IDE Integrated Development Environment

JJA June-July-August

KZN KwaZulu Natal

LMDZ Laboratoire de Métérologie Dynamique Zoom

MJO Madden-Julian Oscillation

MAM March-April-May

MPI-ESM 1.2-LR Max Planck Institute Earth System Model, Low-Resolution version 1.2

MCC Mesoscale Convective Complexes

MP Mpumalanga

MOM6 Modular Ocean Model version 6

NOAA GFDL National Oceanic and Atmospheric Administration, Geophysical Fluid Dynamics

Laboratory

NW Northwest

NEMO Nucleus for European Models of the Ocean

ORCHIDEE Organising Carbon and Hydrology In Dynamic Ecosystems

RCM Regional Climate Models

RCP Representative Concentration Pathways

RMSE Root Mean Square Error

SST Sea Surface Temperatures

SON September-October–November

SSP Shared Socioeconomic Pathways

SADC Southern African Development Community

SOI Southern Oscillation Index

SWIO South-West Indian Ocean

SRES Special Report on Emission Scenarios

SAT Surface Air Temperature

TC Tropical Cyclone

TTT Tropical-Temperate Troughs

2-D Two-Dimensional

CHAPTER 1: INTRODUCTION

1.0 Background

1.1 Climate change and variability

South Africa is vulnerable to climatic ambiguity in the future as a result of global climate change. Droughts, floods, and other severe weather and climate phenomena are frequently experienced in southern Africa, with disastrous effects on the region's agriculture, economy, water supplies, and well-being of people (Coetzee et al. 2023). Southern Africa region is especially susceptible to catastrophic climate and weather events and the impacts of climate change since its economies are heavily dependent on weather and climate-sensitive industries (Mpandeli et al. 2018).

The awareness that climate change is taking place during times that affect human activities rather than just in the distant past has enhanced the significance of climate (Neelin, 2010). Climate is an average of weather events, and the definition of climate varies depending on the period utilized in the average. For example, the average climate from 1950 to 1970 differs from the average from 1980 to 2000 (Volodin and Gritsun, 2018). This average fluctuates from decade to decade and more so across various centuries. Climate variability is the term used to describe these variations. This involves the ice ages and the prolonged warm climate that the dinosaurs thrived in, together with phenomena such as El Niño, which causes the tropical Pacific Ocean to warm and cool periodically, and the prolonged drought that has ravaged the Sahel region of Africa over the last few decades (Neelin, 2010). Since humans may now alter the climate, climate change has acquired a new dimension. Anthropogenic climate change is human-caused and is different from El Niño, an example of natural climate variability. Acid rain, ozone hole, and warming temperatures are examples of human-caused climate change (Nanda, 2021).

1.1.1 Anthropogenic climate change

The main contributing element to human energy production is the main cause of emission of greenhouse gases (GHG) through fossil fuel burning by humans, particularly carbon dioxide (CO2) (Min et al.2022). As a result, the generation of energy in the future is inextricably tied to human-caused global warming and anthropogenic GHG emissions. The evaluation of future climate change brought on by human activity is

based in large part on projections of how the system of the world's energy will change over the coming century (Hook, 2011).

There is evidence that supports the fact that anthropogenic climate change has caused climate extremes to be more intense and occur more frequently over the land (Zittis et al. 2022). Co-occurring climatic extremes in various areas are projected to occur with a high frequency of CO2-enhanced global warming as climate extremes spread across a growing proportion of the land area. The geographic distribution of climate extremes' co-occurrence and the degree to which its alterations can be linked to global climate change are uncertain (Zhou and Zhang, 2023). The magnitude of the dependence among climate drivers and the average and variation of climate variables are all altered by anthropogenic climate change (Sun et al. 2022).

The Intergovernmental Panel on Climate Change (IPCC) utilizes climate models that depend on different emission scenarios to represent potential future production of fossil fuels trajectories and their associated CO2 emission (IPCC, 2007). The Special Report on Emission Scenarios (SRES) was released by the IPCC in 2000 and remains to be a vital component of climate change modelling (Hook and Tang, 2013). What is vital for future projection of climate change, is the variety of future pathways for society, its system of energy, and the associated emission of GHGs (Riahi et al. 2017). These pathways, also known as emission scenarios, are fed into climate models to help translate the projected emissions into climatic changes. Throughout its work, the IPCC has employed a variety of emission scenarios (Nakicenovic et al. 2000).

1.2 Problem statement

According to Driga and Drigas (2019), human actions that have resulted in the release of GHGs into our atmosphere are mostly to blame for the Earth's accelerating climate change. Global warming now poses grave dangers to several climate-sensitive industries due to the altered climate factors caused by these rising GHG emissions. The socioeconomic environment and South Africa's location in the arid subtropics make it sensitive to the impacts of climate change (Nembilwi et al. 2021). Southern Africa's likelihood of experiencing catastrophic storms, such as powerful tropical cyclones (TC) and extremely strong thunderstorms, is rising due to climate change. As a result of climate change, there are more incidents of fatalities, injuries, and infrastructure damage (Scholes and Engelbrecht, 2021).

Compared to the rate of global warming over the past five decades, temperatures have been rising sharply throughout Africa, and at the majority of locations, the increases are statistically significant. The regions of

subtropical southern Africa, subtropical North Africa, and portions of central tropical Africa have had the highest trends (Collins, 2011). The overall rate of temperature increase in these areas is over two times as fast as the rate of rising temperature on land worldwide (Engelbrecht et al. 2015). In addition, there is also evidence of flood events over South Africa's east coast, in KwaZulu Natal (KZN) (Bouchard et al. 2023).

The KZN and the Eastern Cape (EC) provinces in South Africa experienced extremely excessive precipitation in April 2022, with some areas receiving more than 300mm in just under 24 hours (Singh et al. 2022; Mashao et al. 2023; Mudefi, 2023). A cut-off low (COL) that veered off the mid-latitude westerly wave and traveled across South Africa's east coast and the interior was responsible for the occurrence (Thoithi et al. 2022). COLs are synoptic scale baroclinic systems and are capable of producing extreme weather and heavy precipitation events in this region and neighbouring locations. COLs are frequent in South Africa throughout April. The low-level maritime winds carrying moisture from the southern Indian Ocean further aggravated the effects of the COL on the 11th and 12th of April 2022 (Singh et al. 2022).

Flooding caused by heavy rains over South Africa's northeast, including the province of Mpumalanga (MP), is typically linked to TC activity from the South-West Indian Ocean (SWIO) (Mpungose, 2022) and midtropospheric COLs. However, cloud bands can occasionally cause flooding when slow-moving (Rapolaki et al. 2019). Heavy rainfall and flooding can also be brought on by intense thunderstorms buried in tropical lows and mesoscale convective complexes (MCC) (Chikoore et al. 2021). In February 2000, extremely severe rains were experienced over the northeastern regions of South Africa, Mozambique, and Zimbabwe. Numerous people died due to the disastrous flooding, and the region's infrastructure was seriously damaged, severely inhibiting agricultural and economic growth (Smithers et al. 2001). Tropical weather systems that travelled from the east to the west across the subcontinent were responsible for most precipitation, which fell between February 5th and 10th and February 22nd and 25th in 2000 (Dyson and Van Heerden, 2001).

The national average precipitation in South Africa is only 450 mm annually, which is much less than the average worldwide precipitation of 860 mm annually (Mabhaudhi et al. 2019). Due to its closeness to the warm Indian Ocean, the eastern region of the country experiences greater amounts of precipitation during summertime (Mpungose et al. 2022). According to Ratna et al. (2013), because of tropical-temperate troughs (TTT), the Indian Ocean is the primary provider of precipitation in the subtropical regions, accounting for 30% to 60% of all precipitation. As a result, most of the country's high-producing agricultural and forestry land,

which includes the MP forestry sector, is found in the east. According to Van der Merwe et al. (2022), climate is the most important site variable for the development of invasive pine species in MP. South Africa.

The performance of agriculture, as observed by Mutengwa et al. (2023), is significantly affected by the impacts of climate variability and change on water supplies. More than 60 of the population in rural southern Africa bases its lifestyle in rural areas and entirely depends on natural resources and agriculture. As a result, these impacts are already undermining the development and growth of the economy (Nhamo et al. 2019). Additionally, as outlined by Steiner et al. (2020), climate variability and change have an anticipated impact on the supply and demand sides of agricultural foods. While local systems prepare and respond to changes in short-term climate causes, they hinder longer-term food security. According to Nhemachena et al. (2020), the socioeconomic effects of climate change on agriculture include decreased yields and output, decreased agriculture Gross Domestic Product (GDP), increased risks of hunger and food insecurity, and an increase in the number of people affected.

Due to future climate conditions, future projections of climate show that crop yields will decline, and latest research shows that yields are being reduced (Ray et al. 2019). Extreme weather conditions that negatively affect southern Africa's agriculture include floods, extreme heat, regular droughts, rising temperatures, and unpredictable weather (Odongo et al. 2022).

Projected changes in rainfall and temperature over southern Africa have been the subject of some research. In addition, there are no studies that have been done on climate variability and change specifically focusing on eastern South Africa. This study intends to cover the gap by investigating historical and projected variability and change of climate over eastern South Africa (KZN and MP) under high and low mitigation focusing on the near-future (2021-2050) and the far-future (2070-2099) periods.

1.3 Research questions

- What are the historical trends in surface air temperatures (SAT) and rainfall characteristics over eastern South Africa?
- How well do models from the Coupled Model Intercomparison Project Phase 6 (CMIP6) simulate the observed climate of eastern South Africa?
- What are the projected changes in SATs over the study area in the future from 2021 to 2099?
- To what extent will climate change alter rainfall characteristics over the study area?

1.4 Research aim

The study aims to investigate historical and projected variability and change of climate over eastern South Africa under high and low mitigation focusing on the near-future (2021 to 2050) and the far-future (2070 to 2099) periods.

1.5 The specific objectives of the study

- Analyse trends in SATs and rainfall over eastern South Africa from 1961 to 2020
- Evaluate the performance of six CMIP6 models against historical observations (1961 to 1990)
- Analyse projections of SAT over the study area for the near and far-future periods
- Map and quantify future projections of rainfall over the study area

1.6 Chapter outline

The study covers six chapters: *Chapter one* presents the introduction of the whole study which consists of the background, problem statement, research questions, research aim, and specific objectives of the study. *Chapter two* presents a literature review which consists of the introduction, climate of South(ern) Africa, climate trends and change in South Africa, climate models and climate modelling, future climate projections over South Africa, impacts, vulnerability, and adaptation to climate change, and lastly, the summary of the chapter. *Chapter three* presents the research methodology which consists of an introduction, study area, observed data, climate models, model verification, trends analysis, future projections, instrumentation, and the summary of the chapter. Chapters four and five are the results chapters. *Chapter four* deals with historical trends and model verifications. *Chapter five* presents the future climate projections from the model ensembles. *Chapter six* presents the key findings, recommendations of this work, and the conclusion.

CHAPTER 2: LITERATURE REVIEW

2.0 Introduction

This chapter focuses and reports on the studies that have already been done and that are related to this study. The studies are for enhancing this study and to show a broader view of climate variability and change in a region. The purpose of this chapter is to provide the background knowledge of the research topic, identify what other studies have found, and bring out what is not known in this study field. It also discusses the climate models and scenarios.

2.1 Climate of South(ern) Africa

2.1.1 Dominant weather systems

Dominant weather systems in South Africa include COLs, TCs, and cloud bands (Harrison, 1984; Singleton and Reason, 2007; Hart et al. 2013; Moses et al. 2023). COL is a weather system that is greatly affected by the interception of the Mascarene High (Xulu et al. 2023). Furthermore, it is a deep low-pressure system that is strongest in the mid-troposphere and forms at 500 hectopascals (hPa) (Muofhe et al. 2020). A COL is formed by the separation of an upper westerly wave from the predominant mid-latitude westerly wind which is cut off by that westerly wind. The COLs are low-pressure systems that are no longer connected to the westerly wave and become detached from the autonomously rotating planetary circulation (Ndarana et al. 2020).

The COL loses its momentum and may spread across the region over several days or spread slowly before dissipating. COLs are associated with mid-tropospheric instability and deep convection, which can also cause extreme weather patterns across an area (Barnes et al. 2021). This was experienced in April 2019 when a COL in eastern South Africa (KZN, Durban) caused flooding that killed at least 85 people and displaced thousands (Thambiran et al. 2023). COLs are the main cause of flood damage in South Africa and consist of semi-annual variations with peak values between March and May and between September and November (Singleton and Reason, 2007). COLs are least frequent from December to February however, that is when they are most commonly connected with blocking Mascarene High blocking (Xulu, 2017).

The COL in the region of 2.5°E to 32.5°E/20°S to 45°S tends to have precipitation over the mainland. Blockage of the Mascarene High could cause stagnation of westerly wave propagation, which could exacerbate the formation of COL that rotates independently of the westerlies, resulting in further blockages in southern Africa (Xulu et al. 2020). A COL that is completely developed circulates independently, leading to further blocking from Mascarene High. Blocking from COL is another form of quasi-stationary west-east tracking, resulting in long periods of unstable weather over the subcontinent (Abba, 2020).

The COLs occur throughout the entire year, on average about 11 of them making landfall in southern Africa each year (Singleton and Reason, 2007; Barnes et al. 2021; Taljaard, 1985). Autumn and spring, are seasons of transition, and that is when the COLs occur mostly (Singleton and Reason, 2007; Favre et al. 2012). COLs lead to heavy rainfall in parts of South Africa and contributes more to South Africa's annual rainfall. In the tropics, propagation of COL is additionally erratic, as they tend to migrate westward (Favre et al. 2013).

TCs are cyclones over sub-tropical or tropical waters with organised convection and pronounced circulation of cyclonic surface wind (In the northern hemisphere the circulation is anti-clockwise and in the southern hemisphere is clockwise) (Keriwala and Patel, 2022). TCs take place over the SWIO in the summer from November to April (Pillay and Fitchet, 2019) and affect the eastern parts, including South Africa's Limpopo, MP, and KZN provinces (Mpungose, 2022; Chikoore et al. 2021; Meyiwa, 2019). They are among the deadliest, most destructive, and most damaging weather systems on Earth (Lamers et al. 2023). Severe TCs cause devastating winds, torrential downpours, coastal storm surges, and severe flooding, usually causing significant damage to property and fatality (Do and Kuleshov, 2023). Late in February 2000, TC Eline triggered devastating floods in South Africa, Zimbabwe, and Mozambique and a tropical depression early in the same month (Reason and Keibel, 2004).

More than 1300 people died and over three million people were left homeless due to TC Idai, which struck Zimbabwe, Mozambique, and Malawi in March 2019 (Zimba et al. 2020). Health concerns in the afflicted populations were made worse by the storm's extensive flooding and loss of infrastructure, including medical institutions (Dembedza et al. 2023). In the wake of the storm, outbreaks of cholera were recorded, underlining the heightened risk of infectious illnesses brought on by extreme weather conditions. Similar to TC Eloise, which ravaged Zimbabwe, South Africa, Eswatini, and Mozambique in January 2021, it displaced people, severely damaged houses, and raised the danger of infectious illnesses (Aderinto, 2023).

Conditions for TCs to develop include Sea Surface Temperatures (SST) that are greater than 27°C and a cloud cluster that exhibits continuous deep convection (Chang and Smith, 2021). In the Indian Ocean, latitudes between 5°S and 14°S are particularly favourable for cyclogenesis (Jury and Pathack, 1991). TC generation is restricted to specific seasons and latitudes. Furthermore, for active cumulus and cumulonimbus formation in the cloud cluster and the TC formation, the relative humidity up to the middle level must be rather high. The central pressure and surface wind speed are important factors for the development of TCs (Fang et al. 2022). The TC's eye forms when the speed of the wind is above 60 knots, and the central pressure falls below 1000 hPa. TCs are fixed in easterlies and tend to migrate westward, which is influenced by large-scale flow (Rohli and Li, 2021). The supply of moisture and energy is essential for TC to maintain its intensity (Trenberth, 2011). When TCs touch down over land, they weaken, and their wind speeds are also lowered by surface friction at the land's surface (Wang and Matyas, 2022). Due to the reduced SST in the mid-latitudes, TCs also begin to deteriorate (Ginis, 2021).

In the southern hemisphere's subtropical belt, Northwest (NW) cloud bands constitute a significant aspect of the weather (Mahlobo et al. 2019). The cloud bands at their southeast end link a cold front to the Intertropical Convergence Zone (ITCZ) at the NW end, and they range in length from 3,000 to 8,000 km (Xulu et al. 2020). An easterly wave is typically present at the bottom of the NW cloud band closest to the equator. In the connection involving the mid-latitude frontal belt and ITCZ, NW cloud bands play a significant role. These cloud bands show up during summertime (Reid et al. 2019; Hart et al. 2013).

NW cloud bands are widespread near South America, across Paraguay through the South Atlantic, as well as in southern Africa (Chikoore and Jury, 2021). Furthermore, cloud bands frequently surround Australia and extend from the area near Indonesia throughout the middle of Australia to the southeast coast. NW cloud bands also predominate across southern Africa (Flamant et al. 2022). There are enduring cloud bands that connect the tropics and the mid-latitudes, and the cloud band that connects southeast Africa with the Congo basin is less enduring.

Significant cloud bands develop in TTTs and prolonged NW to southeast convergence zones, which connect the tropics to the mid-latitudes. These cloud bands occur when waves in the westerlies become connected to disruptions in the tropics (Howard et al. 2019). The zones, which are linked to maximum rainfall, are

channels for the large-scale movement of energy of latent heat and moisture form from the tropics to the midlatitudes. A band of clouds and rain are linked to the TTT (Erasmus, 2019) and as a result, cloud bands play a significant role in producing rainfall in the south of the Zambezi Valley.

When the NW cloud band moves slowly, it spreads south-eastward and causes floods and severe, persistent rains. Mahlalela et al. (2020) observed that throughout most of South Africa, including the greater part of the EC, there are one to two less/more days of cloud band than normal in the dry/wet springtime. A more robust Angola Low frequently serves as the source zone for cloud bands (Munday and Washington, 2017).

2.1.2 Rainfall climatology

According to Roffe et al. (2019), South Africa is one of the few nations in the southern African area to have rain in every season. In South Africa, during the summer season, is when precipitation rates are at their peak (Ibebuchi, 2023). Except for a tiny portion along the south coast, the southern African subcontinent gets most of its precipitation during the summer season. Furthermore, the Western Cape province receives most of its rainfall during winter season, and this is because mid-latitude cyclones pass through this area during winter, bringing frontal rainfall (De Kock et al. 2022). During the autumn season, the majority of the country's eastern regions, including the coasts of KZN, show relatively low average rainfall at a maximum of 4 mm/day, whereas the western region has average rainfall below 3 mm (Engelbrecht et al. 2013).

South Africa has its driest weather during the winter season (Engelbrecht et al. 2009). The increasing strength of lower and mid-level subtropical high-pressure systems across southern Africa has a significant impact on the winter season. At the same time, the ITCZ and other powerful summer systems weaken and move north of the equator (Dedekind et al. 2016). Winter precipitation in South Africa is mostly in the country's southwest, with little or no precipitation occurring elsewhere. Cold fronts are carried to the west coast during the winter season by the South Atlantic high-pressure system's northward movement (Odoulami et al. 2021). South Africa's west coast experiences precipitation as a result of cold fronts' interaction with the continuous winds over the cold Benguela area (Du Plessis and Schloms, 2017).

Except for the NW regions of South Africa, the country has wetter weather during the neutral year, when neither El Niño nor La Niña occurs. However, neither the La Niña nor the El Niño periods exhibit a preponderance of precipitation outside of South Africa's eastern regions and southwestern Cape regions are

not very sensitive to El Niño Southern Oscillation (ENSO) forcing (Sazib et al. 2020). The MP province is the source of the majority of GHG emissions, as it is home to multiple coal-fired power plants. Due to the rising atmospheric moisture, this region is likely to experience a decrease in rainfall throughout the September-October-November (SON) period (Shikwambana et al. 2020). Due to GHG warming the surface of the Earth, more water vapour enters the atmosphere. As the spring season changes to the summer season, the additional moisture increases the quantity of energy required to heat the atmosphere, which can change the occurrence of the periods of rainfall (Shikwambana et al. 2023). This implies that more moisture will cause the atmosphere to take longer to absorb energy and produce rainfall. The return of mild temperatures on the ocean and the land, as well as the suppression of powerful high-pressure systems that produce rain over coastal regions, are characteristics of the spring season (Ncube, 2019).

2.1.3 Temperature variability

The Earth is gradually becoming warmer. Globally, anomalies in terrestrial air temperature have been steadily increasing since 1880 (Wang et al. 2018). The warmest years on record were discovered after 1976, and a more pronounced increasing trend is acknowledged globally in both the northern and southern hemispheres following that year (Ndlovu et al. 2021). Globally, people are affected by this consistently increasing trend and extremes in air temperature (Fan et al. 2020), however, marginalized, impoverished, agricultural, and less resilient populations are probably going to be more affected (Ndlovu et al. 2021).

Variations in the ENSO, a teleconnection that has been demonstrated to influence temperature in specific regions of Africa, are probably not the primary cause of climate change across the continent. Rather, climate change is probably caused by other natural climatic variability and/or human action (Collins, 2011). KZN's inland air temperatures are more extreme than those along the coast due to factors like low water vapour pressure deficits, ocean breezes, water's higher specific heat capacity than soil, and moderate air temperatures that permit moderate intra-seasonal, intra-seasonal, and intra-day variations in upper and lower air temperatures (Ndlovu et al. 2021).

Wet or hazy days and, occasionally, snow on high land or mountain summits are linked to extreme low temperature (ELT) occurrences. Snow seldom falls over South Africa due to its geographic position, except for the southern mountain peaks (Stander et al. 2016). When snow falls, it disrupts property and economic activity and can result in the death of homeless people (Chikoore et al. 2024; Stander et al. 2016).

Consequences of ELT occurrences in South Africa are severe frosts on winter crops (e.g. oats, and wheat), the death of young and fragile animals, and financial losses (Archer et al. 2021). The ridding anticyclones from the South Atlantic Ocean and mid-tropospheric COL pressure systems in the sky are the primary weather systems linked to ELT conditions over South Africa (Ndarana et al. 2021). The majority of cold air advection from the higher, colder latitudes, such as the South Atlantic High ridges across the southern part of Africa, is caused by cold frosts, which typically come before ridging anticyclones (Chikoore et al. 2024; Ndarana et al. 2021). Sea-surface temperature fluctuation in the tropical Indian and Pacific oceans is connected to the frequent occurrences of summer heat wave events, which frequently occur in conjunction with meteorological droughts (Mbokodo et al. 2020, 2023; Klopper et al. 1998).

2.1.4 Impacts of the ENSO

The ENSO is one of the major climate factors that affect the tropical Pacific SST (Shikwambana et al. 2023). South Africa's annual temperature and precipitation trends are significantly impacted by ENSO, which is characterized by the fluctuation of the eastern-tropical Pacific Ocean's surface temperatures (Bradshaw et al. 2022). Extreme cyclical climatic phenomena including heatwaves, droughts, and flooding can be brought on by ENSO anomalies (Goddard and Gershunov, 2020). ENSO comprises three phases: El Niño, La Niña, and the neutral phase (Ohde, 2018). When the surface temperatures of the eastern tropical Pacific Ocean rise above average, an El Niño event takes place, which causes droughts to occur on land and warmer-than-average temperatures over southern Africa. La Niña episodes are caused by water surface temperatures below normal, which causes more rain and cooler temperatures to fall over southern Africa (Van der Merwe et al. 2023). When neither El Niño nor La Niña occurs and SSTs in the equatorial Pacific are close to average, the neutral state takes place.

In the Western Cape area, wind speed fluctuates during El Niño or La Niña periods as it is weaker or stronger than usual (Philippon et al. 2012). According to Hoell et al. (2017), El Niño and La Niña occurrences cause a mid-tropospheric convection dipole across the tropical west and central Pacific, resulting in circulation abnormalities over southern Africa. As a result, abnormal circulations change the vertical movements and moisture fluxes, forcing seasonal rainfall abnormalities across southern Africa.

According to Mbokodo et al. (2023), the ENSO affects the KZN Drakensberg's summer rainfall variability, and there is a substantial association between summer rainfall and the Southern Oscillation Index (SOI) for

previous periods. Southern Africa continues to suffer from droughts brought on by the ENSO phenomenon, which have a severe effect on the environment, economic growth, and way of life (Tongwane et al. 2022). The region of Southern African Development Community (SADC) requested international assistance to feed nearly 40 million people as a result of the 2015–2016 ENSO drought (Hove and Kambanje, 2019). Because of greater investment in agricultural irrigation and improved crop types, grain production has been increasing gradually despite the difficulties associated with water constraints. According to Shikwambana and Malaza (2022), forward-thinking actions for adaptation are crucial to support communities that do farming in building systems of resilience to cope with alterations and variations in the climate as well as other stressors. This is because the agricultural sector in southern Africa is vulnerable currently and in the projected future.

2.2 Climate trends and change in South Africa

Not all parts of South Africa receive rainfall during the same season. The greater part of South Africa experiences summer rainfall (Ncoyini et al. 2022), but Cape Town and the surrounding southwestern Cape districts have winter precipitation primarily from cold fronts associated with extratropical cyclones that move east through the South Atlantic (Landman et al. 2017). Reduced rainfall during winter and the intensity over an extended period have had a substantial impact on the City of Cape Town's water constraints (Mahlalela et al. 2019).

Even though the definition of drought in arid regions is disputed, drought persists in the province of Northern Cape, South Africa, due to climate change (Calverley and Walther, 2022). Over the past few decades, unexpected harsh drought occurrences have caused water supply shortages that have impacted the agricultural industry in various parts of South Africa, including the EC, KZN, North West, Limpopo, and Free State provinces (Baudoin et al. 2022). As a result of absence of water, the Western Cape province saw a drop in tourism during the drought period. Furthermore, due to climate change and warming temperatures, extreme wildfire outbreaks have taken place on the coast of the south-Western Cape over the past ten years (Liu et al. 2023).

Drought, changes in land use, and extreme fire danger conditions all contributed to the latest Knysna fire, which was a disastrous event in the province of Western Cape (Quiroz et al. 2023). Climate change has raised the likelihood of both drought, and wildfire activity in South Africa and the frequency of heavy rainfall events (Clarke et al. 2022). The abnormal rise in global temperatures brought on by socioeconomic activity

is expected to increase South Africa's flood probability by more than 80% each year. The warmer Indian Ocean will most certainly experience more TCs in the future, increasing the likelihood of coastal flooding (Lin et al. 2020). Flooding may have an impact on the fuel load, vegetation, and fire patterns. The eastern interior and east coast parts of South Africa, as well as the Limpopo River basin region in southern Africa, experience the largest number of heat-wave days (approximately three on average per year) (Meque et al. 2022; Mbokodo et al. 2023).

Temperature extremes, including cold waves, warm waves, and recurrent heat waves, can have an impact on South Africa (Mengistu et al. 2024; Mbokodo et al. 2020). Southern Africa has seen temperature rises over the last 50 years that are more than twice as high as those seen worldwide, according to Engelbrecht et al. (2015). A rise in extreme weather events and climatic phenomena (e.g. drought) is the main effect of climate change globally (Dube et al. 2022a).

A persistent shift in the composition of the atmosphere or alterations in land use are examples of external influences that can cause climate change (Celik, 2020). Given the high levels of inequality and entrenched poverty in South Africa, the effects of climate change are projected to present significant obstacles to the country's national development (Mthembu and Hlophe, 2020). The global problem of global warming is expected to develop due to the increased rate of GHG emissions, changing the features of severe weather and climate events (Karl and Trenberth, 2003; Zittis et al. 2022).

2.3 Climate models and climate modelling

2.3.1 Regional climate models (RCM) and Global climate models (GCM)

Knowledge of potential changes in the climate must be made available to prepare for the effects of climate change, and climate models can provide this knowledge (Giorgi, 2019). A mathematical depiction of a real climate system, which is the climate model, is based on the conservation of momentum, energy, and mass (Tehrani et al. 2022). Climate models are important tools for researching potential changes in the climate under various circumstances of GHG emissions (Agbor et al. 2023). The physical and dynamic processes that exist in the atmosphere and their interactions with other elements of the Earth System are represented by these numerical models. These models' complexity necessitates trade-offs between computing costs, horizontal resolution, and occasionally, domain size (Doury et al. 2023).

The area of the field that is concerned with collecting and analysing observations must unavoidably interact with climate modelling. RCMs have a higher spatial resolution than GCMs because they operate over narrower domains that encompass an area of interest (Cheung et al. 2023). Despite using the same physical laws that are expressed in terms of mathematical equations as global models, RCMs are frequently used to generate projections of how the climate could shift locally (Nguyen et al. 2023). RCMs have been extensively utilized to study local climates, and it has been discovered that these models offer extraordinary advantages (Wen et al. 2023). They are more effective at resolving coastal and mountainous locations, for example, where a distance of 50 km might result in a major shift in climate. Furthermore, they can also record the mean statistics of daily rainfall on the sizes of a few grid boxes (Demessie et al. 2023). RCM is useful for projecting future climate change and simulating the recent past (Fan et al. 2014). It is commonly acknowledged that RCMs were initially developed as a short-term solution to a transient issue, specifically the inability to efficiently downscale the outputs of GCM at the regional level. Currently, however, a large number of GCMs are operated at a spatial resolution that is even higher than that of the majority of RCMs (Tapiador et al., 2020).

Future projections of several atmospheric and oceanic variables are provided by GCMs. These models are created and used on a worldwide scale, taking into account several potential future situations (Pourali et al. 2023). In recent years, GCMs have grown in importance and usefulness as a tool for tackling the problem of climate change (Tayyebi et al. 2023; Watanabe et al. 2010). Particularly when used to model projections of climate change at a country size, such as South Africa, the geographical resolution of GCM is somewhat imprecise. The resolution that can be achieved with GCMs depends on the processing resources available (Li et al. 2023).

2.3.2 Shared Socioeconomic Pathways (SSP)

Using illustrative emission scenarios known as SSPs, which are coupled with Coupled Model Intercomparison Project Phase 5's (CMIP5) Representative Concentration Pathways (RCP), climate models from CMIP6 are combined to project future climate change (Ge et al. 2021; Eyring et al. 2016). Researchers and pioneers in the field of climate change devised emission scenarios to make it easier to assess future climatic factors including adaptation, vulnerability, and mitigation (Zandersen et al. 2019). To assist the comprehensive study of future climate effects, vulnerabilities, adaptations, and mitigation, the climate change

research community devised a new scenario framework, which includes the SSPs (Van Vuuren et al. 2014). For researchers to research the effects, adaptations, and minimizing of climate change, the newly developed scenario framework for climate change research envisages integrating pathways of future radiative forcing and their related climate changes with different socioeconomic development pathways (O'Neill et al. 2014). The pathways were created over the last years through a cooperative community effort, and they reflect conceivable significant worldwide developments that collectively would create various obstacles to climate change mitigation and adaptation in the future (O'Neill et al. 2017). The five primary SSPs (SSP1-1.9, SSP1-2.6, SSP2-4.5, SSP3-7.0, and SSP5-8.5) are equally spaced and stretch to lower 2100 radiative forcing and temperatures, and the emission scenarios are different (Meinshausen et al. 2020). SSPs and RCPs are different and belong to different phases (Eyring et al. 2016). Figure 2.1 and Figure 2.2 below show SSPs and RCPs that belong to CMIP6 and CMIP5, respectively.

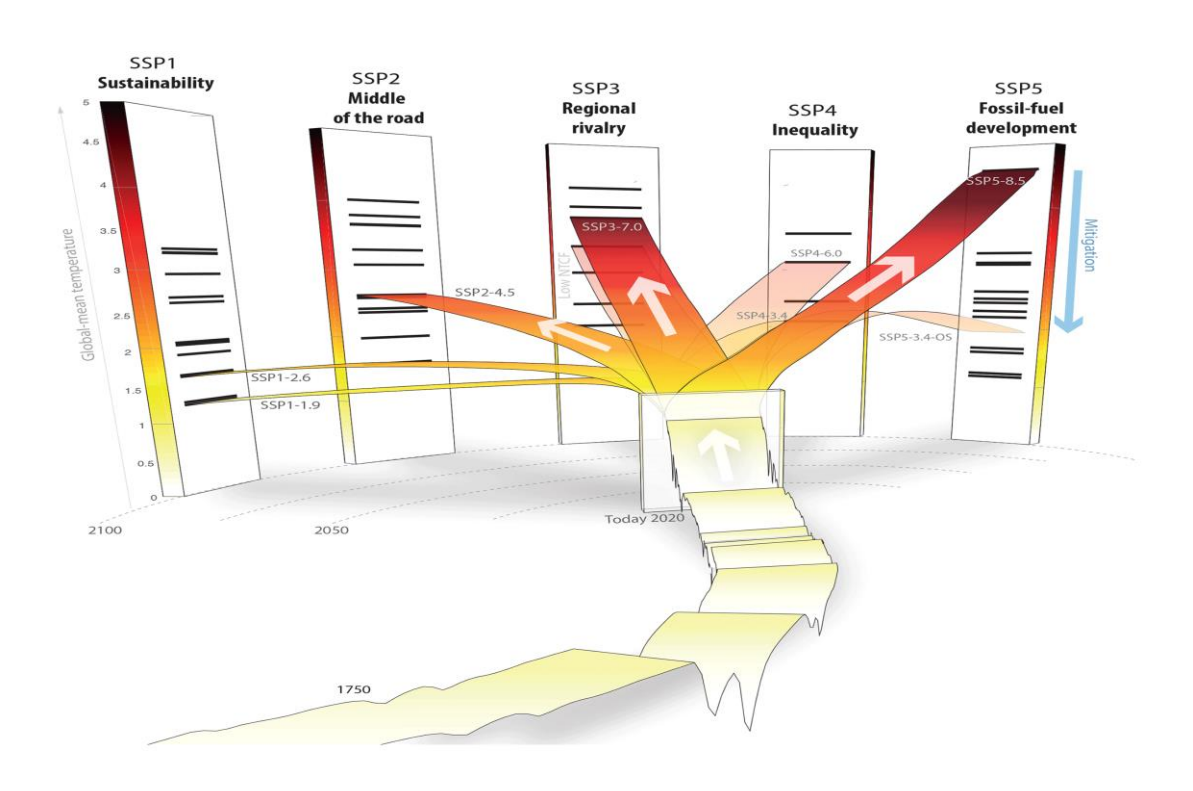


Figure 2.1 The five SSP families and their scenarios (Source: Meinshausen et al. 2020)

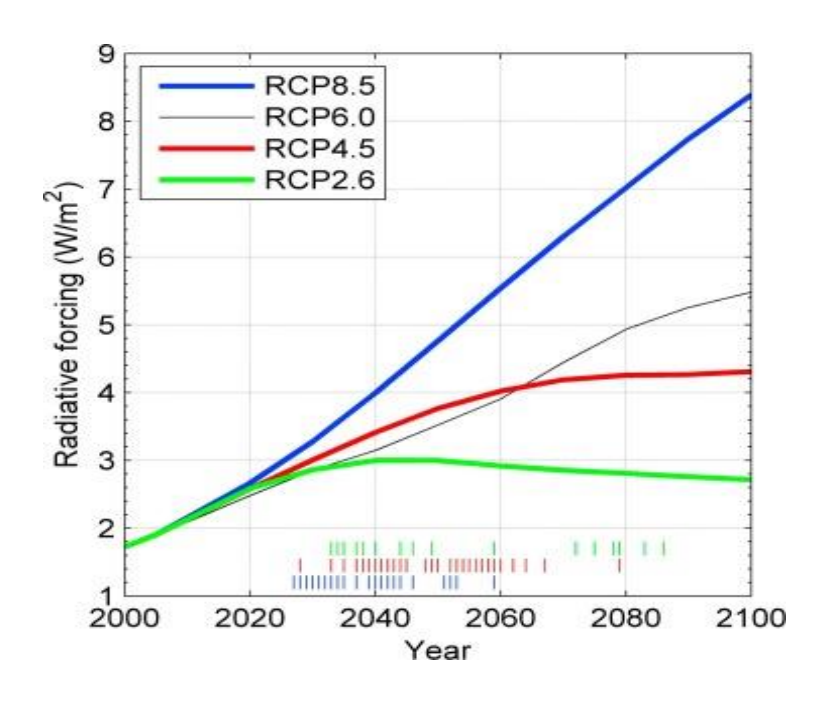


Figure 2.2 Trends for four RCPs from 2000 until 2100 (Source: Maule et al. 2017)

2.3.3 Verification/validation of climate models

For the study of changes in the climate that might arise from elevated levels of CO₂ and other GHGs in the atmosphere, climate models constitute a distinctive and potentially formidable instrument (Gates et al. 1990). These models are the only ones that can take into account the multitude of interrelated physical processes that make up the climate system at once, and their objective numerical solution offers the chance to investigate the characteristics of both past and potential future climates under various circumstances. However, validating the simulations against the observed climate is required to be able to correctly assess model projections (Abdolalizadeh et al. 2022). This allows for identification of the systematic flaws in the simulations, especially errors that are shared by several models. The projections of future climate changes must be evaluated while accounting for these inaccuracies or model biases. Naturally, the availability of pertinent observed data is necessary for the climate model validation (Tapiador et al. 2017). Observed data for some variables of relevance are either not accessible at all or are only accessible to a small portion of the globe. The paucity of surface and upper air observations is a major challenge particularly in Africa. To assess the models' performance, the climate models are validated (Feng et al. 2023) and the overall effectiveness of the CMIP6 models can be assessed using a Taylor diagram (Taylor, 2001; Chen et al. 2023).

2.3.4 CMIP6 models and the IPCC Sixth Assessment Report (AR6)

The CMIP6 multi-model ensemble, which is newly developed, offers additional options for studying the climate system and producing regional climate projections under several future scenarios, in addition to improving upon phase 5 (Taylor et al. 2012). The Earth System Model (ESM) and coupled Atmosphere-Ocean General Circulation Model (AOGCM) simulations of the world's climate are included in CMIP6 (Grose et al. 2020). The IPCC AR6 will heavily rely on the new CMIP6 ensemble to assess processes of climate change and produce revised national climate change projections. The new CMIP6 ensemble will also offer fresh perspectives on the climate systems and climate change relevant to the area. Some GCMs contain climatic processes and earth system aspects that were left out in earlier generations for the CMIP6 projections, which are carried out within a newly developed framework of socioeconomic and emissions pathways (Bouramdane, 2022).

Any advancement in how these models are assessed in comparison to the climate that has been seen may raise confidence in some climate projections. The world is very interested in any future projections that deviate from those in CMIP5 (Hamed et al. 2022). This applies to situations in which there is improved model agreement for confined limits of projected change, or in situations in which projected changes from CMIP6 are beyond the limits of CMIP5 for a certain forcing scenario. A collection of models with stronger climate sensitivity compared to CMIP5 is present in CMIP6, which is a significant new feature (Kaur et al. 2023). Higher climate sensitivity points to the hot model issue in CMIP6 models (Hausfather et al. 2022), and a broader spectrum of warming responses to CO2-forcing and greater model uncertainty in future warming estimates are suggested by higher climate sensitivity.

The IPCC AR6 is based on the CMIP6 program (Zhang et al. 2023). The application of physics-based emulators to guarantee consistency between the sea-level projections and the AR6-assessed Equilibrium Climate Sensitivity (ECS) and Global Surface Air Temperature (GSAT) was the key advancement in AR6 (Slangen et al. 2023). With a very high degree of confidence, the IPCC AR6 asserts that the collection of the CMIP6 model develops the trend of historical global surface temperature and variability that has been observed with anomalies sufficiently small to support the attribution and detection of human-caused warming (Engdaw et al. 2023).

2.4 Future climate projections over South Africa

As with farmers everywhere else, climate change is causing temperatures to rise and more extreme weather throughout Africa (Field, 2012). The fact that Africa's agricultural systems still rely mostly on rain and have few technology inputs makes it particularly vulnerable to climate change. There is unmistakable proof that global average temperatures have risen. These changes started to be noticeable in Africa in 1975, and temperatures have been rising at a pace of roughly 0.03°C each year since then (Hartmann et al. 2013). The majority of the African locations for which statistics are available have shown a rise in the frequency of high heat events as well as prolonged heat waves (Girvetz et al. 2019).

According to Engelbrecht and Monteiro (2021), South Africa will grow drier and warmer in the next 19 years, between 2021 and 2040, at a level of global warming of 1.5°C. Additionally, it is anticipated that southern Africa will become typically drier in scenarios of low-mitigation climate change (Petja et al. 2021). Such changes will limit the area's ability to adapt as it is already known for being dry and warm. (Archer et al. 2018). Southern Africa is going to keep experiencing climate change even with moderate to high mitigation, however, the magnitude of change will be smaller, potentially allowing for greater opportunity for adaptation (Kapuka et al. 2022).

Additionally, climate change is expected to affect the characteristics of extreme weather events as well as shifts in typical temperature and rainfall patterns. The majority of the interior of southern Africa is likely to see generally drier weather and more frequent dry periods (Engelbrecht et al. 2009; Christensen et al. 2007; Haensler et al. 2011). Floods would occur more frequently in northern Mozambique than in the South African province of Limpopo, according to projections for TC tracks (Malherbe et al. 2013). In South Africa, COL-related flood events are projected to occur less frequently as a result of a poleward shift in the westerly wind regime. A generally higher temperature may conceivably result in stronger thunderstorms across South Africa (Engelbrecht et al. 2013). An increase in heat-wave days and high fire-danger days is projected to occur consistently and extremely in their regularity of occurrence. Furthermore, a decrease in the availability of soil moisture is projected, even for areas where increases in rainfall are reasonable, because of improved levels of evaporation (Engelbrecht et al. 2015).

2.5 Impacts, vulnerability, and adaptation to climate change

2.5.1 Impacts of climate change

Southern Africa is particularly susceptible to the negative impacts of climate change, including health concerns (Muyambo et al. 2023). The region has also experienced some of the most intense effects. One of the most obvious and destructive effects of climate change in the area is the rising intensity and frequency of synoptic features that can cause flooding and excessive damage, such as TCs (Salarieh et al. 2023). These occurrences have the potential to relocate a sizable population in addition to causing serious harm to crops, houses, and infrastructure. Injury, infections, and mental health issues are among the health effects of such incidents that can be severe (Parker et al. 2022). Climate change influences the patterns of rainfall and temperature in addition to causing severe weather events, which has a big impact on the security of food and agriculture. Droughts can be caused by changes in patterns of precipitation, which lower the production of food and exacerbate starvation (Agostoni et al. 2023). The spread of vector-borne illnesses such as dengue and malaria fever, which are already major regional public health issues, can potentially be accelerated by increasing temperatures (Beermann et al. 2023).

During the entire 21st century, climate change is projected to increase more and have negative effects (Haile et al. 2020). Climate change has increased the likelihood of severe weather events, such as powerful rainstorms that cause widespread floods worldwide. Due to climate change and other human-caused activities, flooding is projected to rank among the most prevalent disasters in the upcoming years. South Africa is concerned about the potential of flooding, with the provinces of KZN, EC, North West, and Limpopo being the most at risk (Munyai et al. 2021).

The KZN and EC provinces, which saw the worst floods in April 2022, have both been affected by significant flooding. Floods that carried away bridges, homes and other structures caused massive property damage, over 400 fatalities, and almost 50,000 displacements of people in KZN (Durban) (Volgraff and Cele, 2022). In addition to deaths, the EC flood catastrophe led to significant harm to the infrastructure, which had a detrimental effect on the socioeconomic as well as environmental conditions (Dube, 2022). According to Dube et al. (2022b), the rising number of extreme weather events is alarming since they provide complicated difficulties to the socioeconomic growth of communities in these locations, with the most underprivileged and vulnerable individuals suffering the most.

2.5.2 Vulnerability to climate change impacts

South Africa has serious concerns about climate change (Pandy and Rogerson, 2021). During the past 50 years, annual average temperatures have climbed by a minimum of 1.5 times the recorded 0.65°C world average, and the occurrence of severe precipitation events has gone up (Van Der Walt and Fitchett, 2022). The IPCC's Fifth Assessment Report (AR5) for RCP 8.5 projects interior warming of 3-6°C by 2081-2100 relative to 1986-2005, but less certain changes of rainfall concerning magnitude as well as direction (Ziervogel et al. 2014). These changes are projected to keep occurring.

The availability of water, availability of food, well-being, infrastructure, services provided by ecosystems, and biodiversity in South Africa are all seriously threatened by climate change (Moseki et al. 2022). These effects provide significant obstacles to national growth given South Africa's extreme levels of inequality and poverty (Khine and Langkulsen, 2023). Due to rising industrialization and urban island structures, metropolitan areas are more likely to experience temperature rise and heat waves. On the other side, due to a lack of or insufficient infrastructure, such as water storage facilities and construction infrastructure, rural regions may also be more susceptible to droughts and floods. In terms of exposure, sensitivity, and adaptation capability, rural regions in South Africa are significantly more susceptible than metropolitan ones (Zhou et al. 2022).

Due to climate change, natural catastrophes in South Africa such as droughts, floods, and thunderstorms are expected to cause even greater economic and social damages (Ngcamu, 2022). More than 100 disaster incidents were documented between 1900 and 2017, causing 21 million people to be impacted, 2200 deaths, and a total economic loss of about US\$4.5 billion. Fortunately, because of its relative richness and great adaptation ability, South Africa is thought to have among the best resistance to climate change in Africa (Vincent, 2007).

2.5.3 Adaptation

Understanding adaptation to changes in the climate that occur for a long or short-term period is the subject of an expanding body of research both domestically and abroad (Gbetibouo, 2009). Despite this, the majority of adaptation strategies continue to concentrate on lowering susceptibility to current climate exposure, including through early warning systems, catastrophe risk reduction, and controlling water demands (Olorunfemi, 2011).

The results of climate change have piqued the curiosity of both individual farmers and agricultural associations, and the majority have already started adapting to past changes. For example, agriculture businesses in the southern Cape have shifted from crops to pasture and improved their water-storage capacity (David, 2022), while vineyards that can tolerate warmer temperatures have replaced apple orchards in the Western Cape region (Theron et al. 2022).

The availability of food for households is expected to be seriously threatened by climate change's projected considerable negative effects on smallholder subsistence farmers (Rankoana, 2022). Farmers are more likely to increase agricultural output and enhance their standard of living if they respond to climate change by taking a variety of adaptation techniques. Additionally, coping with climate change helps to increase food security for households and farm household welfare as a whole (Shisanya and Mafongoya, 2016). To significantly lessen the effects of climate change, increase the net income of smallholder farmers, and improve farmers' availability of food, adaptation measures including improved variety of crops and early growing crops, livelihood diversification, agrochemical application, watering, as well as reduction of livestock have been shown to be effective (Ogundeji, 2022).

Coordinating efforts are necessary to put into place measures that increase the resiliency of the disadvantaged people in the informal settlements because the danger of flooding is caused by multiple elements cooperating to create catastrophic circumstances, especially in urban areas (Anwana and Owojori, 2023). Southern Africa is the region of Africa most vulnerable to the effects of climate change because of its lack of flexibility and reliance on agriculture. Understanding climate change vulnerabilities and dangers will aid in creating adaptation plans and identifying ways to lower the risk of natural disasters (Eriksen et al. 2021).

2.6 Summary

This chapter has presented a background on the research topic using previous studies that are relevant to climate variability and change in South Africa. Furthermore, it has focussed in detail on the climate of South Africa, climate trends and change in South Africa, climate models and climate modelling, future climate projections over South Africa, and lastly, impacts, vulnerability, and adaptation to climate change. From this review it is evident that South Africa is vulnerable to climate change, most parts of South Africa receive rainfall in summer with the exception of the Western Cape region which receives majority of its rainfall in the winter season, and climate change is projected to rise in the next coming years.

CHAPTER 3: DATA AND METHODOLOGY

3.0 Introduction

This chapter describes how the research on the historical and projected climatic variability and change in eastern South Africa under high and low mitigation was done. The study area, observed data, climate models, model verification, trends analysis, future projections, and instrumentation are main points of emphasis of this chapter. It also explains the datasets and methodologies utilized in this investigation. To gather as much information as possible for the study area's climatic variability and change knowledge, data analysis is crucial (Ncube, 2019).

3.1 Study area



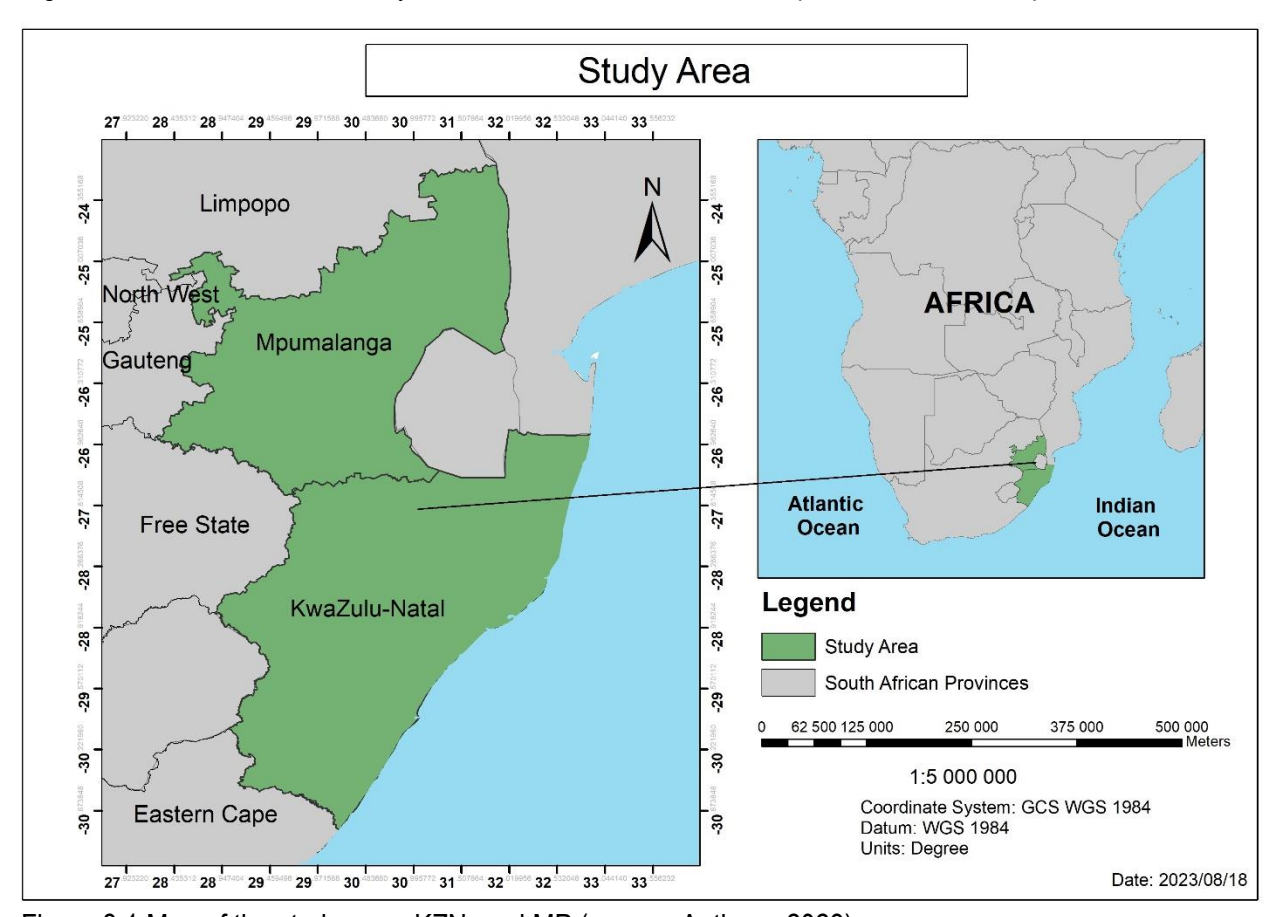


Figure 3.1 Map of the study area, KZN, and MP (source: Authors, 2023).

The research was conducted in the provinces of KZN and MP in South Africa. The study focussed on historical trends (1961-2020) and future climate projections (2021-2099) for these provinces on South Africa's east coast. These two provinces are vulnerable to climate change and they have been affected by floods in the past. Furthermore, climate extremes are expected to increase and intensify over the eastern regions of South Africa (Mashao et al. 2023).

3.2 Observed data

Both observational and climate projection data were collected from Copernicus Climate Change Service (C3S) (Hersbach et al. 2023) which is managed by the European Centre for Medium-Range Weather Forecasts (ECMWF). It consists of all climate data for exploration. The ECMWF provides a detailed record of the world's atmosphere, land surface, and ocean waves from 1950 onwards, whereas C3S gives reliable weather and climate data (Chevuru et al. 2023). The variables that were employed included monthly rainfall, SAT, relative humidity, sea level pressure, winds (eastward and northward), and geopotential heights. Using these variables provided information on how rainfall and temperature evolved in the past. The ERA5 reanalysis was used as an observation (Hersbach et al. 2020).

3.3 Climate models

Climate models project future climate change under different circumstances of GHG emissions (Dessai et al. 2009; Agbor et al. 2023). The CMIP6 models were used to get information on how the climate has changed under different circumstances of GHG emissions. The ECS was used as a guideline to choose correct models that are not over-estimating. The following CMIP6 models in Table 3.1, have a good skill, are the latest established CMIP models, they perform best, and have been used before in similar studies (such as Singo et al. 2023; Mauritsen et al. 2019; Boucher et al. 2020). In terms of yearly SST, models from the CMIP6 have a much reduced global-mean absolute bias than those from CMIP5 (Zhang et al., 2023).

Table 3.1 The CMIP6 models used for projected future climate change study

Models	Resolution (lat. × long.)	Institution, country	Source
Australian Community	1.25° × 1.875°	Commonwealth	(Liu et al. 2023)
Climate and Earth		Scientific and Industrial	
System Simulator		Research	

Coupled Model version		Organisation (CSIRO-	
2 (ACCESS-CM2)		BOM), Australia	
Institut Pierre Simon	1.26° × 2.5°	IPSL, France	(Boucher et al. 2020)
Laplace Climate Model			
Low-Resolution			
version 6A (IPSL-			
CM6A-LR)			
Beijing Climate Center	1.125° × 1.125°	Beijing Climate Center	(Guo et al. 2022)
Climate System Model		China Meteorological	
Medium Resolution		Administration, China	
version 2 (BCC-CSM2-			
MR)			
Geophysical Fluid	1° × 1.3°	National Oceanic and	(Zhang et al. 2023)
Dynamics Laboratory		Atmospheric	,
Earth System		Administration,	
Model version 4		Geophysical Fluid	
(GFDL-ESM4)		Dynamics Laboratory	
		(NOAA GFDL), USA	
Alfred Wegener	0.9° × 0.9°	AWI, Helmholtz Centre	(Semmler et al. 2020)
Institute Climate Model		for Polar and Marine	
Medium Resolution		Research, Germany	
version 1.1 (AWI-CM-			
1-1-MR)			
Max Planck Institute	1.9° × 1.9°	Max Planck Institute for	(Mauritsen et al. 2019)
Earth System Model,		Meteorology, Germany	
Low-Resolution			
version 1.2 (MPI-ESM			
1.2-LR)			

3.3.1 ACCESS-CM2

ACCESS-CM2 is part of the contributions of Australia to the CMIP6. Moreover, ACCESS-CM2 has been designed for many applications and research related to climate modelling (Bi et al. 2020). The Climate Science Center of CSIRO Oceans and Atmosphere has created ACCESS-CM2 to be a fully coupled climate model (Bi et al. 2022). Even while ACCESS-CM2 has made several important advancements over its predecessor, the Australian Community Climate and Earth System Simulator version 1.3 (ACCESS 1.3) (Bi et al. 2013), which took part in CMIP5, there are still some shortcomings in the simulated climate.

3.3.2 IPSL-CM6A-LR

IPSL-CM6A-LR climate model was developed at IPSL and in CMIP5 it is referred to as IPSL-CM5A-LR (version 5A). The IPSL-CM6A-LR consists of the LMDZ (Laboratoire de Métérologie Dynamique Zoom) atmospheric model version 6A-LR (Hourdin et al. 2020), the ORCHIDEE (Organising Carbon and Hydrology In Dynamic Ecosystems) land surface model version 2.0, and the Nucleus for European Models of the Ocean (NEMO) oceanic model Version 3.6. According to Boucher et al. (2020), the climatology of the model is significantly better than that of its previous versions based on a variety of indicators (especially those pertaining to temperature, precipitation, wind, and radiation). Several well-known biases and flaws (such as the double ITCZ, and ENSO dynamics) still exist, despite their reduction. IPSL-CM6A-LR model compared to IPSL-CM5A-LR employed in CMIP5, the ECS, and transient climate responsiveness have both increased (Mignot et al. 2021).

3.3.3 BCC-CSM2-MR

One of the models produced by BCC operating in CMIP6 is the BCC-CSM2-MR model (Xin, 2019). The Beijing Climate Center Atmospheric General Circulation Model (BCC-AGCM) serves as the foundation for the atmospheric component of BCC-CSM2-MR. According to Lu et al. (2021), the horizontal resolution of the atmospheric component in BCC-CSM2-MR is about 1.125° longitude by 1.125° latitude, and it has forty-six hybrid vertical levels. Tropical atmospheric variability simulations, such as the Madden-Julian Oscillation (MJO) and the stratospheric quasi-biennial oscillation, have been significantly improved by BCC-CSM2-MR than its precursor in CMIP5 (Wu et al. 2019).

3.3.4 GFDL-ESM4

The GFDL-ESM4 is the fourth generation of GFDL and is constructed using the same foundation as GFDL's atmosphere model version 4 (AM4.0) and Modular Ocean Model version 6 (MOM6) (Zhang et al. 2023). However, it places more emphasis on chemistry and ecosystem comprehensiveness, with a reduced horizontal resolution (about 0.5°) for the ocean model and a higher amount of chemistry prognostic tracers, increased vertical levels (49), a higher top and more vertical resolution of the stratosphere, and increased sophisticated ocean and land biogeochemical models (Stock et al. 2020). ESM4 has a transient climate sensitivity of 1.6 K and an ECS of 3.2 K (Dunne et al. 2020).

3.3.5 AWI-CM-1-1-MR

For the first time, the AWI-CM takes part in the CMIP6 (Semmler et al. 2020). The average warming anticipated by climate models in the preceding intercomparison project (CMIP5) is comparable to the expected global warming in AWI-CM. According to Danilov et al. (2004), the AWI-CM has a sea ice-ocean component called Finite Element Sea Ice-Ocean Model (FESOM). A medium resolution "MR" mesh that adheres to the mesh design approach is used to run the FESOM model (Semmler et al. 2019).

3.3.6 MPI-ESM 1.2-LR

The MPI-ESM1.2 is the most recent version of the MPI-ESM, serving as the basis for the CMIP6 and ongoing projections that focus on seasonal as well as decadal climate, and the MPI-ESM1.2-LR is the lower-resolution version (Azran et al. 2023). As scientists increasingly switch to employing the most recent modelling system, the release of the MPI-ESM1.2 model seeks to meet the institutions' objectives for scientific modelling in the next years. According to Martinez and Iglesias (2023), MPI-ESM1.2 will be employed in the current CMIP6 operations as well as other model intercomparison studies.

3.4 Model verification

CMIP6 models' performance was verified using statistical approaches (Engelbrecht et al. 2015) and visual verification. To evaluate the strengths and limitations of the models modelling precipitation, a Taylor diagram was employed. According to their correlation, root-mean-square difference, and the ratio of their variances, patterns can be compared statistically to one another using a Taylor diagram (Taylor, 2001). The performance of these models was verified to evaluate how well they simulate the observed climate.

3.4.1 Visual verification

Visual verification is also referred to as eyeball verification and is used to assess how well climate models have performed over time (Ebert, 2001; Kumar and Sarthi, 2019). In terms of spatial verification, the eyeball approach continues to be the most popular (Ouma et al. 2022). To identify the projection errors through comparison, one may use this approach to compare the projection and the ERA5 observations side by side. Whilst the outcome is not quantitative and the interpretation might be subjective, the eyeball approach occasionally provides a good picture of the variable under investigation (Mahlobo, 2013).

3.4.2 Statistical verification

The strength of the association between a group of models and data is summarized in a two-dimensional (2-D) graph known as a Taylor diagram (Taylor, 2001; Taylor, 2005). It is used to assess how well models and ERA5 observations match each other (Zhou et al. 2021). The Taylor diagram comprises the following:

3.4.2.1 Root Mean Square Error (RMSE)

The RMSE is the square root of the mean squared error (MSE). According to Yan et al. (2023), the MSE indicates the standard deviation of the variations between expected and actual values. It demonstrates how crowded the data are in the vicinity of the line of best fit. To verify the validity of experimental findings, RMSE is frequently employed in climatology, regression analysis, and projection (Fouotsa Manfouo et al. 2023).

$$RMSE = \sqrt{\frac{1}{n} \sum_{j=1}^{n} (y_j - \hat{y}_j)^2}$$
 Equation 3.1.

In equation 3.1 above, y_i is the actual value for the ith observation, \hat{y}_i is the predicted value for the ith observation, and n is the number of observations.

3.4.2.2 Correlation coefficient (r)

According to Ali and Medhat (2021), the correlation coefficient (r) is a statistical metric that determines the strength of the link between two variables that are linearly associated. Correlation coefficient values vary between -1.0 to 1.0 (Fu et al. 2020). However, if a computed value is more than the 1.0 and -1.0 thresholds, there is a measurement error in the correlation (Li et al. 2022).

$$r = \frac{n(\sum xy) - (\sum x)(\sum y)}{[n\sum x^2 - (\sum x)^2][n\sum y^2 - (\sum y)^2]}$$

Equation 3.2

In the equation above n is the number of values, $\sum x$ is the sum of the first values list, $\sum y$ is the sum of the second values list, $\sum xy$ is the sum of the product of the first and second values, $\sum x^2$ is the sum of squares of first values and $\sum y^2$ sum of squares of second values.

3.4.2.3 Standard deviation (δ)

It is customary to give the standard deviation for a mean, which is a measure of variability or dispersion. Variability refers to how widely the individual recorded scores or values that are observed vary from each other (Vetter, 2017). Furthermore, the variance's square root is used to determine the standard deviation (Budhidarma, 2023). It is determined as the square root of variance by calculating the variance between each point of data in relation to the mean (Baker et al. 2021). The standard deviation, which measures how widely distributed the data are, is determined by the distance between a point's data value and the mean (Chimoto et al. 2023).

$$s = \sqrt{\frac{(x_i - \bar{x})^2}{n-1}}$$
 Equation 3.3.

In equation 3.3 above, x_i is the value of observed data, \bar{x} is the mean value of the data set and n is the number of data points in the data set.

3.5 Trends analysis

According to Longobardi and Villani (2010), a trend is a change that occurs over time displayed by a random variable, and it can be detected by parametric and non-parametric procedures. Trends tests were done on the historical record based on ERA5 reanalysis from 1961 to 2020. Mann Kendall trend test was used for trends in temperature (Gadedjisso-Tossou et al. 2021) and the RClimDex for trends in heavy rainfall (Wang and Zhao, 2022). The Mann-Kendall test examines the direction of the difference between data that were measured earlier and later. RClimDex is an R-based tool that calculates precipitation and temperature indices

(Sohrabi et al. 2009; Zhang and Yang, 2004). Furthermore, it is available for free on the Expert Team on Climate Change Detection Indice (ETCCDI) website (Chikoore et al. 2024). RClimDex was used to calculate trends of the selected indices of key variables of the study. TX10P and TX90P are temperature indices and they represent cool and hot days, respectively (Mbokodo et al. 2023). Furthermore, R10mm, R20mm, and R50mm are rainfall indices and they represent heavy rainfall days, very heavy rainfall days, and frequency of rainfall exceeding 50 mm/day, respectively (Sohrabi et al. 2009; Tangang et al. 2018).

3.6 Future projections

When focussing on climate projections, two scenarios were used, and this study employed SSP5-8.5 (worst-case low mitigation scenario) and SSP2-4.5 (medium challenge to mitigation and adaptation) (Siabi et al. 2023). These two scenarios had to be used because the future climate change was not known and to provide future projections together with the CMIP6 models. Southern Africa is going to keep experiencing climate change even with moderate to high mitigation, however, the magnitude of change will be smaller, potentially allowing for greater opportunity for adaptation (Mertz et al. 2009). The focus was on the projections of each model (from the 6 models) under the above-mentioned scenarios and the second step was to ensemble those 6 models together to be an ensemble. The study also focussed on seasonal changes in SAT and rainfall under SSP2-4.5 and SSP5-8.5 which were made by subtracting reference climate (1961-1990) from the future periods (2021-2099). The future projections were divided into near-future (2021-2050) and far-future (2070-2090) periods. Temperature change, rainfall change, and extremes (floods) were the primary variables.

3.7 Data Display

3.7.1 Grid Analysis and Display System (GrADS)

GrADS is an interactive desktop interface that accesses, modifies and visualises Earth science data (Matthews et al. 2008). GrADS provides two data models for managing gridded and station data (Kumari et al. 2015). According to Bhadauriya (2018), GrADS is compatible with a wide range of data file formats, namely, GRIB (versions 1 and 2), binary (stream or sequential), NetCDF, BUFR (for station data), and HDF (versions 4 and 5). GrADS is freely accessible online and has been used on a number of widely used operating systems worldwide. By inputting FORTRAN-like expressions at the command line, operations are carried out interactively (Ravi, 2018). GrADS, which is designed for meteorological fields, may compute multi-dimensional data through predetermined dimension ranges, although multi-dimensional array operation

features are not provided (Wang, 2019). Scatter plots, line and bar graphs, wind vectors, streamlines, grid boxes, shaded grid boxes, smoothed and shaded contours, and station model plots are some of the graphics used by GrADS to present data. These graphics are stored in PostScript or image formats (Naher, 2016).

3.7.2 Climate Data Operator (CDO)

The CDO is a group of command line tools that were first created to process and analyse data generated by various projection models for climate and numerical weather. The operators include basic mathematical and statistical operations, tools for choosing and sampling subsets of data, and spatial interpolation (Wada et al. 2023). Therefore, supported file formats include several binary formats and widely used output formats from models such as GRIB and NetCDF. According to Kaspar et al. (2010), some of the key CDO characteristics are the availability of over 400 operators, a modular design, and a fairly straightforward UNIX command line interface.

3.7.3 R and R Studio

R is a no-cost, open-source program that lets users create and run data analysis programs. Furthermore, the term "open source" describes a type of software whose source code is made publicly accessible and is typically amenable to suggestions for enhancements or brand-new features created by other parties (Hair Jr et al. 2021). It is utilized for statistical analysis, data processing, and data visualization. R has conditional statements, recursive functions, and input/output instructions much like any other programming language (Krotov, 2017). R Studio is an Integrated Development Environment (IDE) and was thoughtfully designed to anticipate the demands of R users who may progress beyond merely using R for their study and may like to advance to Sweave/TEX/LATEX out of concerns about reproducibility (Racine, 2012).

3.8 Summary

This chapter has shown the process that was followed in completing the research for the aim, and objectives to be achieved. It has presented the study operationalization, observed data, CMIP6 models that were used for this study, methods that were used to verify the models, trends analysis, future projections, and instrumentation. The 1961-2020 period was used as a historical baseline of the study and six CMIP6 models provided climate projections for the near-future (2021-2050) and far-future (2070-2099) periods. The CMIP6 models and SSPs were significant for future projections of climate change over the KZN and MP.

CHAPTER 4: HISTORICAL TRENDS AND MODEL VERIFICATION

4.0 Introduction

It is essential to verify a model against observation to ascertain its accuracy and bias before employing it to project the future (Ncube, 2019). This is the first result chapter. It focuses on analysing the historical trends of SAT and rainfall characteristics during the present day (1961-2020), and model verification using statistical and visual verification. In addition, Taylor diagrams were employed as part of the statistical verification. The performance of the models was verified to evaluate how well they simulate the observed climate. Temperature and rainfall are the main variables of focus in this study and the following seasonal projections were taken into account: December-January-February (DJF), June-July-August (JJA), March-April-May (MAM), and SON.

4.1 Historical trends

Table 4.1 The indices used for SAT and rainfall in Kruger Mpumalanga International Airport and Durban

	Kruger Mpumalanga International Airport Durban				
INDEX	P-value	Slope		P-value	Slope
TX10P	0,053		-0,053	(0 -0,132
TX90P	0,001		0,137	(0,097
R10mm	0,57	,	-0,029	0,624	4 -0,023
R50mm	0,965	<u> </u>	0	0,523	3 0,006

This study examines the long-term trends in temperature and rainfall indices at two locations: Kruger Mpumalanga International Airport and Durban. The indices analysed include TX10P (cool days), TX90P (hot days), R10mm (days with heavy rainfall), and R50mm (frequency of rainfall exceeding 50mm/day). The period of analysis spans from 1961 to 2020.

4.1.1 Trends in SAT

The different trends of the cool days' indices (TX10P) in Kruger Mpumalanga International Airport and Durban for the period 1961-2020 are shown in Figure 4.1 and Figure 4.2. Furthermore, the hot days' indices (TX90P) are shown in Figure 4.3 and Figure 4.4 below. The cool days' index in Figure 4.1 shows that the highest peak

of cool days in Kruger Mpumalanga International Airport occurred for 29 days in 1968. This may suggest that the east side of MP was affected by a low temperature event that prolonged for few weeks. Some plants do not survive during their growing stage in cold weather that prolongs for many days (Moeletsi et al. 2016) and that may suggest that agriculture might have been affected during this period due to low temperatures on the east side of MP. The second highest peak of cool days in Kruger Mpumalanga International Airport took place in 1996 for at least 19 days. In 1979 and 1981, cool days were recorded for over 15 days, and 14 days in 1975, at the airport in MP.

Figure 4.1 also shows low peaks of cool days experienced at the Kruger Mpumalanga International Airport. According to the cool days' index, in 1962 Kruger Mpumalanga International Airport experienced the lowest peak of cool days which occurred only 5 days during the 1961-2020 period. Furthermore, the other fewer cool days occurred in 1961, 1965, 1992, and 2015 for 5 to 10 days. Table 4.1 shows the p-value (0,053) for the cool days' index in Kruger Mpumalanga International Airport which indicates a trend that is not statistically significant at the 5% level. The slope value (-0,053) suggests a slight decrease in the number of cool days over a period. According to the study done by Kruger and Sekele (2013), on extreme temperature indices during 1962-2009, the daily maximum and minimum trends in the stations in the northeast and east of South Africa show an increase and decrease in the warm and cold extremes respectively, compared to other regions in the country.

The cool days' index in Figure 4.2 shows that Durban also experienced its highest peak of cool days in 1968, however, for more than 35 days which are more days compared to the cool days experienced in the Kruger Mpumalanga International Airport. According to these results, Kruger Mpumalanga International Airport and Durban experienced more cool days during the same year. Cold wave trends in 1960 to 2016 were observed increasing for stations in the provinces of KZN, Eastern Cape, Gauteng and Northern Cape at a speed of 0,01 events/day⁻¹ (van Der Walt and Fitchett, 2021). In 1973 and 1996, Durban had its second-highest peak of cool days for at least 15 days, and in 1971 and 1990 experienced cool days for 14 days. According to a study conducted by Van der Walt (2020) on extreme temperature events reports that cold events in KZN led to 30 casualties on 6 July 1996. This shows how cold weather conditions can be detrimental.

Durban experienced the lowest peak of cool days throughout the 1961-2020 period in 1999 and 2014, which lasted for 5 days. Furthermore, as the cool days' index indicates in Figure 4.2, Durban also experienced fewer cool days in 1961, 1985, 1994, 2005, and 2010 for days ranging between 5 to 10. According to Van

der Walt (2020), a cold event linked with snowstorms persisted for at least 10 days and led to the death of people, and livestock and damage to infrastructure in KZN on 22 July 2002. The p-value (0) of the cool days' index in Durban is statistically significant, however, the negative slope value (-0,132) suggests a decrease in the cool days in Durban during the 1961-2020 period and this is also shown by the red dotted declining line in Figure 4.2. The trends in the daily temperature study for the 1960-2003 period in South Africa showed Durban with significant decreases in the diurnal range (Kruger and Shongwe, 2004).

The hot days' index in Kruger Mpumalanga International Airport for the 1961-2020 period is presented in Figure 4.3. Furthermore, at this airport in MP, the highest number of hot days occurred for more than 25 days during the historical baseline of the study in 1992 and 2015. Heat waves occurred in South Africa starting on 7 November 2015 and prevailed over the provinces of MP, Gauteng, North West, and Limpopo (Blunden and Arndt, 2016). Furthermore, according to McBride et al. (2022b), 2015 was one of the hottest years that have ever been experienced in South Africa. The hot days' index in Kruger Mpumalanga International Airport shows several high peaks of hot days, implying that Mbombela is prone to high temperatures. As much as some plants do not survive during cold weather that occurs for a long time, they also struggle to survive during hot days that prolong for many days (Van der Walt, 2020). Hot days were recorded at the airport in MP for more than 20 days in 1970 and between 2018 and 2019, as shown in Figure 4.3. Lastly, some of the years whereby hot days were experienced for over 15 days at Kruger Mpumalanga International Airport were 1962, 1983, and between 2002 and 2003.

The least number of hot days experienced in Kruger Mpumalanga International Airport was less than 5 days in several years, however, 1967 and 2000 were the years with the lesser number of hot days compared to other years. Some of the years in which less than 5 hot days were experienced at the airport included 1974/75, 1978, and 1984. Table 4.1 presents the p-value (0,001) which shows a statistically significant trend and a positive slope value (0,137) that suggests an increase in the number of hot days in Kruger Mpumalanga International Airport. The red dotted line in Figure 4.3 also shows that the hot days increase as the years go by.

The climate in the eastern coastal areas of South Africa is warm and humid due to the warm Agulhas Current (Landman et al. 2017). The hot days' index presented in Figure 4.4 shows a lower number of high peaks of hot days in Durban compared to the higher number of high peaks of hot days in Kruger Mpumalanga International Airport. This suggests that Durban during the 1961-2020 period did not experience hot

conditions like Kruger Mpumalanga International Airport. Meque et al. (2022), report that the interior of South Africa received frequent heatwaves, and the coastal areas of South Africa received less frequency of heatwave events during the summer season from 1981 to 2018. The highest peak of hot days occurred for more than 20 days in Durban between 1991 and 1992. Furthermore, some of the events of high peaks of hot days that occurred at least 15 days and above were recorded in 2010, 2014, and 2016. According to Mbokodo et al. (2023), the high temperatures and heatwave events that occurred in 2015/16 led to the most intense drought in South Africa.

According to the hot days' index in Durban, the least hot days range between 0 to 5 days followed by 5 to 10 days, as shown in Figure 4.4. In 1968 and 1975 Durban experienced less than 5 hot days. Some hot days ranging from 5 to 10 days were recorded in 1984, 1990, 2000, and 2011. The p-value is 0, indicating a statistically significant trend. The slope is 0,097, indicating an increase in the number of warm days.

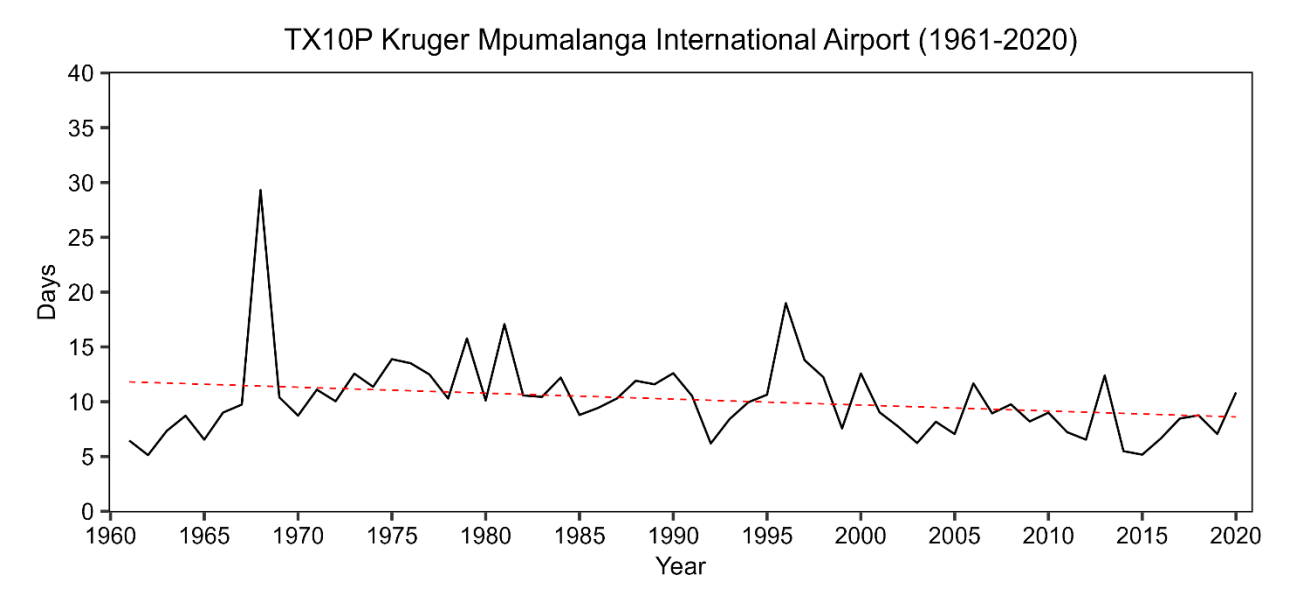


Figure 4.1 This figure shows the cool days' index (TX10P) in Kruger Mpumalanga International Airport for the period 1961-2020. The trend line indicates a significant decrease in the number of cool days over this period.

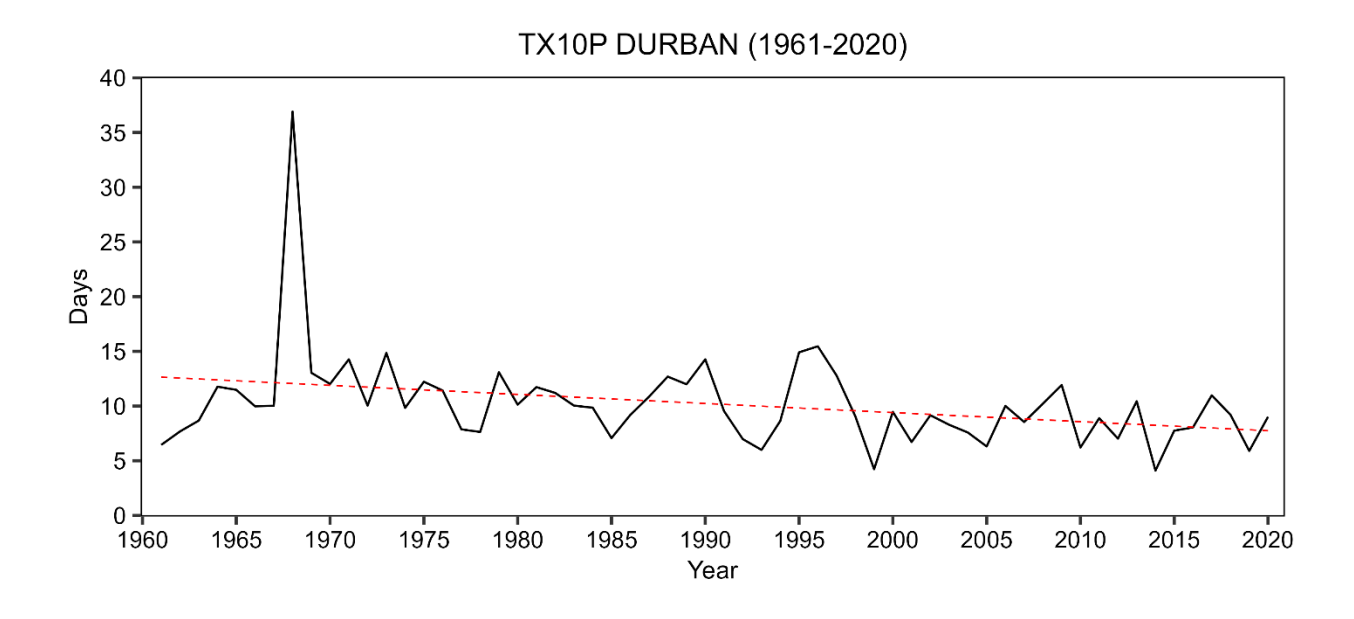


Figure 4.2 This figure shows the cool days' index (TX10P) in Durban for the period 1961-2020. The trend line indicates a significant decrease in the number of cool days over this period.

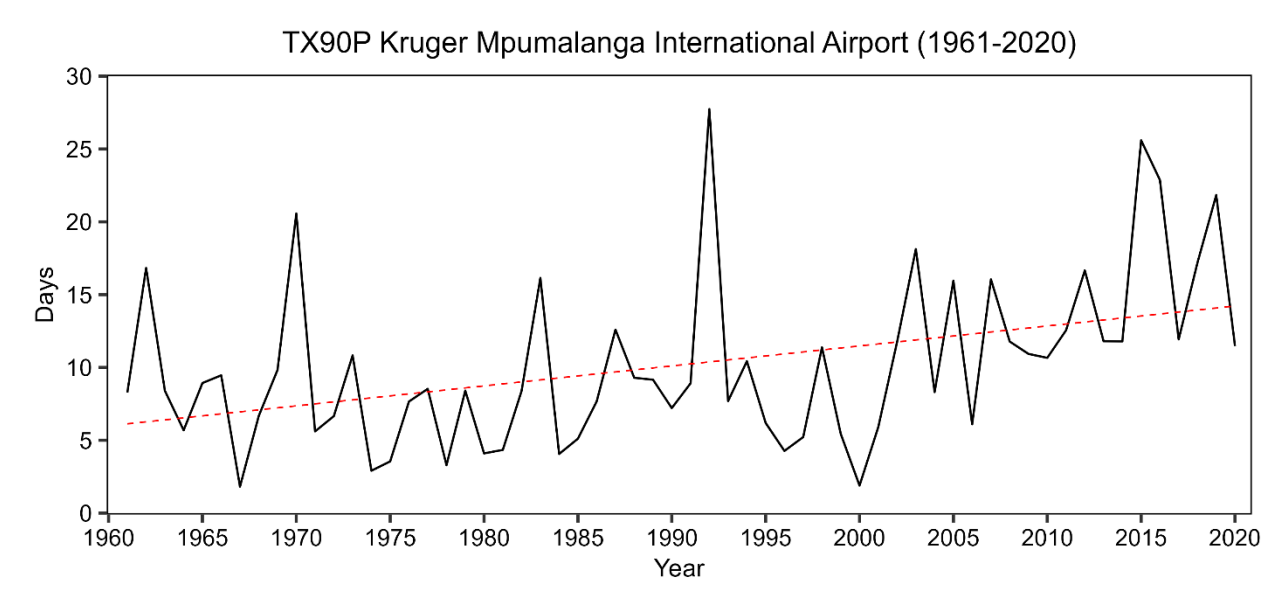


Figure 4.3 This figure shows the hot days' index (TX90P) in Kruger Mpumalanga International Airport for the period 1961-2020. The trend line indicates a significant increase in the number of hot days over this period.

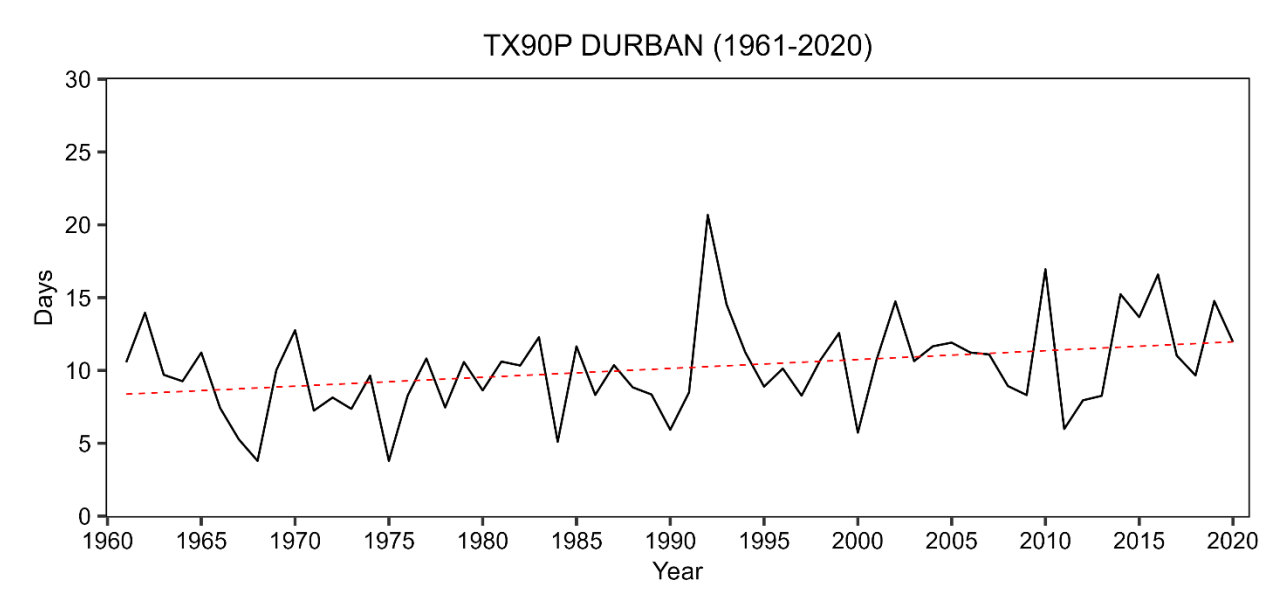


Figure 4.4 This figure shows the hot days' index (TX90P) in Durban for the period 1961-2020. The trend line indicates a significant increase in the number of hot days over this period.

4.1.2 Trends in rainfall

The different trends of the heavy rainfall indices (R10mm) in Kruger Mpumalanga International Airport and Durban for the period 1961-2020 are shown in Figure 4.5 and Figure 4.6. Furthermore, the frequency of rainfall exceeding 50mm/day indices (R50mm) are shown in Figure 4.7 and Figure 4.8 below. The two locations mentioned above in eastern South Africa experienced heavy rainfall days differently according to the indices below. The heavy rainfall index in Kruger Mpumalanga International Airport shows the highest peak in heavy rainfall in 2000, which occurred for over 40 days and led to floods. Furthermore, this may also suggest that areas surrounding the airport may have been affected by the heavy rainfall that took place for over a month in 2000. In February 2000, northeastern South Africa, Mozambique, and Zimbabwe experienced heavy rainfall due to TC Eline that led to the death of people and damage to infrastructure which hindered the development of agriculture and the economy of the region (Dyson, 2000; Dyson and Van Heerden, 2001). The airport in MP received heavy rainfall that occurred over 30 days between 1966 and 1967, and it also received heavy rainfall for at least 35 days in 1975 and between 1977 and 1978. This suggests that northeastern South Africa has been affected by floods during the reference climate and in the recent past of the study. Furthermore, heavy rainfall occurred for over 30 days in 2004, 2006, and 2010. The last event of heavy rainfall days according to Figure 4.5 occurred between 2017 and 2018.

The results show that heavy rainfall was experienced at Kruger Mpumalanga International Airport and the high peaks in rainfall that occurred for at least 30 days are mentioned above. The heavy rainfall index (Figure 4.5) also indicates the years where heavy rainfall took fewer days at the airport during the 1961-2020 period, which is the historical baseline of the study. In this historical baseline of the study, the fewer days whereby heavy rainfall was experienced at the airport in MP, occurred between 10 to 15 days. Moreover, the years in which heavy rainfall took place for fewer days included 1965, from 1982 to 1983, between 1992 and 1993, 2003 and 2004, and from 2015 to 2016, as shown in Figure 4.5. These results suggest that droughts may have occurred in MP where the airport is located because of fewer days of heavy rainfall experienced. According to Table 4.1 above, the p-value is 0,57 for R10mm, indicating no statistically significant trend and the value of the slope (-0,029) suggests a slight decrease in the number of heavy rainfall days at the airport in MP. According to Makungo and Mashinye (2022), rainfall trends in some regions in the northeast of South Africa showed a decrease in rainfall for the 1921-2015 period study.

Figure 4.6 shows the heavy rainfall index in Durban for the 1961-2020 period, and according to this index, the highest heavy rainfall event was experienced in 1986 in Durban for at least 40 days. Durban is located on South Africa's east coast and it is vulnerable to heavy rainfall that leads to floods and negative impacts on the socio-economic development and infrastructures of KZN (Singh et al. 2022). According to R10mm, the second highest peak of heavy rainfall days occurred in Durban and Kruger Mpumalanga International Airport for over 35 days in 1975. Moreover, high heavy rainfall days were also recorded between 1996 and 1997, from 1999 to 2000, 2006, and 2011, and the last heavy rainfall days were recorded between 2016 and 2017, as shown in Figure 4.6 below. These heavy rainfall days recorded in Durban took 35 days and above. In Durban, seven people died and thousands were displaced by extreme rainfall that led to floods and storm surges in July 2016 (Olanrewaju and Reddy, 2022).

Compared to Kruger Mpumalanga International Airport, Durban has more recorded heavy rainfall days throughout the 1961-2020 period of the study, as shown in Figure 4.6. Furthermore, the fewer heavy rainfall days in Durban range between 15 to 20 days, meaning that Durban has experienced more of the fewer heavy rainfall days compared to the airport. The years where heavy rainfall days were fewer, include 1980, between 1982 and 1983, 1991 and 1992, and lastly in 2010 and 2014. These are the years where Durban received less rainfall because of the less heavy rainfall days experienced. Furthermore, these few days of heavy rainfall may suggest that drought may have been experienced during the above-mentioned years because of the below-average rainfall days. The value of p is 0,624, indicating no statistically significant trend and the slope value is -0,023, suggesting a slight decrease in the number of heavy rainfall days. The red dotted line in Figure 4.6 is decreasing as the years go up suggesting that the heavy rainfall days are also decreasing as well.

The index representing rainfall exceeding 50mm/day in Kruger Mpumalanga International Airport for the 1961-2020 period is shown in Figure 4.7. This index shows that the airport received rainfall exceeding at least 50mm/day for more than 4 days in 2000, which is the highest peak of the rainfall days in the historical baseline of the study. The northeast of South Africa was affected by high peaks of rainfall in 1996, 2000, and 2012 which are linked to TCs Bonita, Eline, and Dando (Chikoore et al. 2021; McBride et al. 2022a). The second-highest peak of rainfall days exceeding 50mm/day took place between 1973 and 1974 for at least 3 days. Furthermore, this second-highest event of rainfall days was followed by at least 2 days of rainfall exceeding 50mm/day between 1983 and 1984, 2003 and 2004, and 2013. During the above-mentioned

years, the Kruger Mpumalanga International Airport and its surrounding areas may have been subjected to floods because of the rainfall exceeding 50mm/day they experienced.

The index (R50mm) in Figure 4.7 indicates that Kruger Mpumalanga International Airport has experienced several periods of droughts in the past because of below-average rainfall days. Figure 4.7 shows 0 days of rainfall exceeding 50mm/day from 1961 to 1963, 1965 to 1968, 1970 to 1971, 1976 to 1980, and in 1990, 2010, and 2015. The MP province was one of the provinces that were declared drought disaster areas in November 2015 (Blunden and Arndt, 2016). The p-value (0,965) for the R50mm in Kruger Mpumalanga International Airport shows no statistically significant trend. The value of the slope (0) is neutral suggesting no change in the number of rainfall exceeding 50mm/day throughout the 1961-2020 period.

The frequency of rainfall exceeding 50mm/day index in Durban for the 1961-2020 period is presented in Figure 4.8. Durban had rainfall exceeding 50mm/day for more than 3 days in 1985, 1987, and 1989, and during these years it was only when Durban experienced the highest peak of days of rainfall exceeding 50mm/day. A study conducted by Molekwa (2013), reports that the coastal areas of KZN were affected by severe floods caused by a COL in September 1987. Therefore, this suggests that Durban was also affected by the COL during the spring season in 1987 because it is located on the coast of KZN. Rainfall exceeding 50mm/day that occurred for at least 3 days in Durban, was between 1970 and 1971, from 1995 to 1996, between 2012 and 2013, and in 2017. On 12-14 February 1996, heavy rainfall exceeding 150 mm for 3 days fell over the northeast of South Africa, and Durban was one of the places that were affected by the floods that resulted from the heavy rainfall (De Coning et al. 1998). Durban is shown in Figure 4.8 to have more highest peaks of days of rainfall exceeding 50mm/day compared to Kruger Mpumalanga International Airport and therefore this suggests that Durban received more rainfall exceeding 50mm/day than the airport during the 1961-2020 period.

As much as Durban has many high peaks of rainfall days, it also has many periods whereby it did not experience rainfall days exceeding 50mm/day. Furthermore, some of those years were 1961, 1963, 1974, 1992, 2005, and 2010, and the most recent year according to the historical baseline of the study was 2015. According to Ibebuchi (2021), in 1992 during late summer a significant rainfall deficit occurred in the eastern and northeastern regions of South Africa as a result of El Niño. The strongest and worst drought to ever occur in South Africa since 1921 took place during the summer season in 2015/16 in KZN (Monyela, 2017). The p-value (0,523) for the R50mm index in Durban shows no statistically significant trend (Table 4.1), and the

slope value (0,006) suggests a negligible increase in the number of days of rainfall exceeding 50mm/day (Figure 4.8).

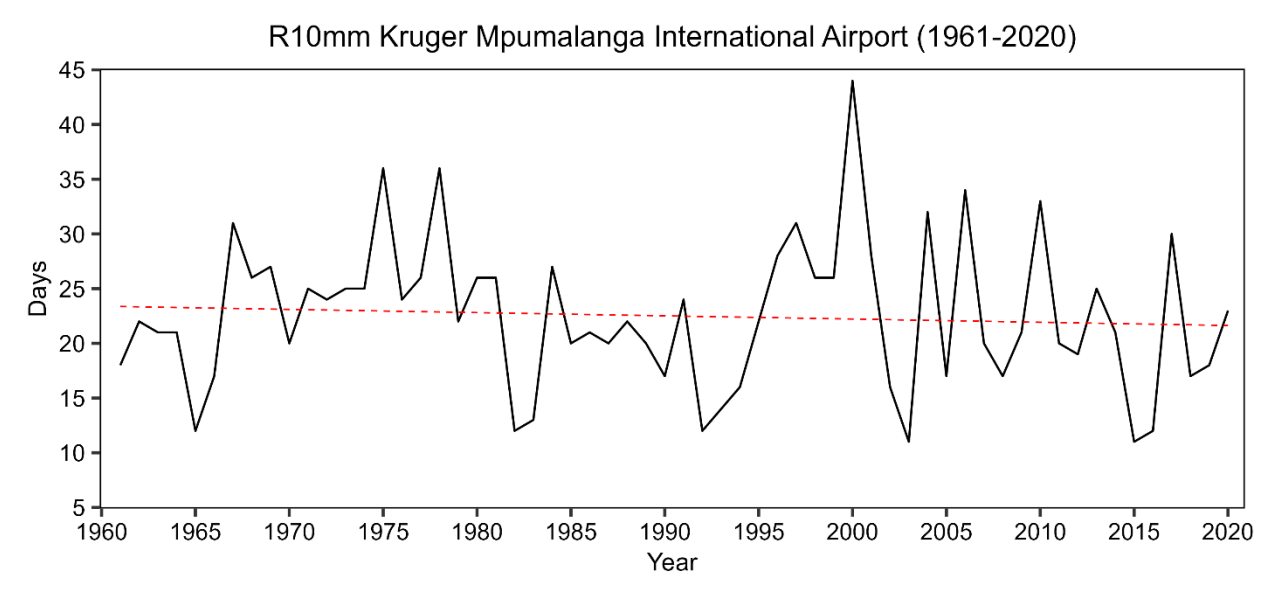


Figure 4.5 This figure shows the heavy rainfall days' index (R10mm) in Kruger Mpumalanga International Airport for the period 1961-2020. The trend line indicates a slight decrease in the number of heavy rainfall days over this period.

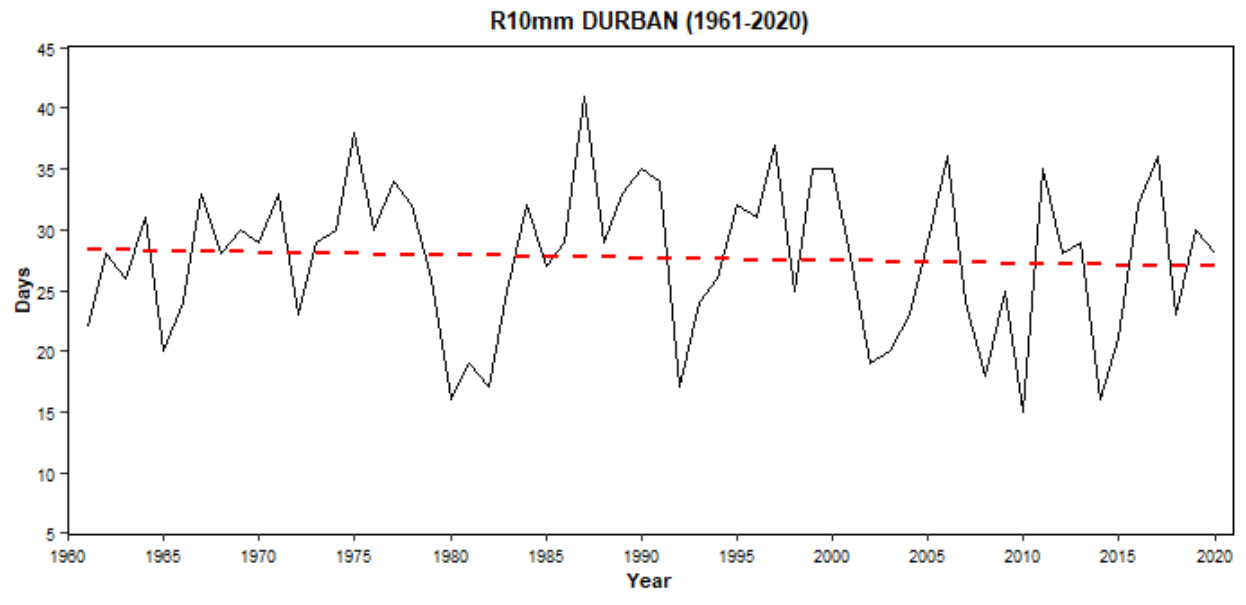


Figure 4.6 This figure shows the heavy rainfall days' index (R10mm) in Durban for the period 1961-2020. The trend line indicates a slight decrease in the number of heavy rainfall days over this period.

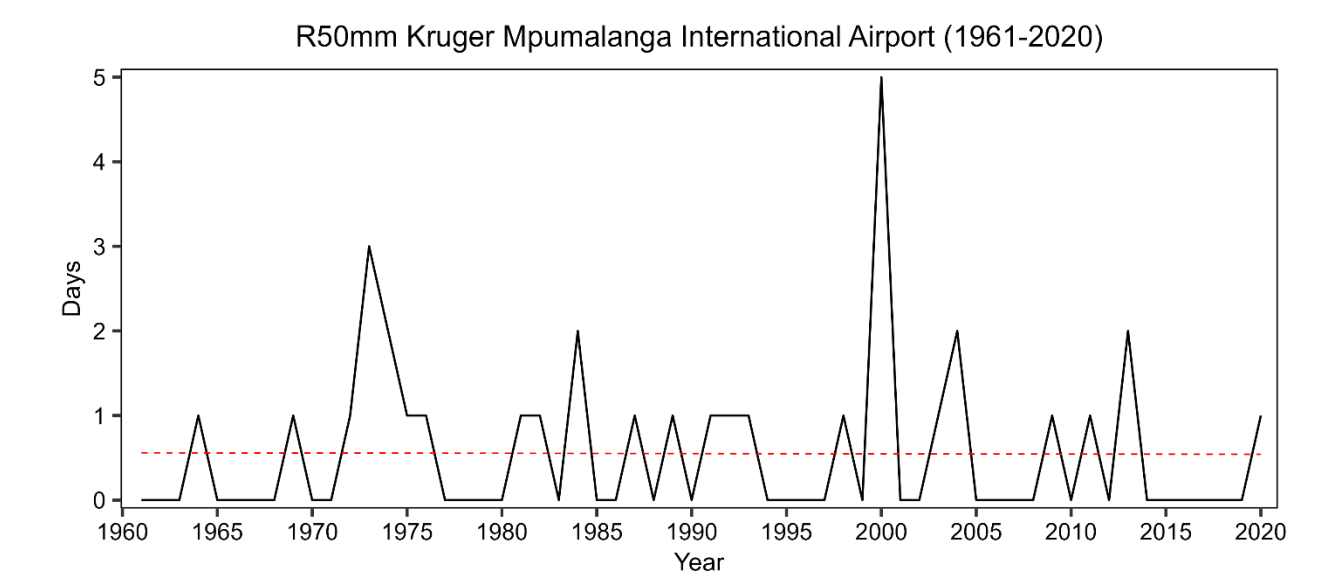


Figure 4.7 This figure shows the frequency of rainfall exceeding 50mm/day index (R50mm) in Kruger Mpumalanga International Airport for the period 1961-2020. The trend line indicates no change in the frequency of rainfall days exceeding 50mm/day over this period.

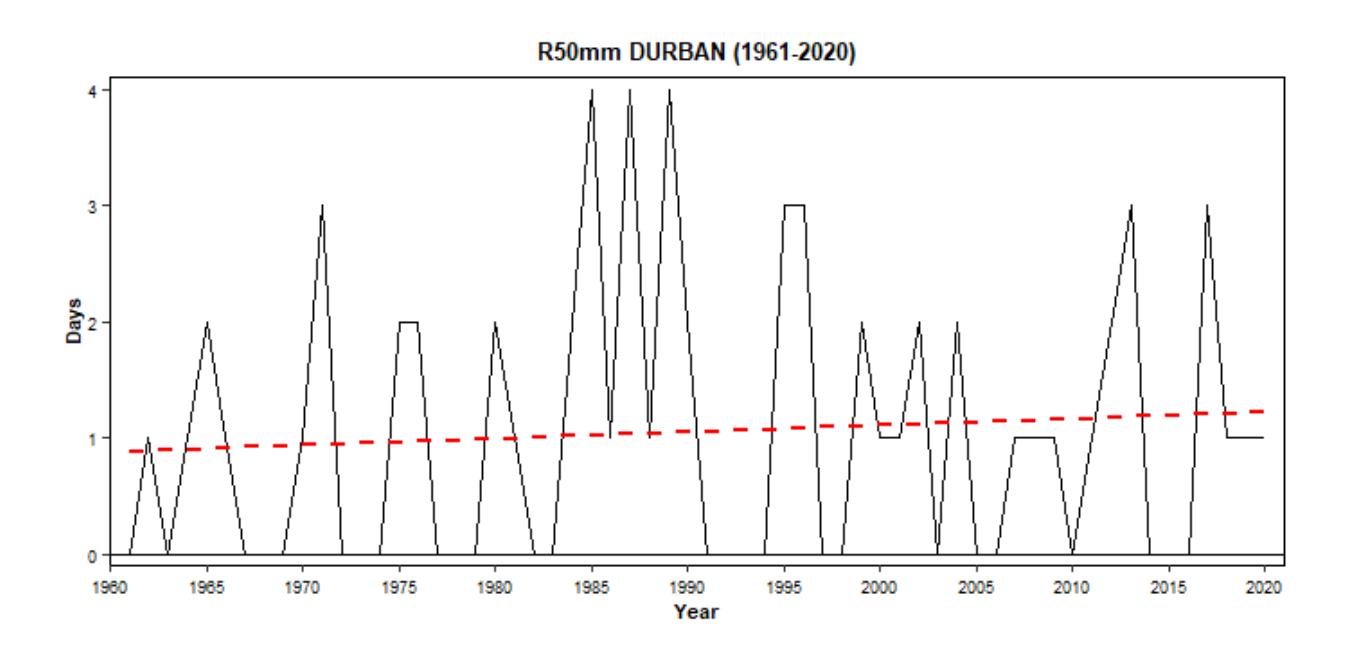


Figure 4.8 This figure shows the frequency of rainfall exceeding 50mm/day index (R50mm) in Durban for the period 1961-2020. The trend line indicates an increase in the number of rainfall days exceeding 50mm/day over this period.

4.2 Model verification

4.2.1 Statistical verification

Model verification was used to evaluate the performance of six CMIP6 models against ERA5 observations. Taylor diagrams shown in Figure 4.9 and Figure 4.10 were used for model validation, hence standard deviation, RMSE, and correlation coefficient are integrated to rank the performance of the models.

Figure 4.9 shows that the observed variability (in terms of standard deviation) is 3.8°C. Models IPSL_CM6A_LR, and MPI_ESM1_2_LR underestimated the observed variability because they lie within the black line representing standard deviation, and the ensemble estimated the observed variability because it lies on the black line. Models AWI_CM_1_1_MR, BCC_CSM2_MR, GFDL_ESM4, and ACCESS_CM2, overestimated the observed variability, however, AWI_CM_1_1_MR, BCC_CSM2_MR, and MPI_ESM1_2_LR estimated close variability to the observation than other models. All models performed well in terms of a high correlation coefficient above 0.9, and the ensemble and ACCESS_CM2 obtained a correlation above 0,95, as shown in Figure 4.9. Regarding RMSE, all models had RSME of less than 2°C, however, model IPSL-CM6A-LR had the highest RMSE.

Results in Figure 4.10 show that the ensemble and AWI_CM_1_1_MR estimated the same value (38 mm) with the observation because they both lie on the black line representing standard deviation and MPI_ESM1_2_LR estimated close variability to the observation value of rainfall than other models. Models IPSL-CM6A-LR overestimated the observed variability because it is furthest from the observation. Models BCC-CSM2-MR, IPSL_CM6A_LR, MPI_ESM1_2_LR, ACCESS_CM2, GFDL_ESM4, and the ensemble, all have a correlation with the measurement above 0.5. Furthermore, AWI_CM_1_1_MR has a correlation of 0.5, and the ensemble achieved the highest correlation above 0.7. In terms of RMSE, all models lie within 50mm/month, however, models GFDL_ESM4 and IPSL_CM6A_LR lie above 40mm/month, with ACCESS_CM2 showing the highest RMSE.

Temperature (1961-1990) 0.1 AWI BCC GFDL IPSL MPI ACCESS ENSEMBLE Observation 0.2 0.3 9 0.4 0.5 Correlation 6 0.6 LΩ 0.7 8.0 0.9 0.95 0.99 0 2 5

Standard Deviation

Rainfall (1961-1990)

Figure 4.9 Taylor diagram showing SAT model verification

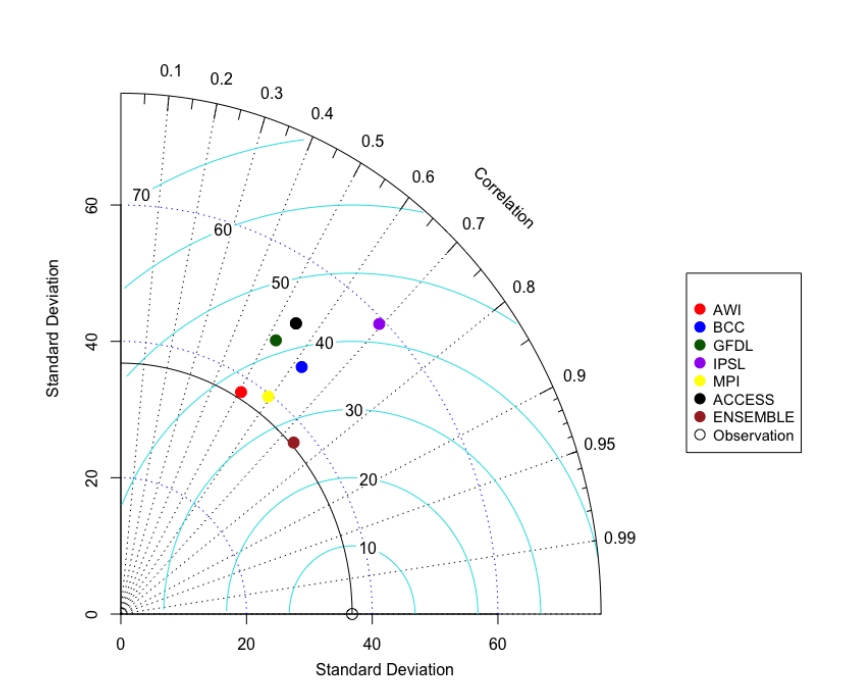


Figure 4.10 Taylor diagram showing rainfall model verification

4.2.2 Visual verification

4.2.2.1 SAT seasonal means

The climate of South Africa generally is warm, and the escarpments in the east and south of the country have the lowest mean temperatures due to the decreasing temperature as the altitude rises. Coastal areas of KZN, northern KZN, and the Lowveld of MP are the warmest areas (Landman et al. 2017). Four different seasonal means for SAT (shown in Figure 4.11 to Figure 4.14) were utilized to show how the models performed against the observation. DJF (summer) is the warmest season with an average temperature ranging above 15°C and below 27°C, as shown in Figure 4.11 (a-h) by the ERA5 and all six CMIP6 models over the study area. Spatial distribution of DJF mean SAT by ERA5, AWI_CM_1_1_MR, IPSL_CM6A_LR, MPI_ESM1_2_LR, GFDL_ESM4, and ensemble mean (ensmean) showed variabilities 15°C - 18°C expanding over west of KZN and south of MP, covering most of Lesotho. High temperatures are experienced over the east coast of the study area, with temperatures ranging above 21°C and below 27°C.

MAM (autumn) mean SATs have cooled down to the lowest peak mean SAT below 15°C, as shown by ERA5 observation in Figure 4.12 (h). Spatial distribution of MAM mean SAT showed west of KZN and south of MP to be cooler than the rest of the study area. However, the east coast of the study area remained warmer. The Indian Ocean and the Atlantic Ocean influence the temperatures that the coastal areas of South Africa experience (Landman et al. 2017). The ERA5 observation and the models AWI_CM_1_1_MR, IPSL_CM6A_LR, MPI_ESM1_2_LR, GFDL_ESM4, ACCESS_CM2, and ensmean showed temperatures below 15°C over the Highveld in MP. The spatial distribution of MAM mean SAT also showed that the interior of the study area had cooler temperatures ranging from 15°C to 21 °C.

During JJA (winter), the observed mean SATs were simulated below 15°C in the north, south, and interior, and 12°C in the west regions of the study area. Furthermore, the mean SATs observed in the east of the study area range above 15°C and below 21°C, as shown in Figure 4.13 (h). The observation showed a significant spatial distribution of 9°C - 21°C over the north, south, west, and east of the study area. JJA mean SATs 18°C-21°C were overestimated by AWI_CM_1_1_MR, IPSL_CM6A_LR, BCC_CSM2_MR, GFDL_ESM4, ACCESS_CM2, and ensmean on the northeast region of KZN. Models AWI_CM_1_1_MR, IPSL_CM6A_LR, MPI_ESM1_2_LR, and GFDL_ESM4 showed SATs that range between 12°C and 15°C over the south of MP, as shown in Figure 4.14 during SON (spring). However, all the models including

ensmean and ERA5 observation simulated the spatial distribution of 12°C - 24°C SON mean SATs over the study area. The spatial distribution of SON seasonal mean SATs with close variabilities to each other over the study area were simulated by ACCESS_CM2 and BCC_CSM2_MR, as shown in Figure 4.14 (d) and Figure 4.14 (f), respectively.

4.2.2.2 Rainfall seasonal means

According to Morishima and Akasaka (2010), rainfall variability in southern Africa has experienced significant modulations, particularly in recent years. South Africa is highly vulnerable to extreme rainfall events which are becoming more frequent leading to increased socio-economic impacts (Mashao et al. 2023). The east coast receives high rainfall and it has the warmest SSTs (Reason, 2017). The high latent heat fluxes caused by the poleward that flows warm Agulhas Current closer to southern Africa's east coast transfers more moisture to the atmosphere than the surrounding waters (Rouault et al. 2003), and this eventually leads to the intensification of a local storm (Singleton and Reason, 2007). The rainfall seasonal means below are shown from Figure 15 to Figure 18.

DJF seasonal mean rainfall over the study area for the period 1961-1990 is shown below in Figure 4.15. DJF rainfall seasonal observation from ERA5 (Figure 4.15 (h)) has shown a minimum of ~ 40 mm to a maximum of ~ 400mm over the study area, with a part of the north of MP receiving less rainfall (40 mm) and southwest of KZN on the boundary of Lesotho receiving high rainfall ranging above 280 mm to below 400 mm. All six models simulated maximum rainfall of about 160 mm/month in some regions of the study area as shown in Figure 4.15 (a-g). Models GFDL_ESM4, ACCESS_CM2, BCC_CSM2_MR, and esmeans' simulations recorded high summer mean rainfall of about 200 mm/month to 280 mm/month in the interior of KZN and AWI_CM_1_1_MR simulated same amount of rainfall in the south of KZN. Model IPSL_CM6A_LR overestimated summer rainfall (160 mm to 360 mm) and MPI_ESM1_2_LR simulated the lowest rainfall (120 mm to 200 mm) over the study area. The warm Agulhas Current in the Indian Ocean accounts for the high rainfall on the east coast of South Africa (Rouault et al. 2024).

The ERA5 observation for MAM seasonal rainfall, simulated low rainfall in most parts of the study area. The rainfall simulations of the ERA5 are below 160 mm/month in most regions of the study area, however, the southwest of KZN, which is the northeast of Lesotho shows higher rainfall that is between 120 mm and 160

mm. All six models simulated a decrease in MAM seasonal rainfall as none of them simulated rainfall above 160 mm/month as shown in Figure 4.16 (a-g). Models AWI_CM_1_1_MR, MPI_ESM1_2_LR, ACCESS_CM2, IPSL_CM6A_LR, and BCC_CSM2_MR, simulated high rainfall in KZN (ranging between 40 mm and 160 mm) than most of MP (between 40 mm and 120 mm). Model GFDL_ESM4 simulated high rain in most of the MP province, ranging between 80 mm to 120 mm except in the north.

During the JJA season, the ERA5 observation showed an equal distribution of rainfall over the study area which is below 40 mm/month, as shown in Figure 4.17 (h). All six models showed a decrease in winter rainfall that is below 120 mm/month over the study area, however, they simulated higher rainfall than ERA5 observation on the east coast of KZN. Models AWI_CM_1_1_MR, and ACCESS_CM2 simulated the highest JJA seasonal rainfall that ranges between 80 mm to 120 mm over the east coast of KZN. The KZN province receives rainfall variability from coastal areas to inland areas (Ndlovu et al. 2021). The ERA5 observation simulated an increase in mean rainfall for SON because the rainfall during this season ranges from above 40 mm/month to 200 mm/month over the study area with MP shown to have received below 120 mm/month during the 1961-1990 period. All six models simulated an increase in rainfall (ranging from above 40 mm/month to 280 mm/month) during the spring season over the interior of the study area and more over the east coast of KZN, as shown in Figure 4.18. Model ACCESS_CM2 overestimated SON mean rainfall ranging from 240 mm/month to 280 mm/month over a small portion of the interior of KZN.

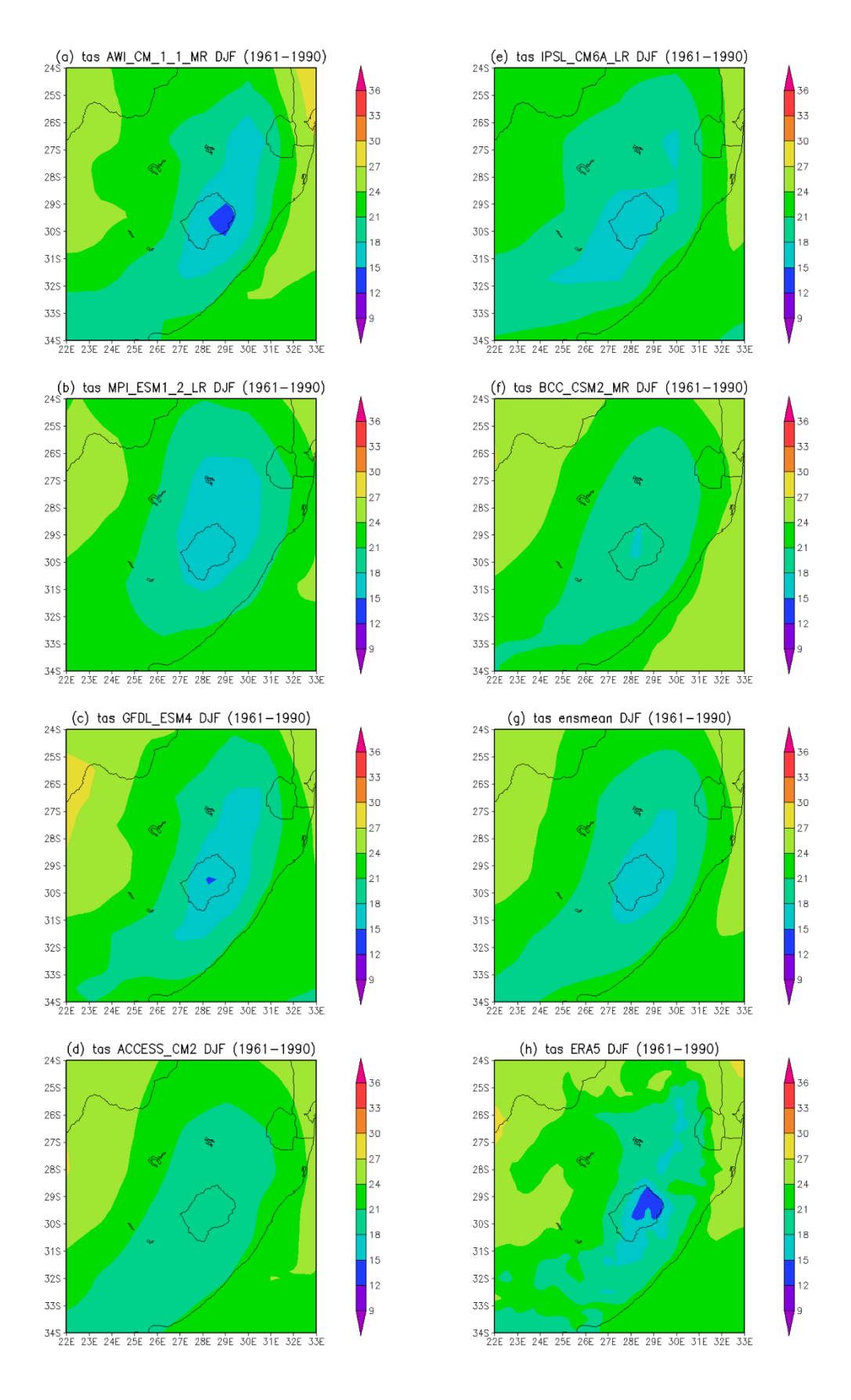


Figure 4.11 DJF seasonal mean SAT for the 1961-1990 period

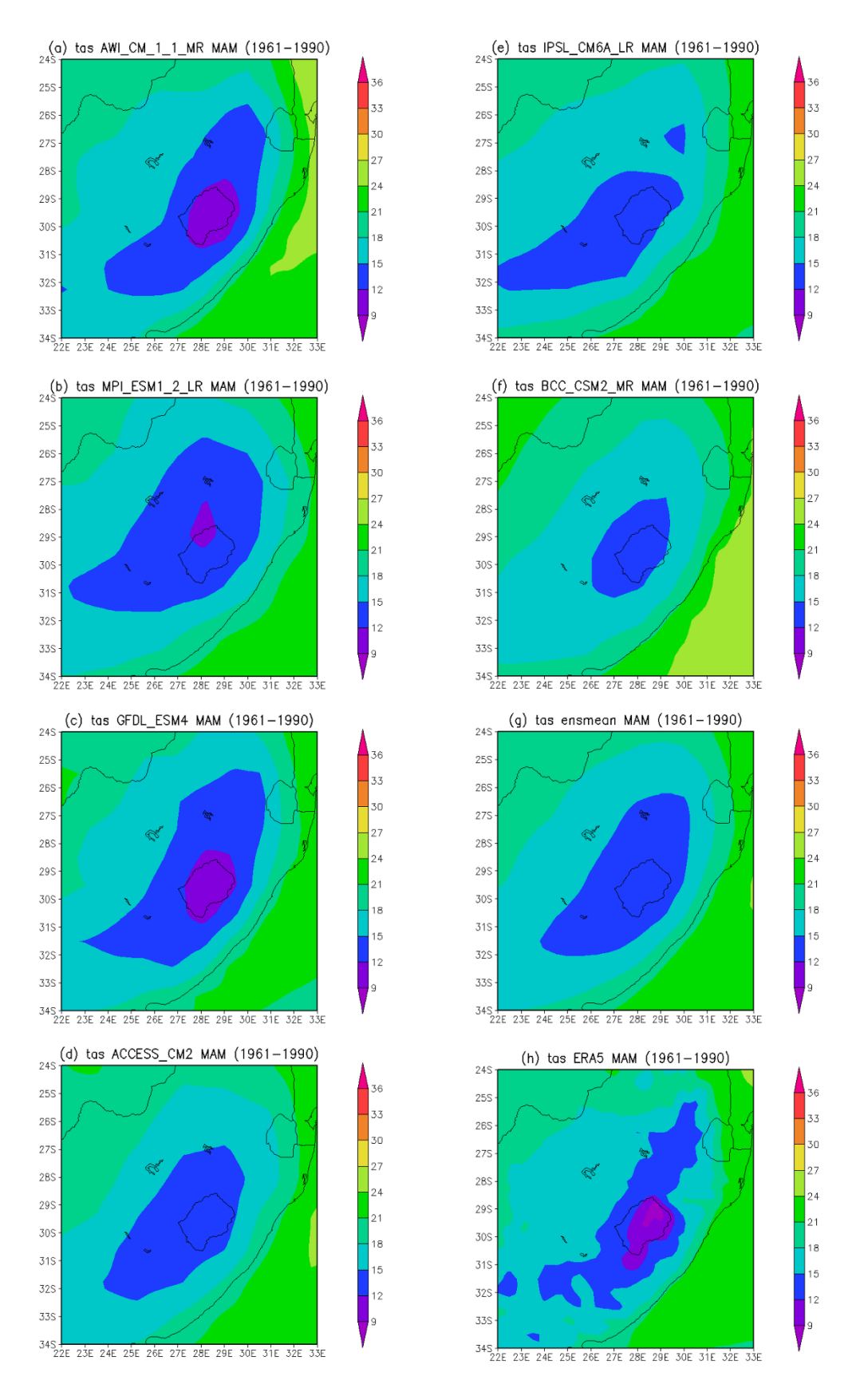


Figure 4.12 MAM seasonal mean SAT for the 1961-1990 period

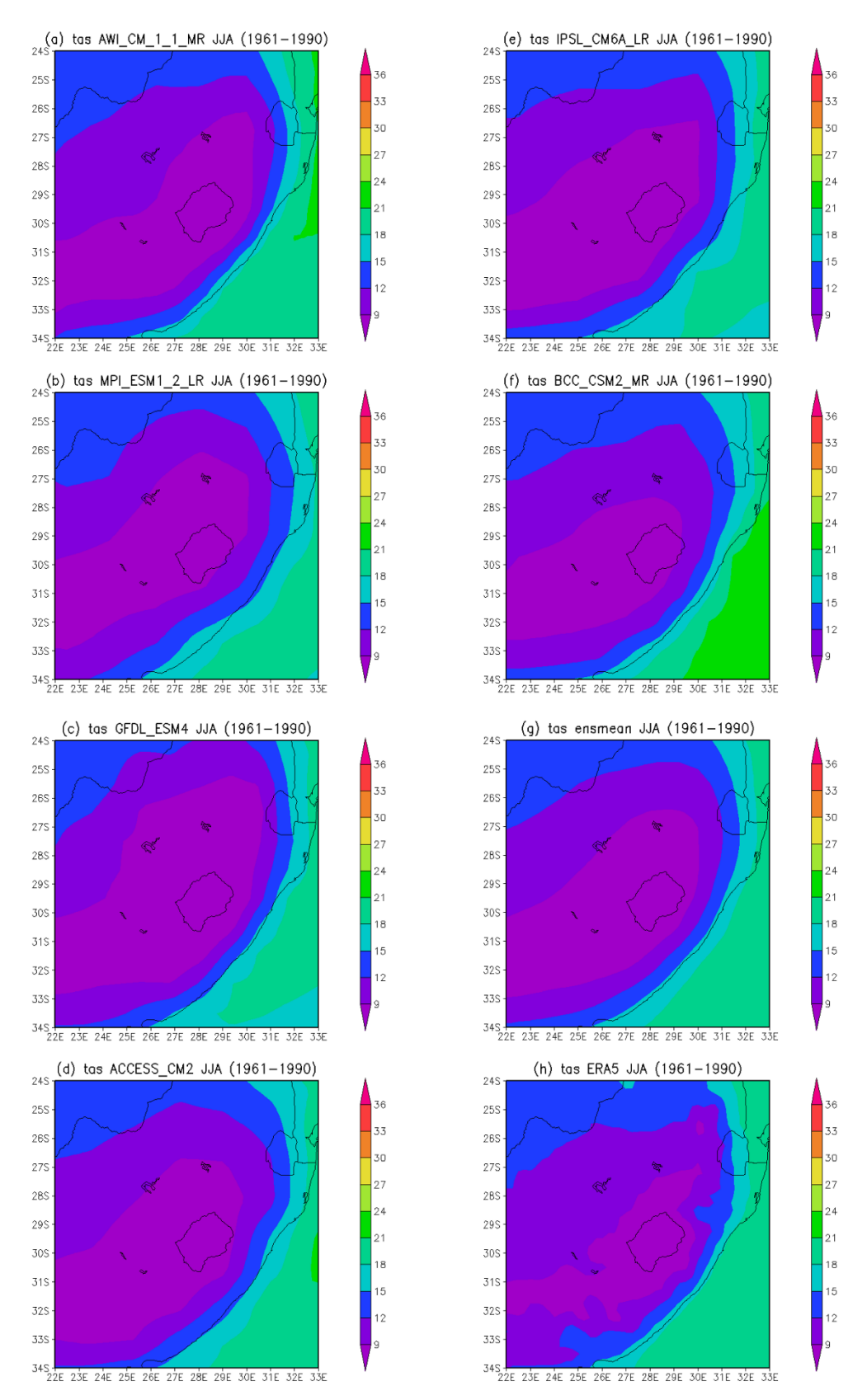


Figure 4.13 JJA seasonal mean SAT for the 1961-1990 period

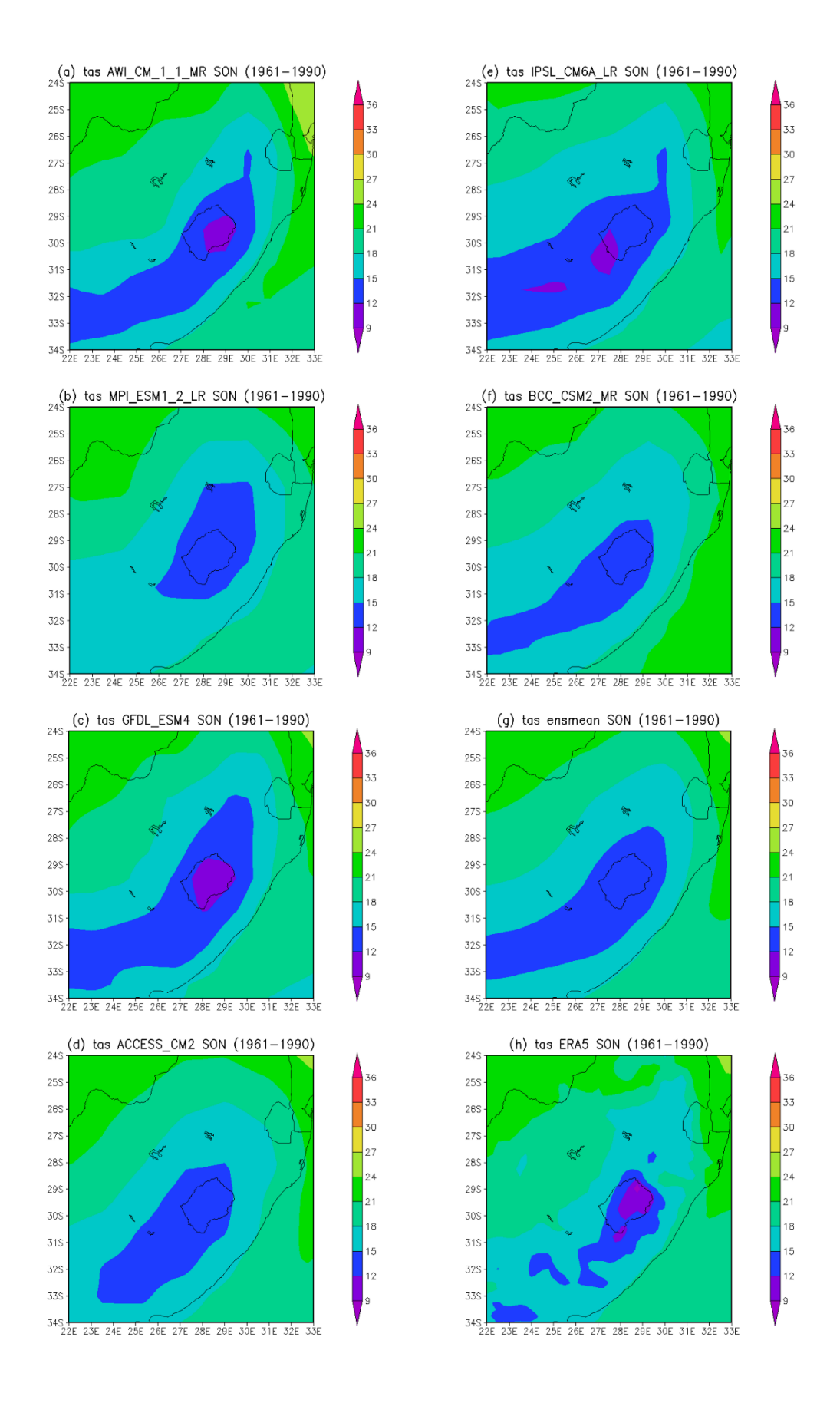


Figure 4.14 SON seasonal mean SAT for the 1961-1990 period

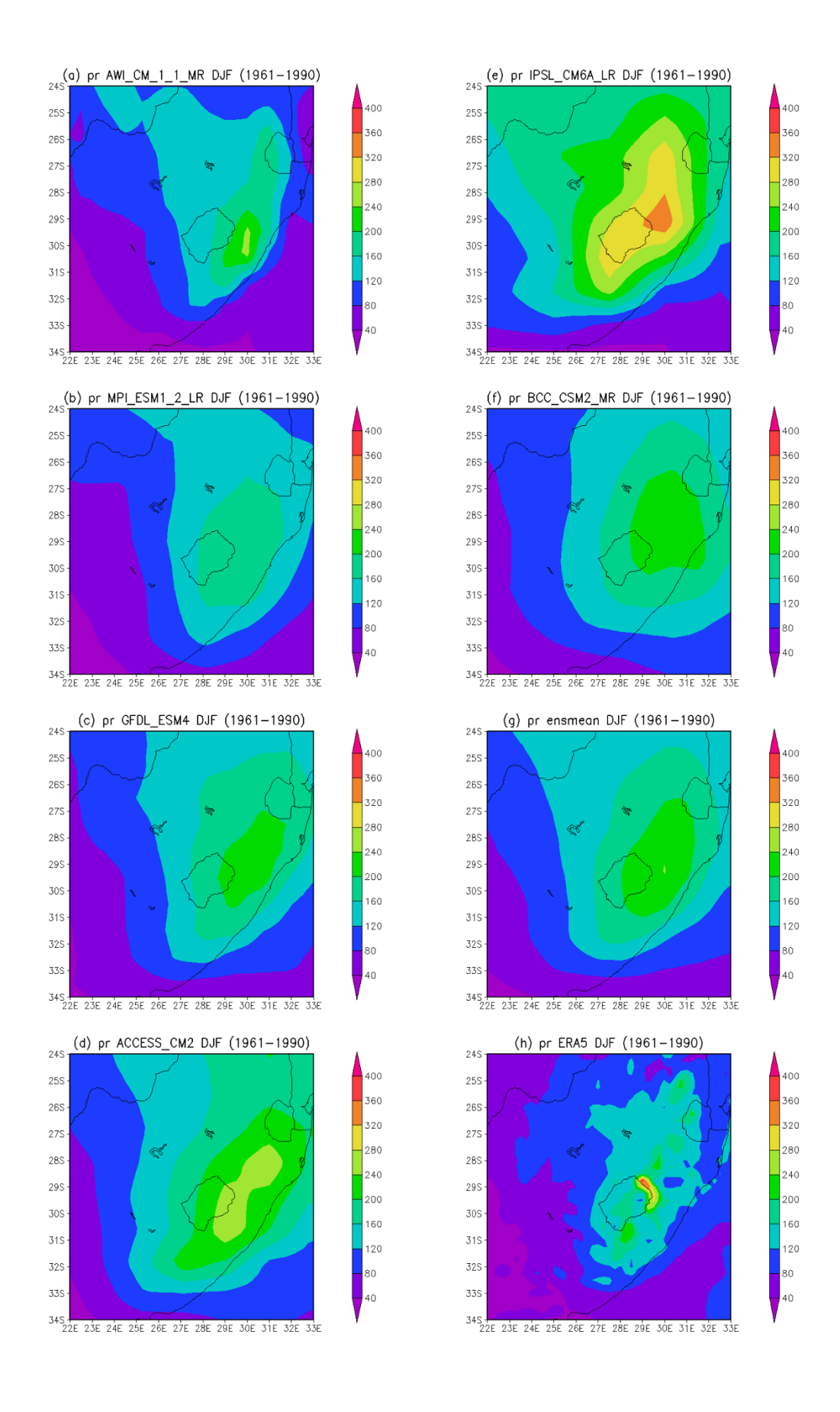


Figure 4.15 DJF seasonal mean rainfall for the 1961-1990 period

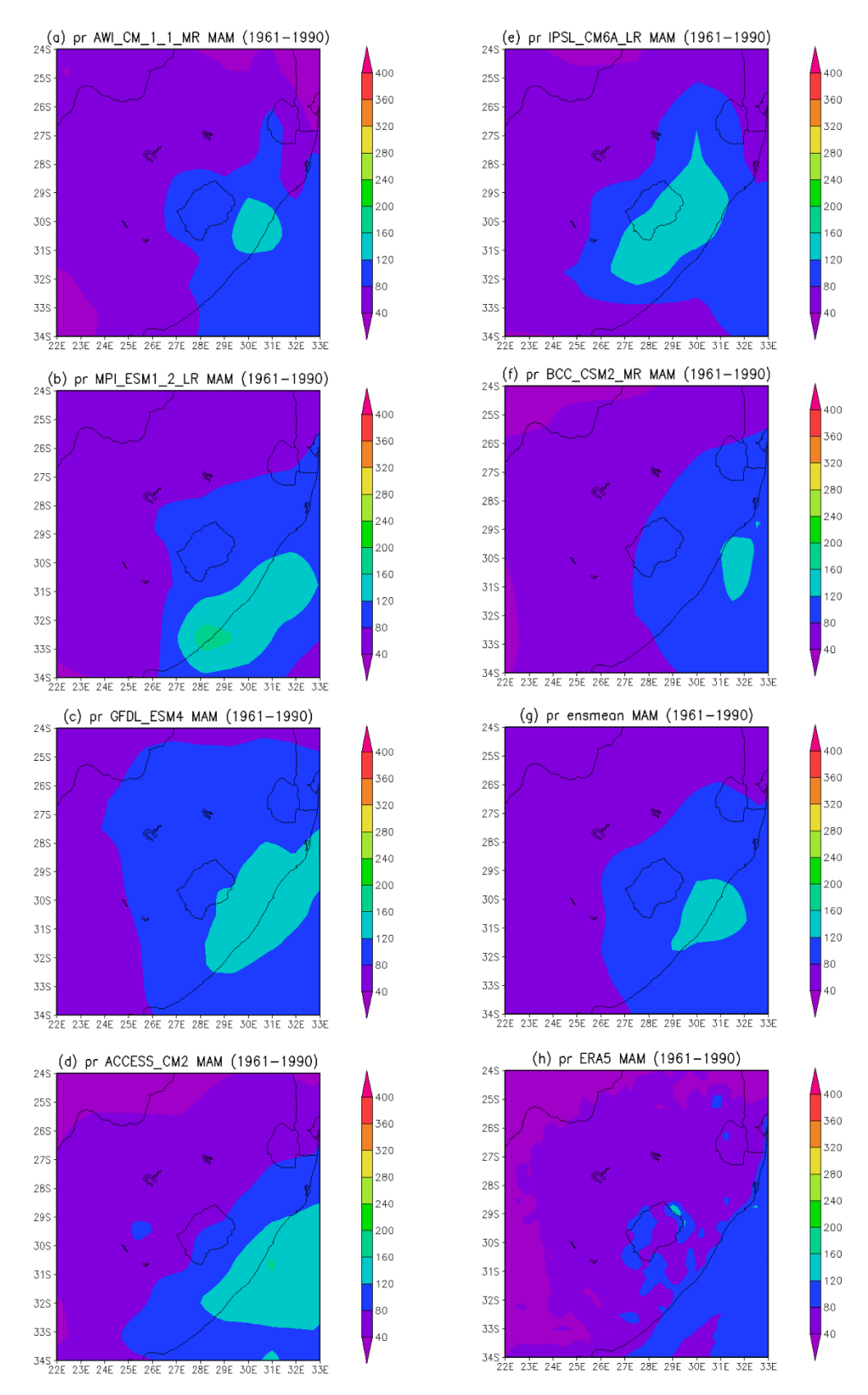


Figure 4.16 MAM seasonal mean rainfall for the 1961-1990 period

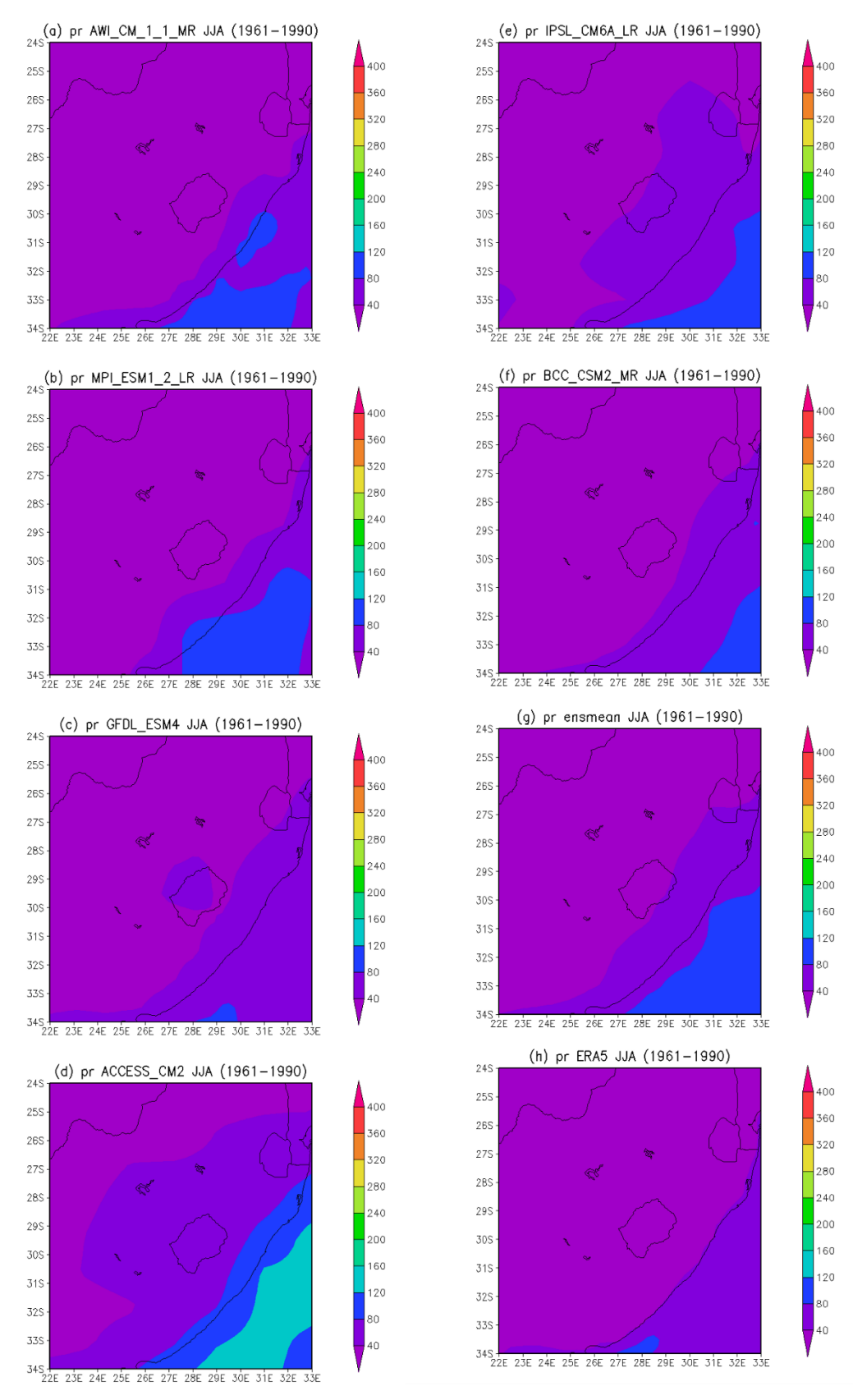


Figure 4.17 JJA seasonal mean rainfall for the 1961-1990 period

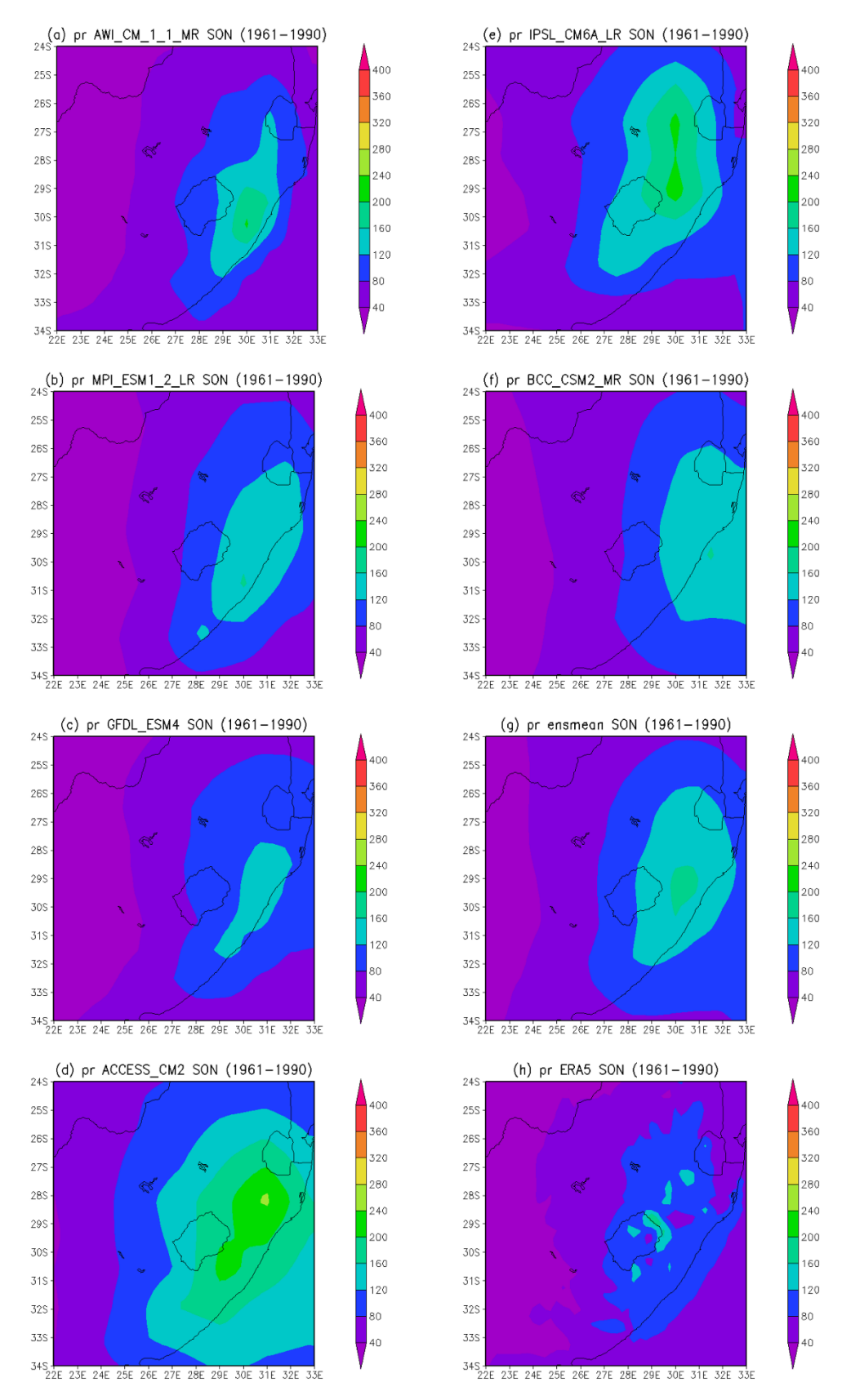


Figure 4.18 SON seasonal mean rainfall for the 1961-1990 period

4.3 Summary

This chapter mainly focussed on analysing the historical trends of SAT and rainfall characteristics during the present day (1961-2020), and model verification using statistical and visual verification. Taylor diagrams containing standard deviation, correlation coefficient, and RMSE were utilized to verify the models' projections over the study area. The six CMIP6 models were verified against ERA5 observation, and seasonal means were used to analyse variations for the reference climate (1961-1990). The ensmean of the models was also presented in this chapter. In 1968, Kruger Mpumalanga International Airport and Durban showed high peak of cool days that persisted for 29 and 35 days respectively, and an increasing trend in hot days and decreasing trend in heavy rainfall days at both locations. Furthermore, this may imply that agriculture in MP might have been affected by low temperatures as some plants cannot survive under cold conditions. Furthermore, the frequency of rainfall exceeding 50mm/day trends varied by location. Statistical verification for Surface Air Temperature (SAT) showed a high correlation (≥0.9) and low Root Mean Square Error (RMSE) with ERA5 data, while rainfall model verification had a moderate correlation (0.5-0.7) and least RMSE, indicating higher uncertainty in precipitation modelling. The highest SATs and rainfall were simulated during the summer season and the lowest SATs and rainfall were simulated during the winter over the study area.

CHAPTER 5: FUTURE PROJECTIONS OVER EASTERN SOUTH AFRICA

5.0 Introduction

According to Lazenby et al. (2018), future projections are important in comprehending the climate change impacts to inform adaptation strategies. This is the second results chapter that focuses mainly on future projections of climate variability and changes over the study area (KZN and MP) during the near-future (2021-2050) and far-future (2070-2099) periods. This chapter outlines how SATs and rainfall over the study area are projected to increase or decrease. The six CMIP6 models and the SSP2-4.5 and SSP5-8.5 emission scenarios were used to derive the projections. Seasonal means in SATs were used to analyse the future projections of SATs for the two emission scenarios. Historical trends in SATs and rainfall are important in the facilitation of future climate change projections for informed policy responses (Ndlovu et al. 2021). This chapter involves projections of seasonal changes in SATs and rainfall between the reference climate (1961-1990), the near-future (2021-2050), and the far-future (2070-2099) periods.

5.1 Future projections of SATs

5.1.1 Near-future (2021-2050)

According to previous research studies, the observations show that as GHG emissions increase also the temperature increases (Bhatti et al. 2024; Zittis et al. 2022). Considering southern African climate projections and trends, the temperature signal is the most robust. The observation in the past century is that trends of SAT in South Africa have been changing between decreasing and increasing, consistent with global changes (Mbokodo et al. 2023). Seasonal means in SAT for near-future projections are presented below for the two emission scenarios.

5.1.1.1 Seasonal mean SAT for SSP2-4.5 and SSP5-8.5

All six models and the ensmean projected DJF seasonal mean SATs under SSP2-4.5 and SSP5-8.5 that range from 18°C to 30°C, with some regions on the east coast of the study area projected to have high SATs during the 2021-2050 period, as shown in Figure 5.1 (a-g) and Figure 5.5 (a-g). Model AWI_CM_1_1_MR is the only model that projected SATs above 27°C to 30°C over some regions on the east coast of MP (Lowveld) and KZN (northeast) provinces. Models AWI_CM_1_1_MR, MPI_ESM1_2_LR, and GFDL_ESM4 projected lower SATs (15°C to 18°C) than other models in the south and southwest of KZN, and those regions include

Free State province and neighbouring Lesotho. The summer season is projected to have higher and warmer SATs than other seasons over the study area under both scenarios. According to Kapuka et al. (2022), southern Africa will continue to experience climate change in the future under moderate and high mitigation, but the magnitude of change will be smaller and there will be more room for adaptation.

During the MAM season, models ACCESS_CM2, IPSL_CM6A_LR, and BCC_CSM2_MR projected variations of SATs ranging from 15°C to 27°C over the study area and the east coast of South Africa. However, models AWI_CM_1_1_MR, MPI_ESM1_2_LR, GFDL_ESM4, and ensmean projected lower temperatures (12°C to 15°C) on the southwest of KZN, and on the south of MP during the MAM season under SSP2-4.5 and SSP5-8.5 mitigation scenarios (Figure 5.2 and Figure 5.6). Furthermore, these regions in South Africa are likely to experience COLs in the near future, as COLs are not only associated with heavy rainfall but with cold weather conditions as well (< 20 °C) (Mashao et al. 2023). The east coast of the study area remains to have higher SATs during autumn than other regions in the 2021-2050 period.

The models projected the JJA season to be the coldest out of all seasons during the 2021-2050 period. Projections of JJA seasonal mean SATs for both scenarios range from below 9°C to 21°C and are distributed differently over different regions of the study area. The Highveld in MP and west of KZN are projected to have the lowest SATs (< 9°C to 12°C) by models GFDL_ESM4 and AWI_CM_1_1_MR respectively, as shown in Figure 5.3 and Figure 5.7. South Africa is vulnerable to temperature extremes such as heatwaves and they are projected to occur more in summer and less in mid-winter (Mbokodo et al. 2020). The models' projections of SATs for the SON season show an increase in the near-future period over the study area from the JJA season, with high SATs (18°C to 27°C) over Lowveld of MP and northeast of KZN as shown in Figure 5.4 and Figure 5.8 below. Models AWI_CM_1_1_MR and GFDL_ESM4 continued to project low temperatures (12°C - 15°C) over the west and south of KZN. The SATs over the western interior of KZN are projected by all six models to be lower than other regions of the study area across all seasons under the SSP2-4.5 and SSP5-8.5 scenarios.

5.1.1.2 Seasonal change in SAT for SSP2-4.5 and SSP5-8.5

Figure 5.9 and Figure 5.10 show the projected seasonal change in SAT for SSP2-4.5 and SSP5-8.5 respectively, between reference climate (1961-1990) and near-future (2021-2050) periods. Across all the seasons the models projected an increase in SATs that range between 1°C and 2°C over the study area under both scenarios. This suggests that conditions are still going to be warmer because of an increase in SATs on the east coast of South Africa. Engelbrecht and Monteiro (2021) suggest that South Africa will become drier and warmer between 2021 and 2040 in the coming years. The west coast of South Africa is projected to be warmer (> 2°C to 3°C) than other regions of the country during the spring season under both emission scenarios.

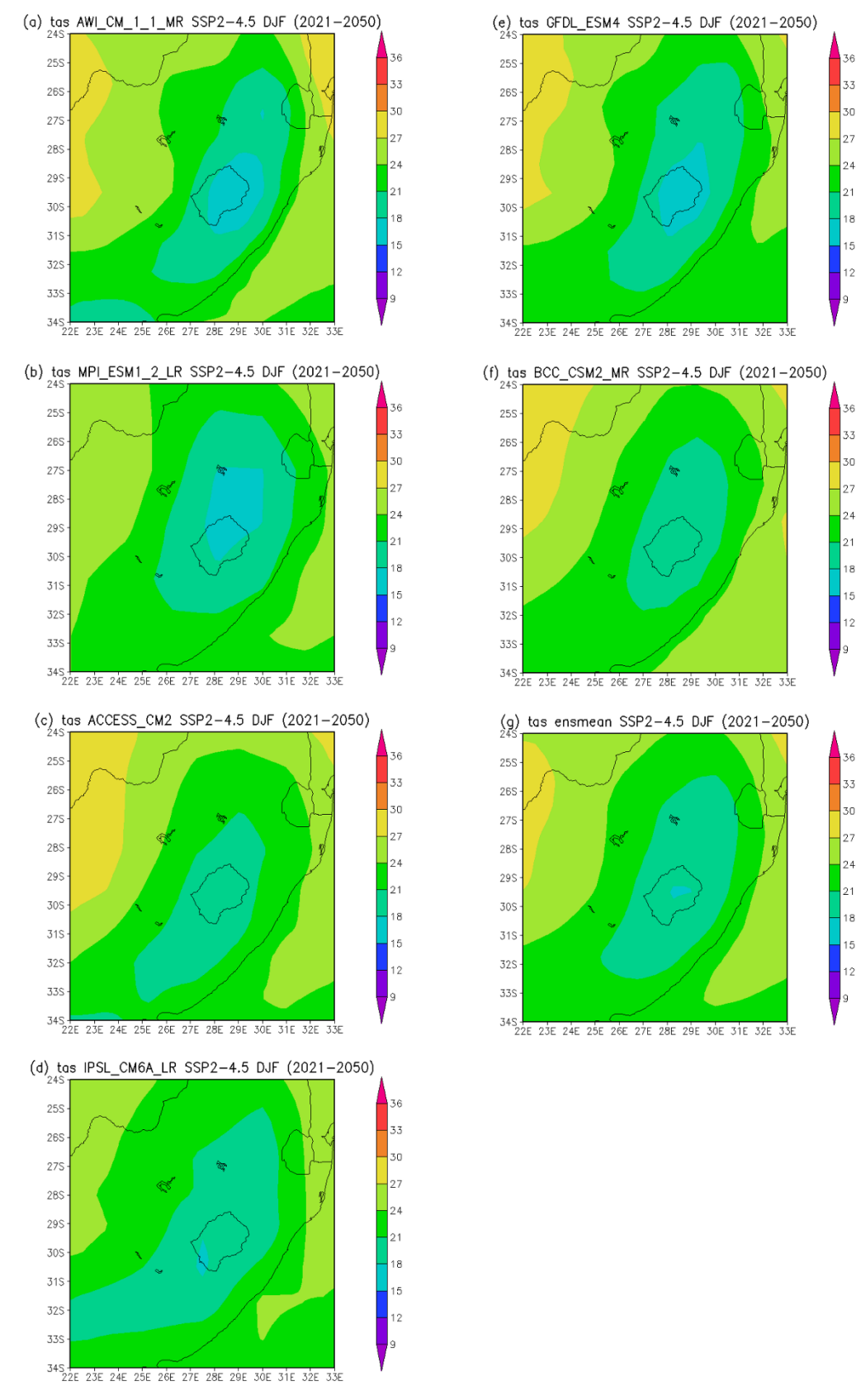


Figure 5.1 DJF seasonal mean SAT for SSP2-4.5 during the 2021-2050 period

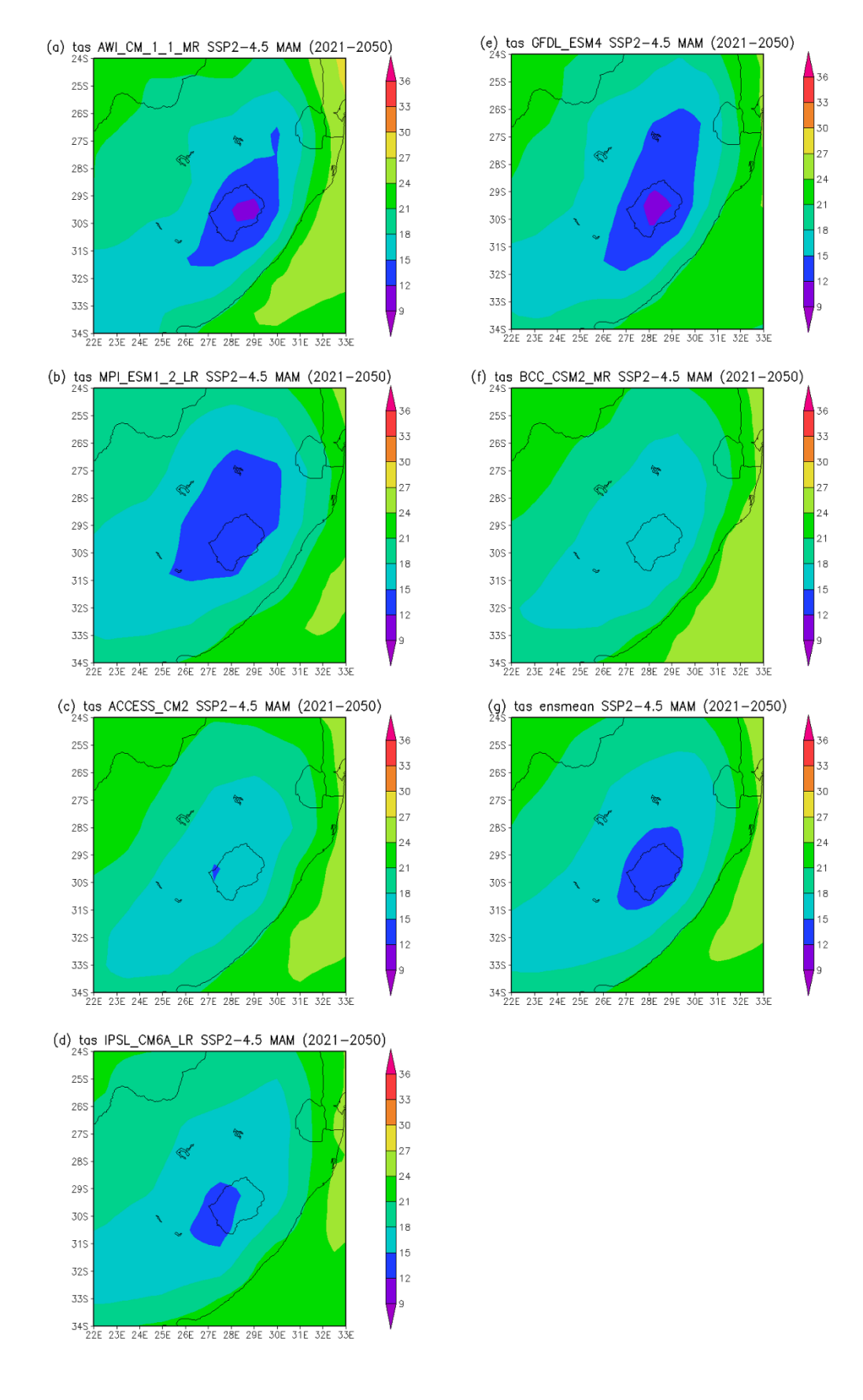


Figure 5.2 MAM seasonal mean SAT for SSP2-4.5 during the 2021-2050 period

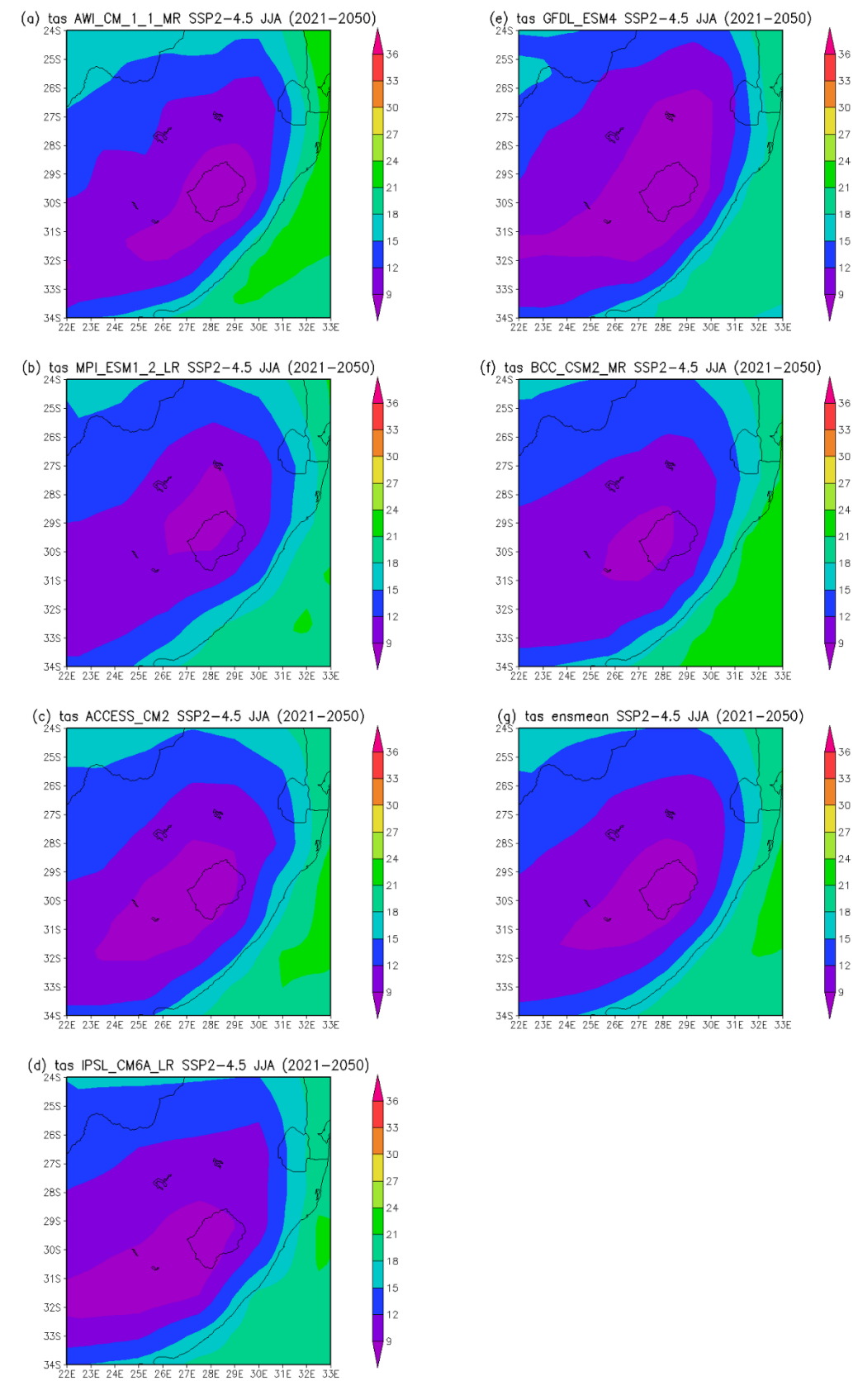


Figure 5.3 JJA seasonal mean SAT for SSP2-4.5 during the 2021-2050 period

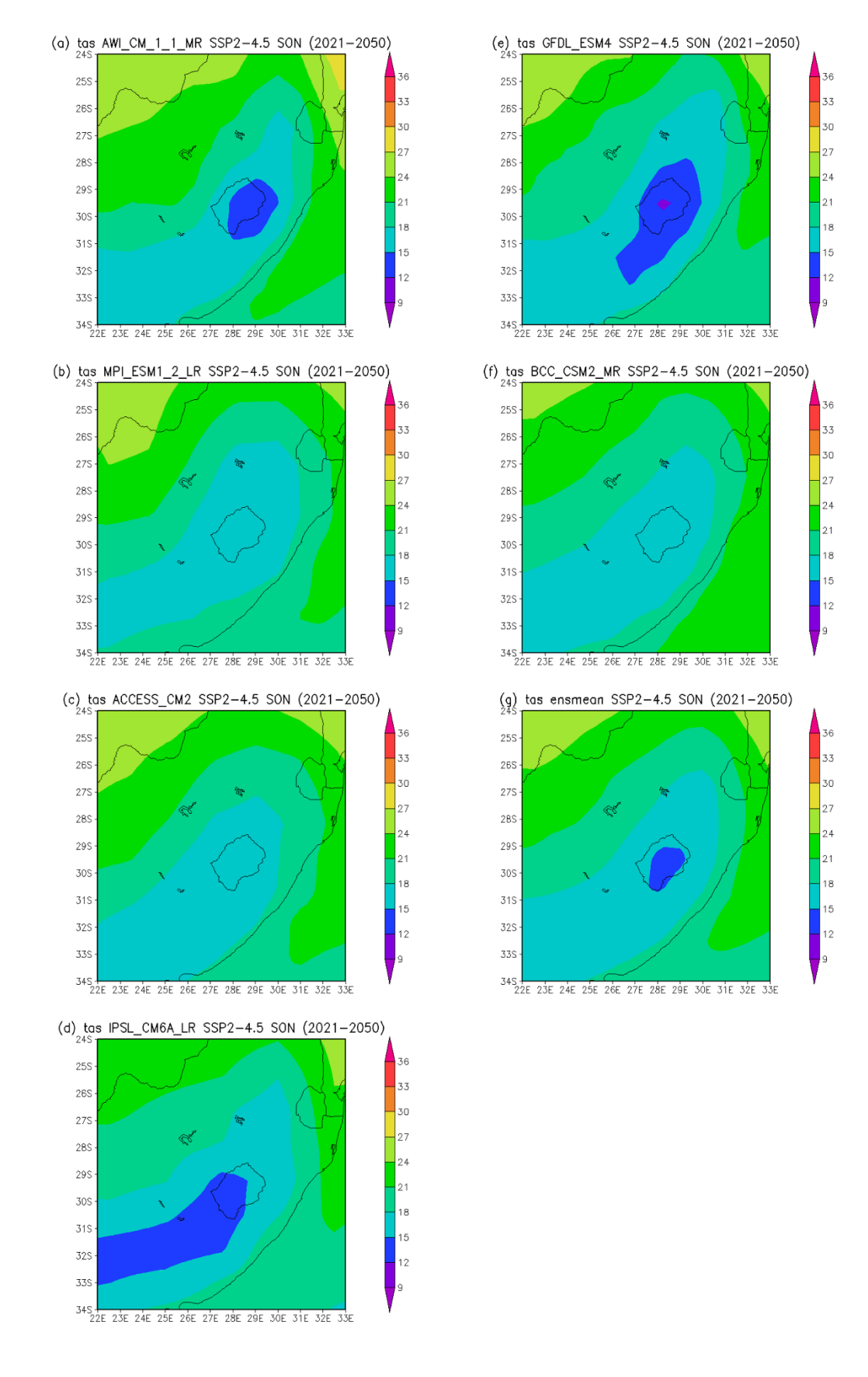


Figure 5.4 SON seasonal mean SAT for SSP2-4.5 during the 2021-2050 period

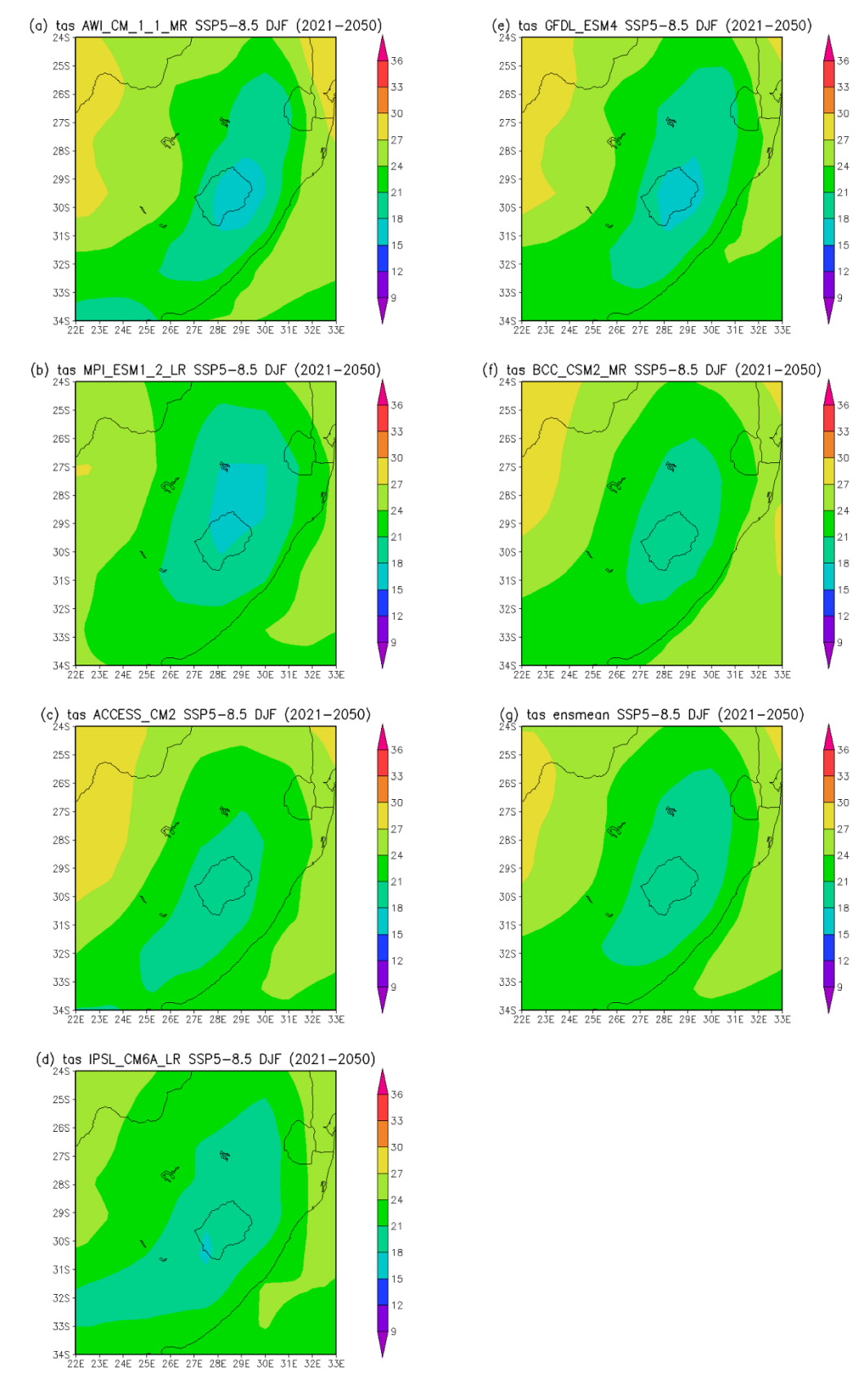


Figure 5.5 DJF seasonal mean SAT for SSP5-8.5 during the 2021-2050 period

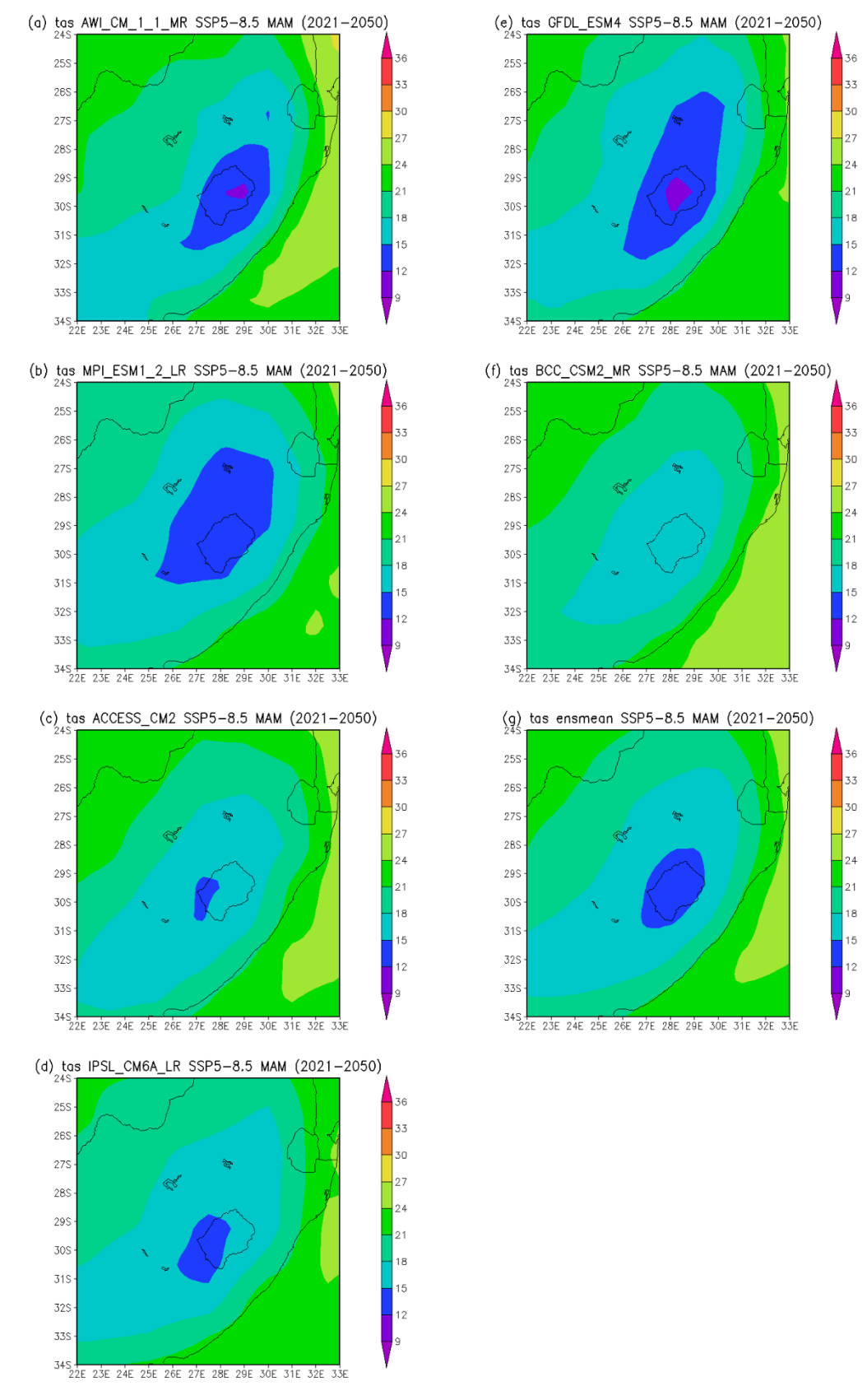


Figure 5.6 MAM seasonal mean SAT for SSP5-8.5 during the 2021-2050 period

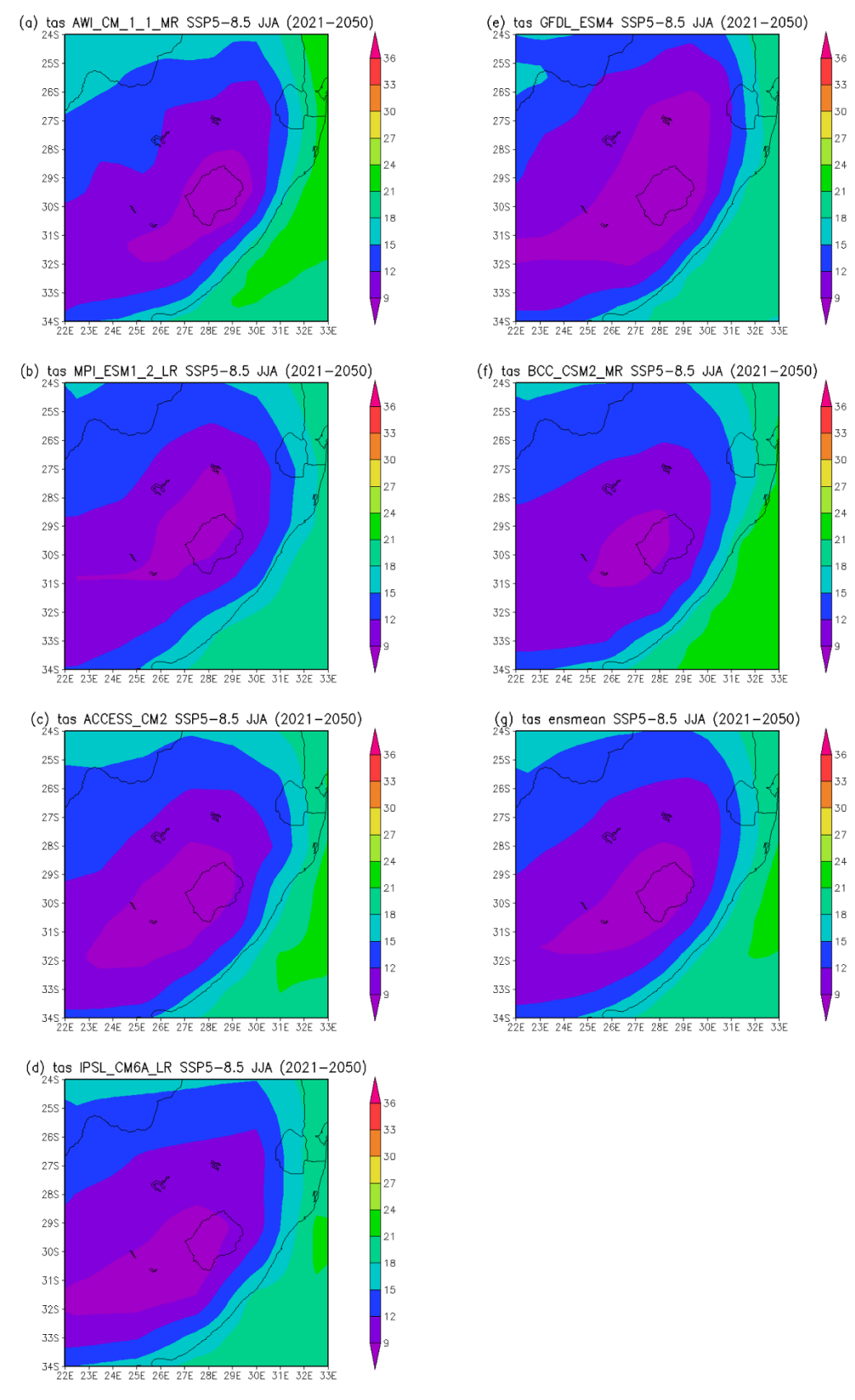


Figure 5.7 JJA seasonal mean SAT for SSP5-8.5 during the 2021-2050 period

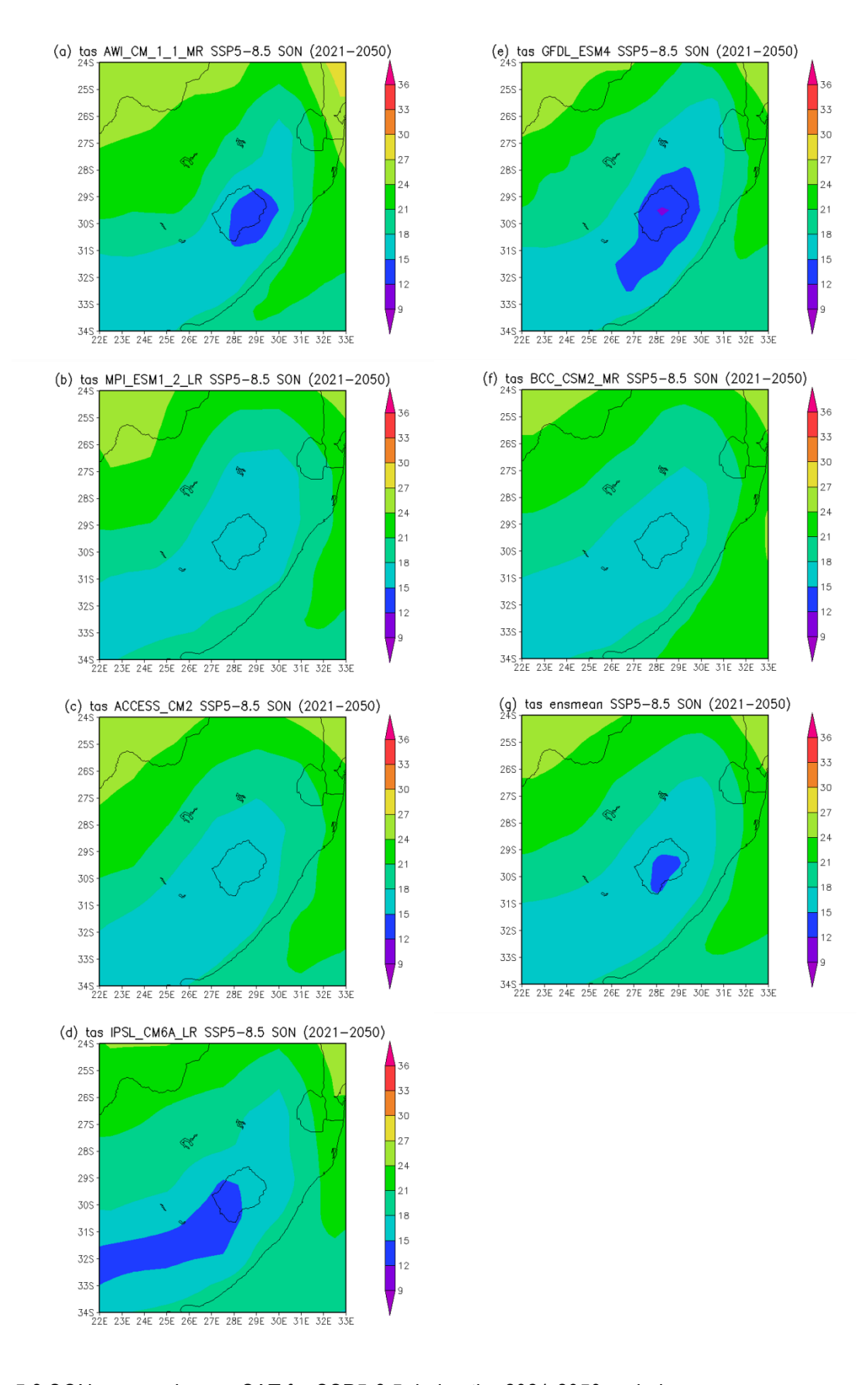


Figure 5.8 SON seasonal mean SAT for SSP5-8.5 during the 2021-2050 period

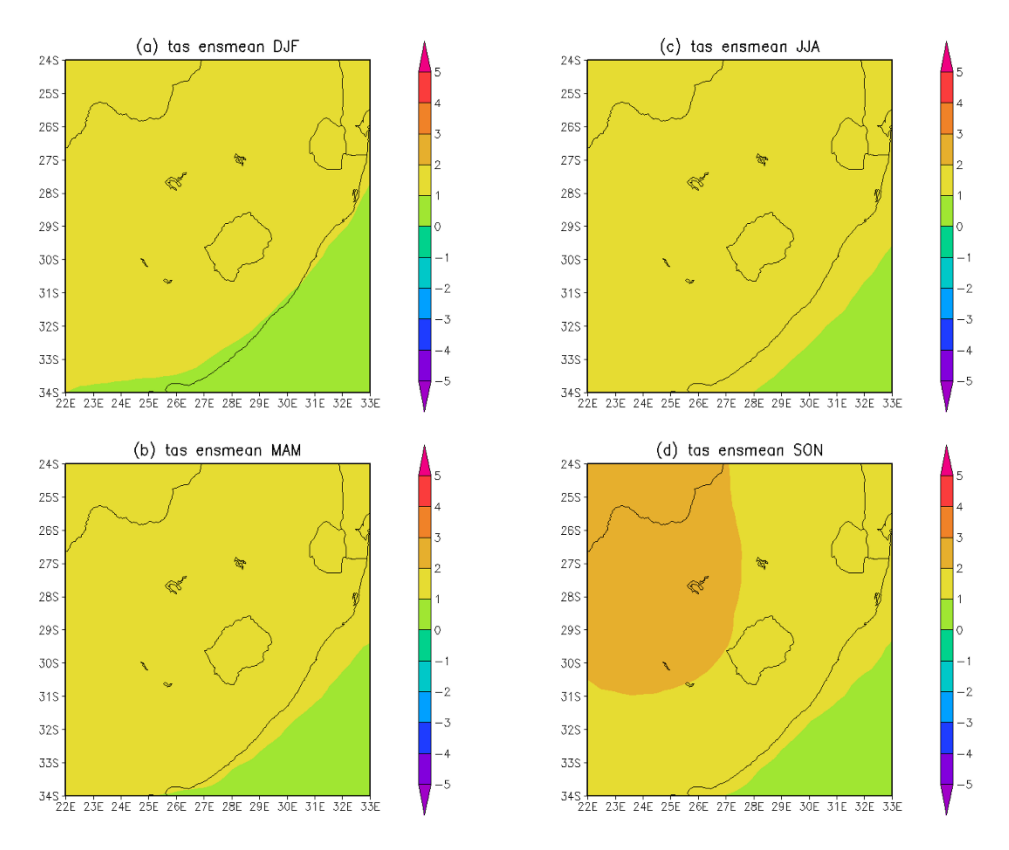


Figure 5.9 Seasonal changes in SAT for SSP2-4.5 between reference climate (1961-1990) and near-future (2021-2050) periods

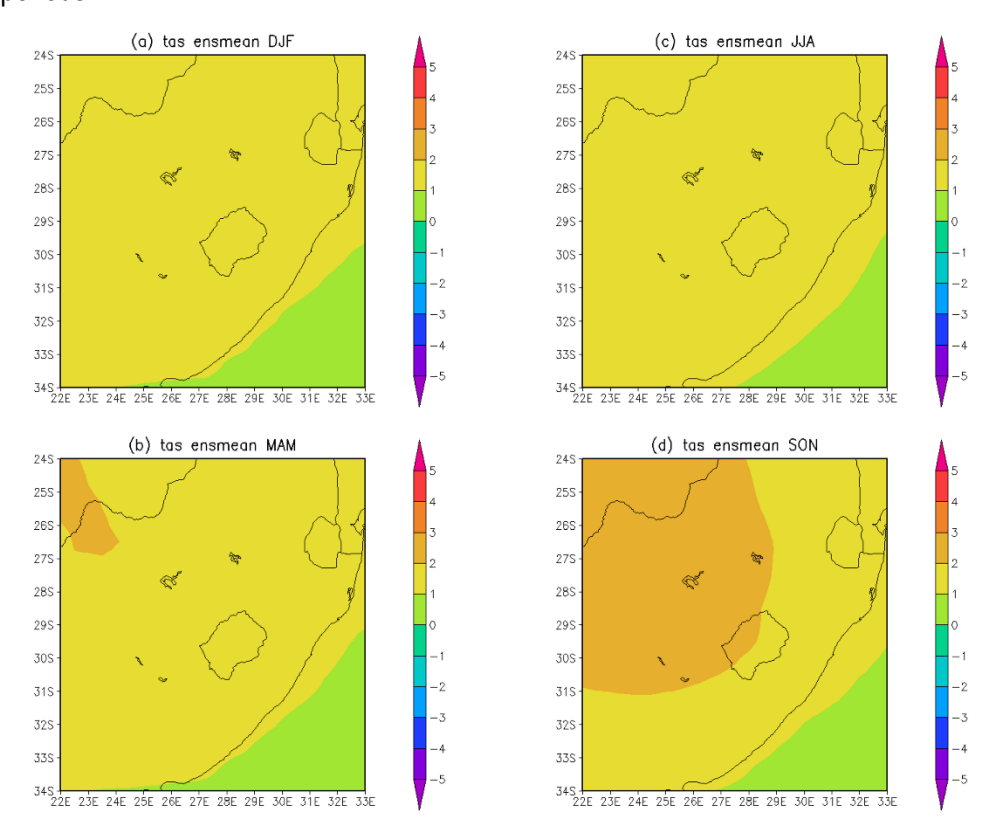


Figure 5.10 Seasonal changes in SAT for SSP5.8-5 between reference climate (1961-1990) and near-future (2021-2050) periods

5.1.2 Far-future (2070-2099)

South African climate, particularly temperature, is regulated by the complex relations between the altitude of the interior plateau, the subcontinent location with respect to the main features of atmospheric circulation, subtropical position, and the oceans on the east and west except for the north (Van Der Walt and Fitchett, 2020). Projections for SAT for the far-future period (2070-2099) are presented below according to seasonal means and seasonal changes for SSP2-4.5 and SSP5-8.5.

5.1.2.1 Seasonal mean SAT for SSP2-4.5 and SSP5-8.5

The projections of the models AWI_CM_1_1_MR, MPI_ESM1_2_LR, IPSL_CM6A_LR, GFDL_ESM4, BCC_CSM2_MR and the ensmean for DJF seasonal mean SATs for SSP2-4.5 during the 2070-2099 period are lower on the Highveld in MP and west and south of KZN (18°C - 21°C). Furthermore, the east of the study area is projected to have higher SATs (21°C to 30°C) in the 2070-2099 period, as shown in Figure 5.11. Overall under SSP2-4.5, the models projected temperature variability over eastern South Africa because of the unevenness of SATs during the summer season. Under SSP5-8.5 only three models (AWI_CM_1_1_MR, MPI_ESM1_2_LR, GFDL_ESM4) projected lower and colder SATs ranging between 18°C - 21°C over the eastern interior of South Africa (Figure 5.15). All six models projected high SATs over a greater portion of the study area under SSP5-8.5 than SSP2-4.5 during the summer season. In the farfuture period, eastern South Africa is projected to be warmer under both mitigation scenarios, and low-pressure systems are likely to occur due to the warm temperatures. According to Engelbrecht et al. (2013), higher temperatures are likely to trigger thunderstorms that lead to heavy rainfall in South Africa.

All six models projected an increase in SATs under both emission scenarios from the 2021-2050 period during the MAM season. Under SSP2-4.5, the models projected SATs that range from 15°C to 27°C over the study area (Figure 5.12). Furthermore, models AWI_CM_1_1_MR, MPI_ESM1_2_LR, and GFDL_ESM4 projected lower SATs of 12°C to 15°C on the west and south of KZN. The projections for MAM seasonal mean SATs for SSP5-8.5 during the 2070-2099 period are not lower compared to the SSP2-4.5 scenario over most of the study area. All six models projected MAM seasonal SATs that range above 18°C to 30°C over the study area, however, models AWI_CM_1_1_MR, MPI_ESM1_2_LR, and GFDL_ESM4 projected lower SATs of 15°C to 18°C on the Highveld in MP, and west and south of KZN, under SSP5-8.5, as shown in Figure 5.16.

During the JJA season, variable SATs are projected over eastern South Africa and are projected to further increase under both emission scenarios from the near-future period (Figure 5.13 and Figure 5.17). The highest SATs projected under both scenarios range from 21°C to 24°C, however, these SATs are projected to occur on the larger part of the east of the study area under SSP5-8.5, as demonstrated by models AWI_CM_1_1_MR, ACCESS_CM2, IPSL_CM6A_LR, and BCC_CSM2_MR in Figure 5.17. This suggests that the east coast of South Africa is projected to be warmer than other regions of the country during the winter season in the far-future period. Colder SATs (< 9°C) are projected by AWI_CM_1_1_MR and GFDL_ESM4 on the west and southwest of KZN under SSP2-4.5.

All six models projected resilient increases in SATs during the spring season from the winter season over the study area. The warmest SATs are projected on the north and east of the study area under both mitigation scenarios, however, under SSP5-8.5 these high SATs occur over larger parts of the above-mentioned regions of the study area, as shown in Figure 5.18. This may mean that much of the warming and drying in the north and east of the study area will occur during the summer and spring seasons. Furthermore, agriculture in MP may be affected in the future because of rising temperatures in southern Africa (Odongo et al. 2022).

5.1.2.2 Seasonal change in SAT for SSP2-4.5 and SSP5-8.5

Different projections of seasonal changes in SATs during the far-future period under both scenarios are presented in Figure 5.19 and Figure 5.20 using the ensmeans of the six CIMP6 models. During the DJF and MAM seasons, under the SSP2-4.5 scenario, SATs are projected to increase between 2°C and 3°C in the far-future period over the study area, which is an increase (by > 1°C) from the near-future period (2021-2050). Furthermore, the SATs are projected to further increase (from 3°C to 4°C) over the Highveld in MP and NW of KZN under SSP2-4.5 during the JJA season, as shown in Figure 5.19 (c). During the SON season, the Highveld and Lowveld in MP and the entire west of KZN are also projected to have SAT increase ranging from 3°C to 4°C and the southeast of MP and the east of KZN are projected to increase from 2°C to 3°C. Projections of seasonal change in SATs for SSP5-8.5 in the 2070-2099 period show an increase from the 2021-2050 period and the SSP2-4.5 of the 2070-2099 period. According to Petja et al. (2021), it is projected that southern Africa will become drier and warmer under low-mitigation climate change futures, thus leaving little room for adaptation in the area that is projected to have high temperatures. Under SSP5-8.5, the study area is projected to be dominated by an increase of 4°C to 5°C during summer, autumn, and winter seasons except for the entire east of KZN which is projected to an increase in SATs that range from 3°C to 4°C.

Furthermore, during the spring season, the Highveld as a whole and a part of Lowveld in MP are projected to an increase in SATs (> 5°C), and the remaining regions of the study area are projected to an increase in SATs that are between 3°C and 5°C (Figure 5.20 (d)).

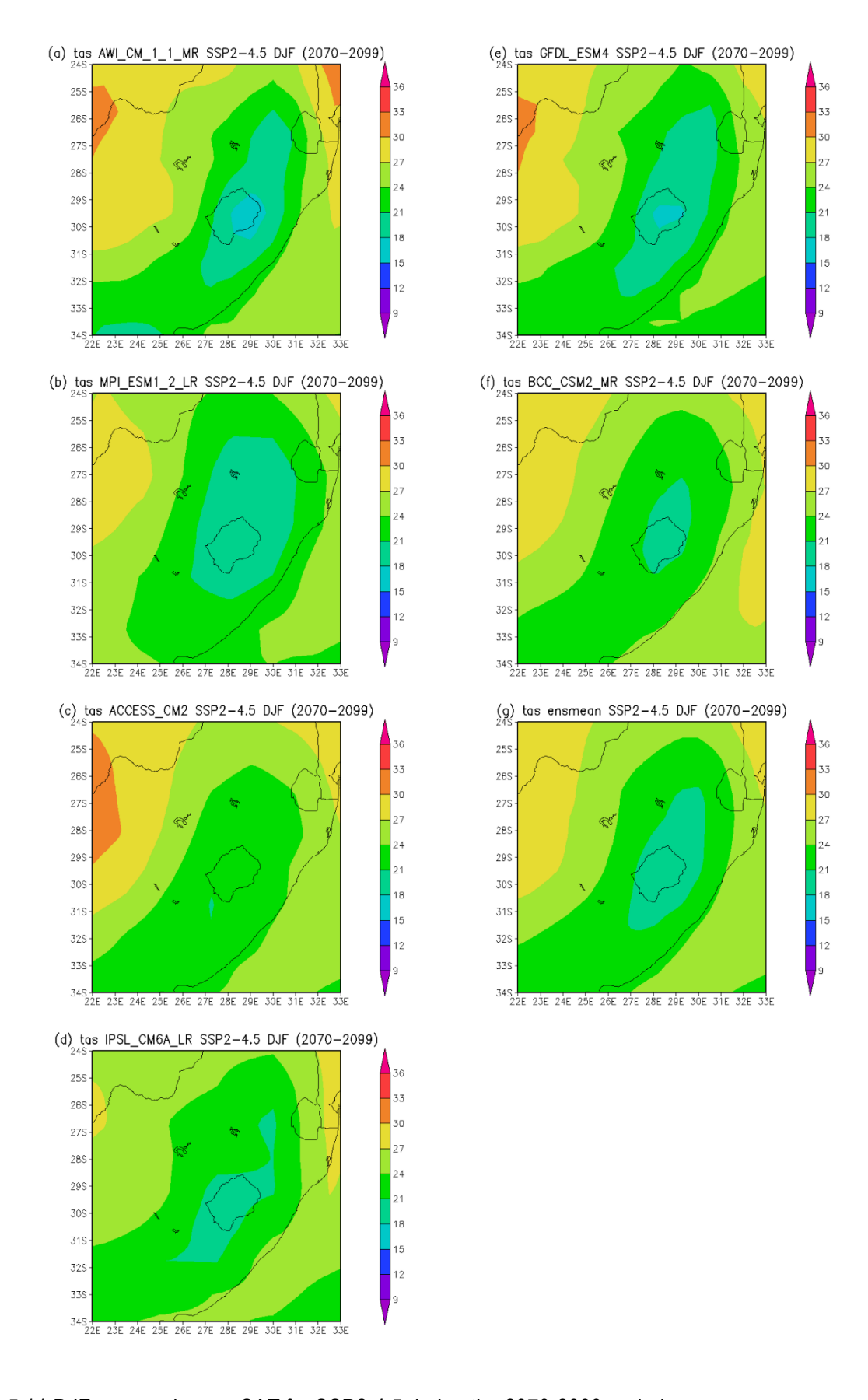


Figure 5.11 DJF seasonal mean SAT for SSP2-4.5 during the 2070-2099 period

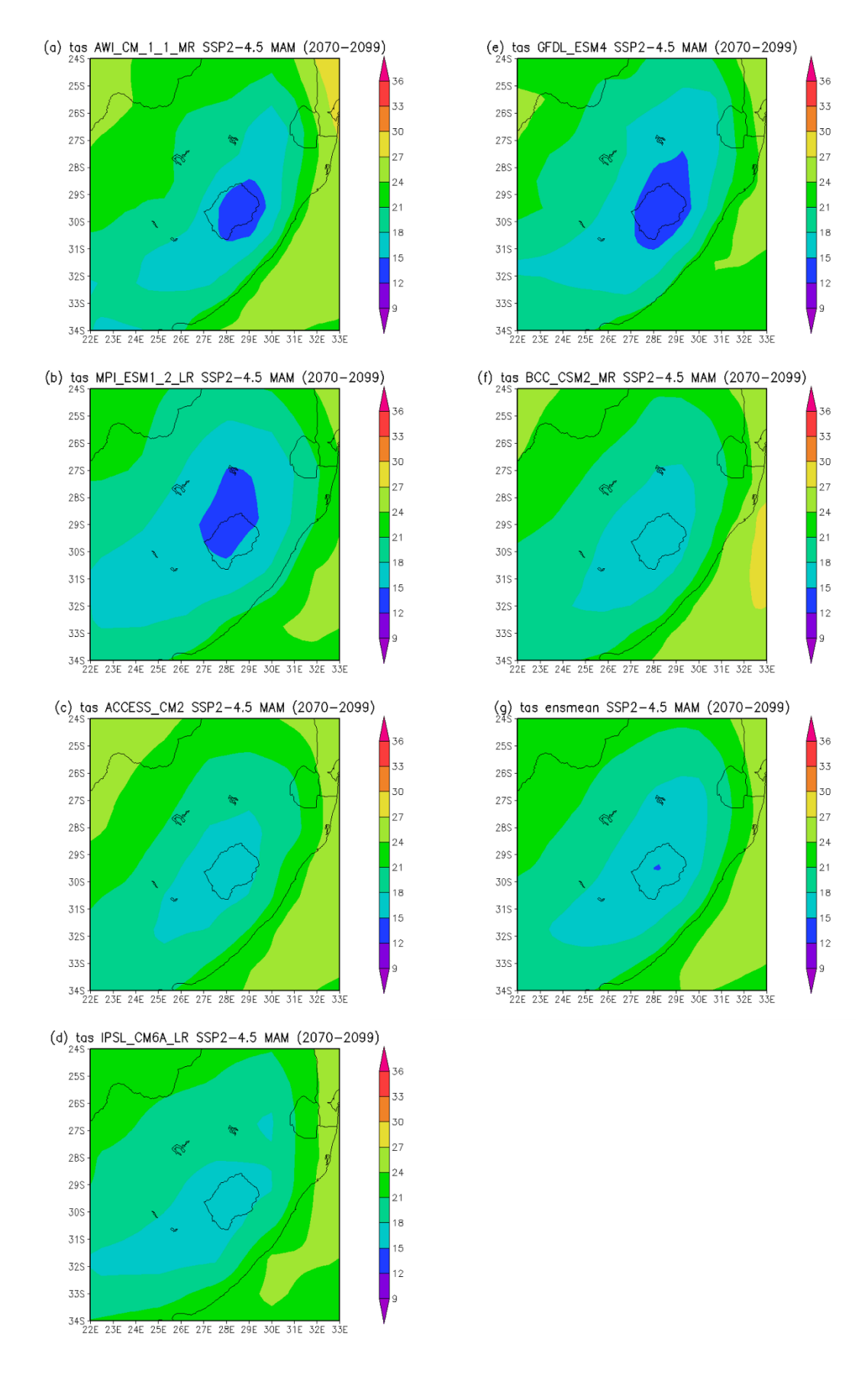


Figure 5.12 MAM seasonal mean SAT for SSP2-4.5 during the 2070-2099 period

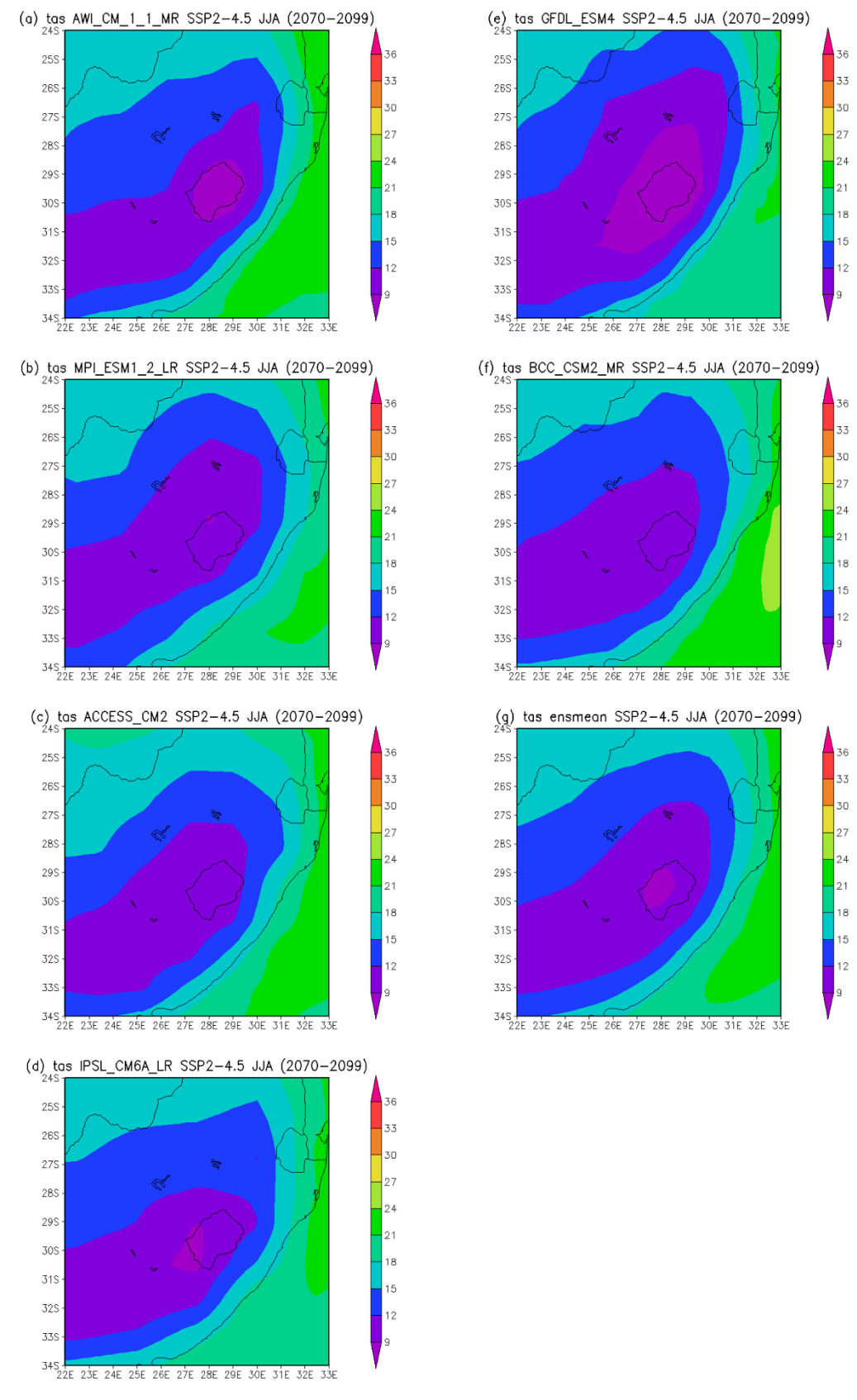


Figure 5.13 JJA seasonal mean SAT for SSP2-4.5 during the 2070-2099 period

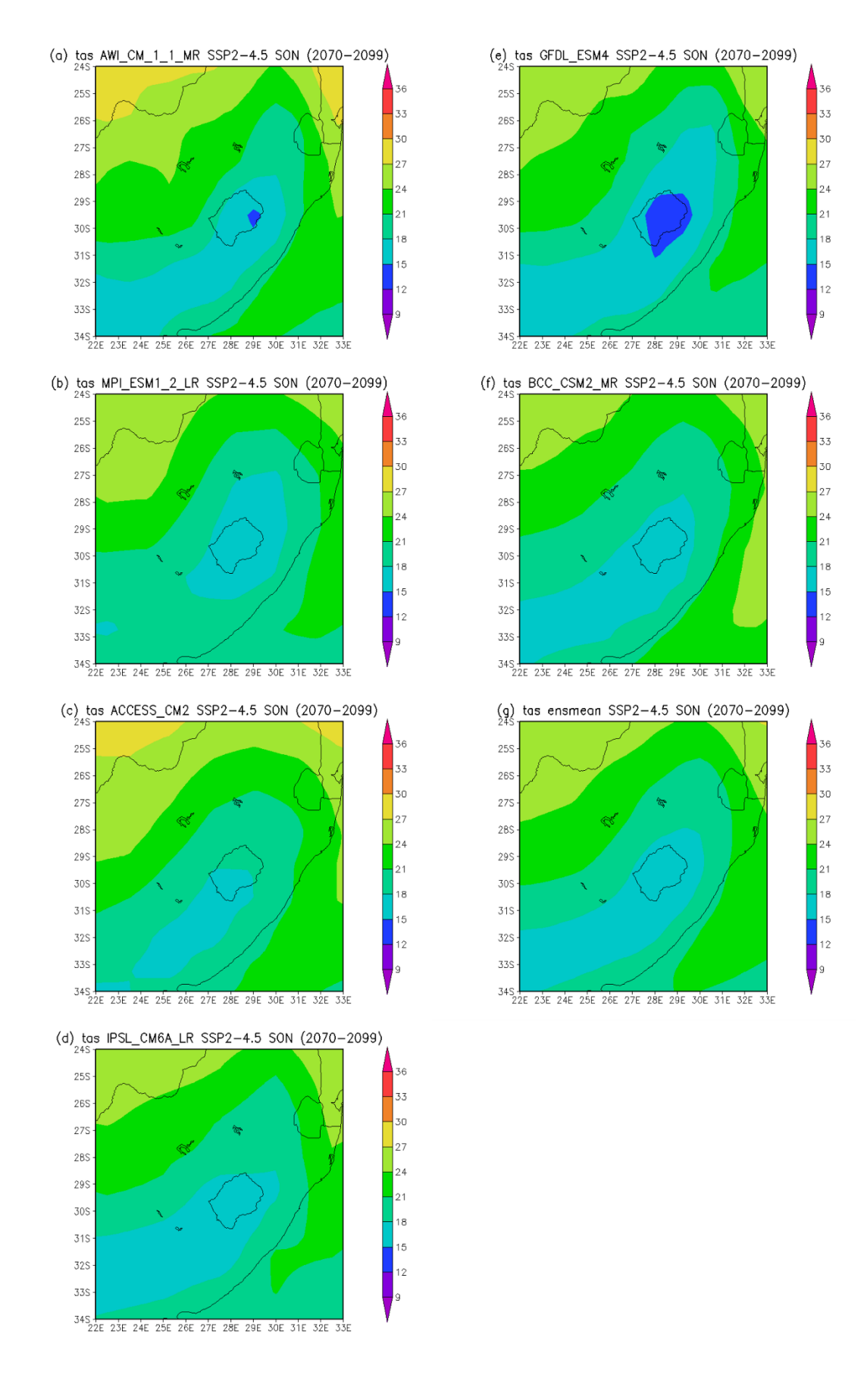


Figure 5.14 SON seasonal mean SAT for SSP2-4.5 during the 2070-2099 period

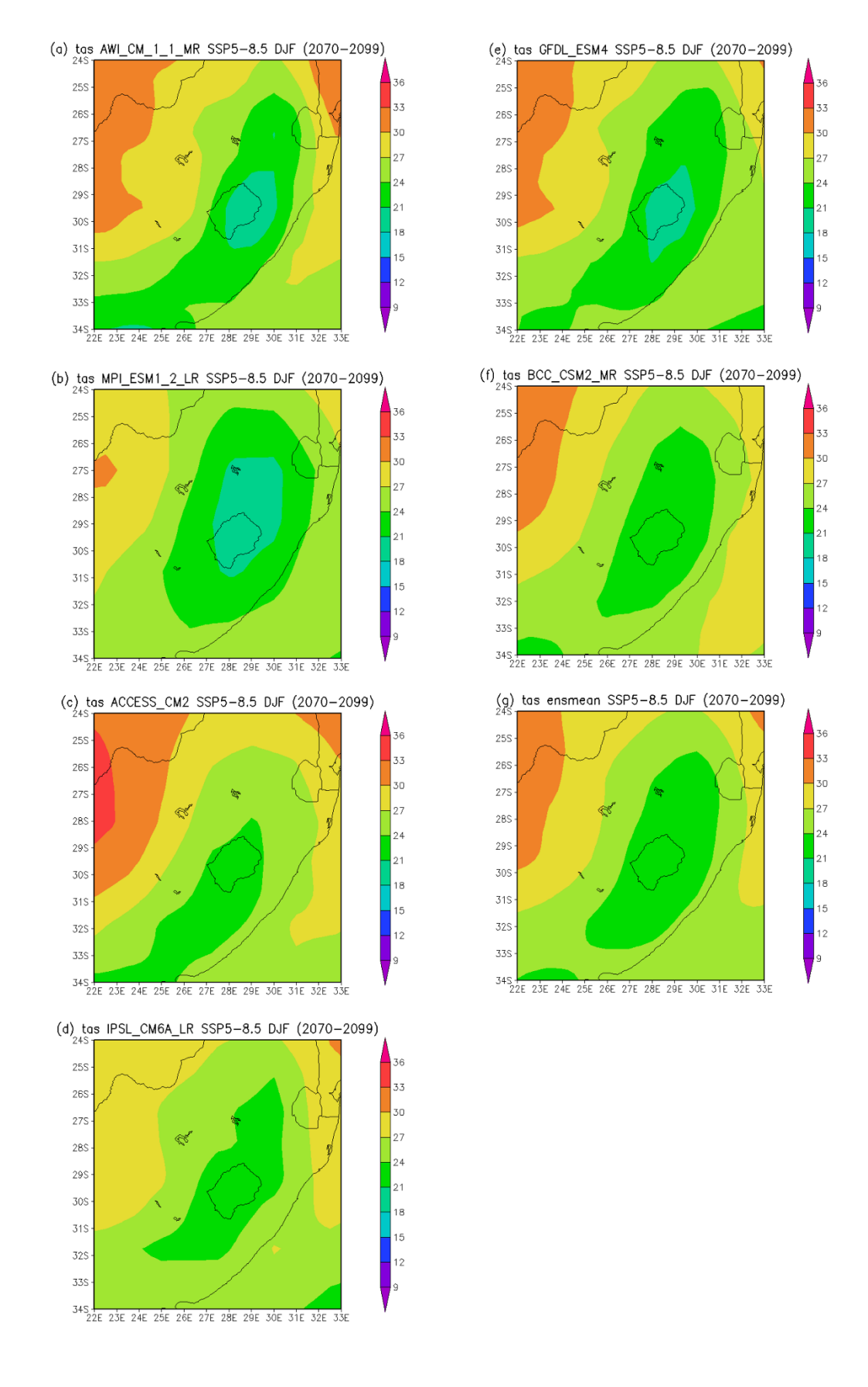


Figure 5.15 DJF seasonal mean SAT for SSP5-8.5 during the 2070-2099 period

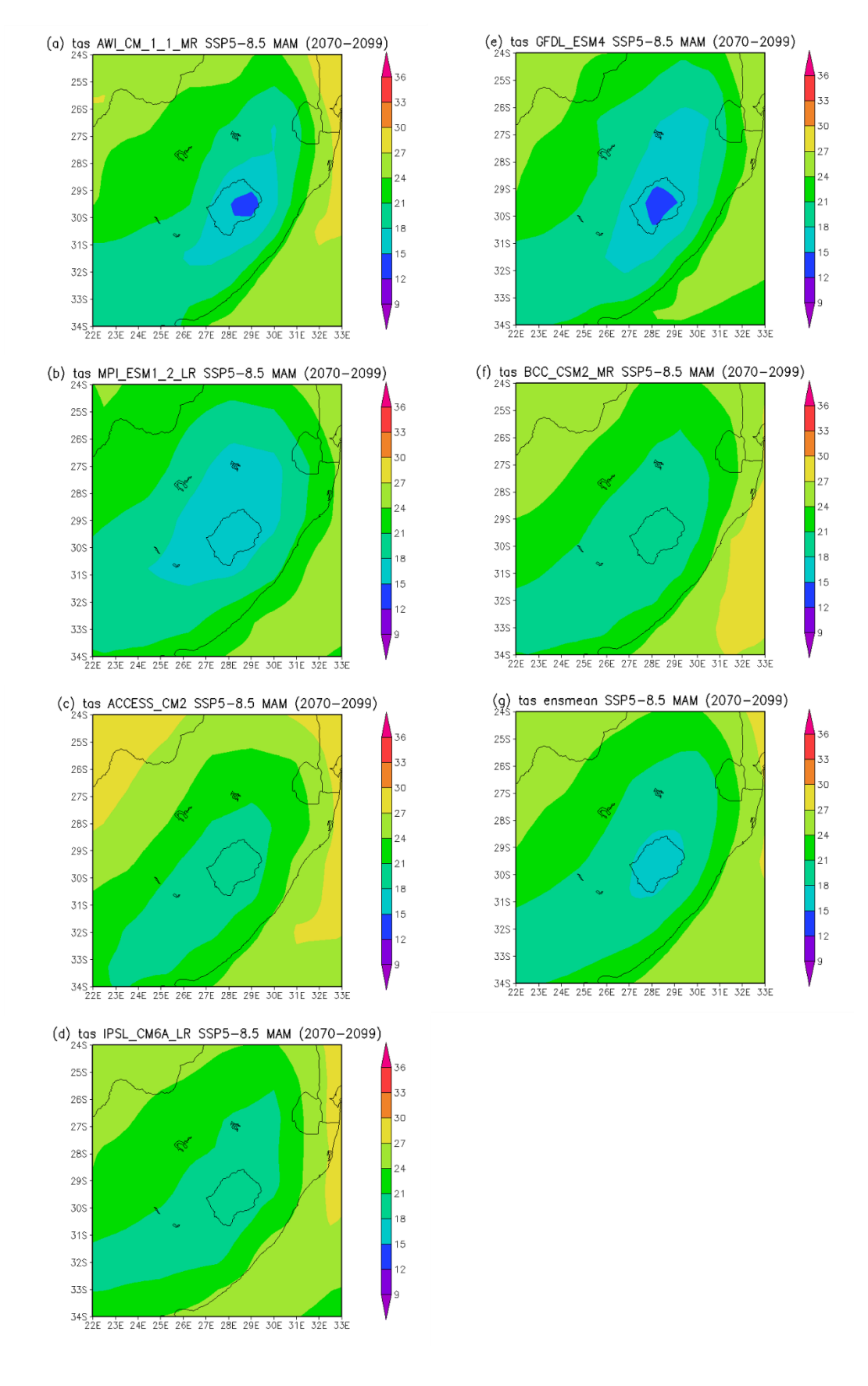


Figure 5.16 MAM seasonal mean SAT for SSP5-8.5 during the 2070-2099 period

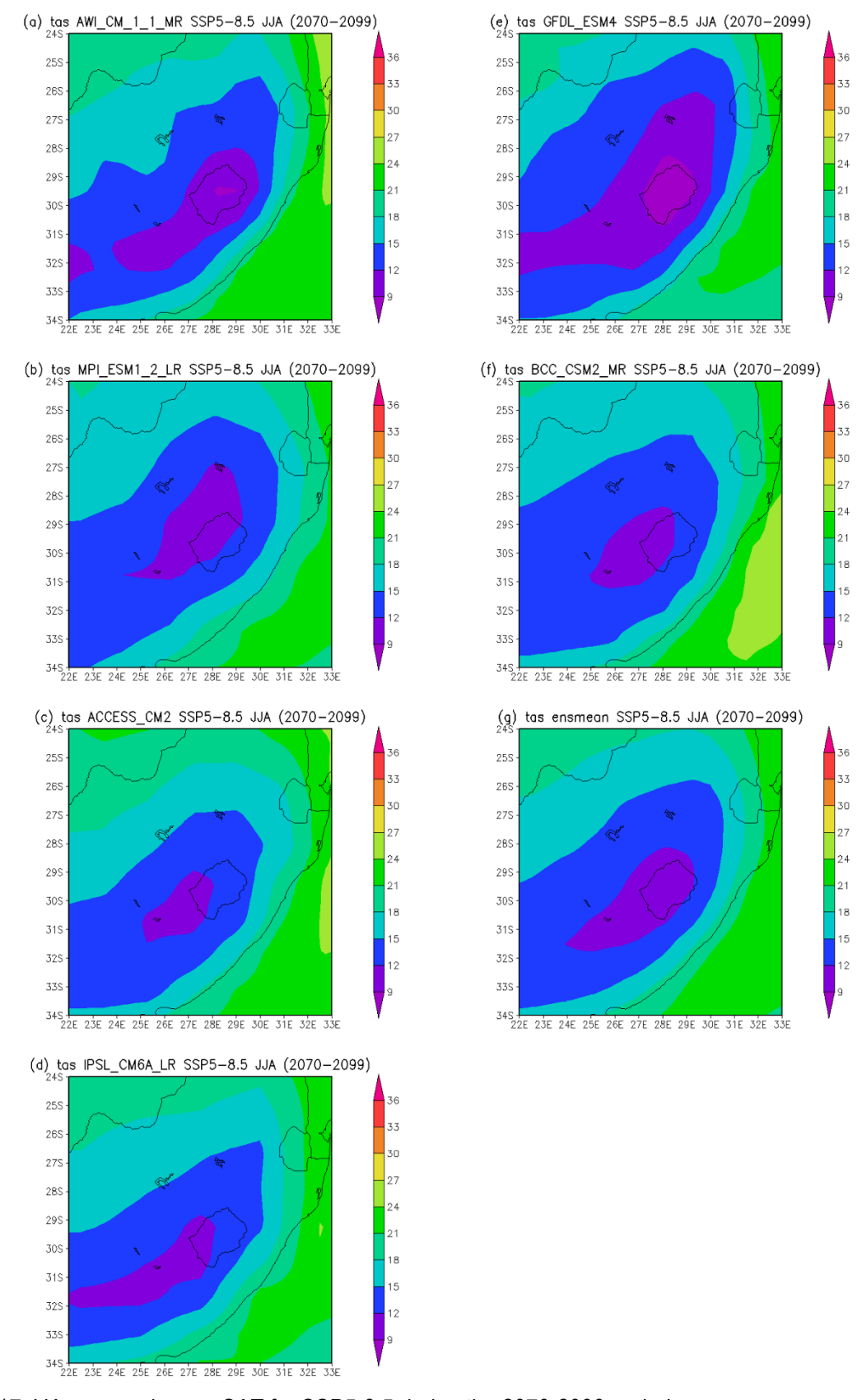


Figure 5.17 JJA seasonal mean SAT for SSP5-8.5 during the 2070-2099 period

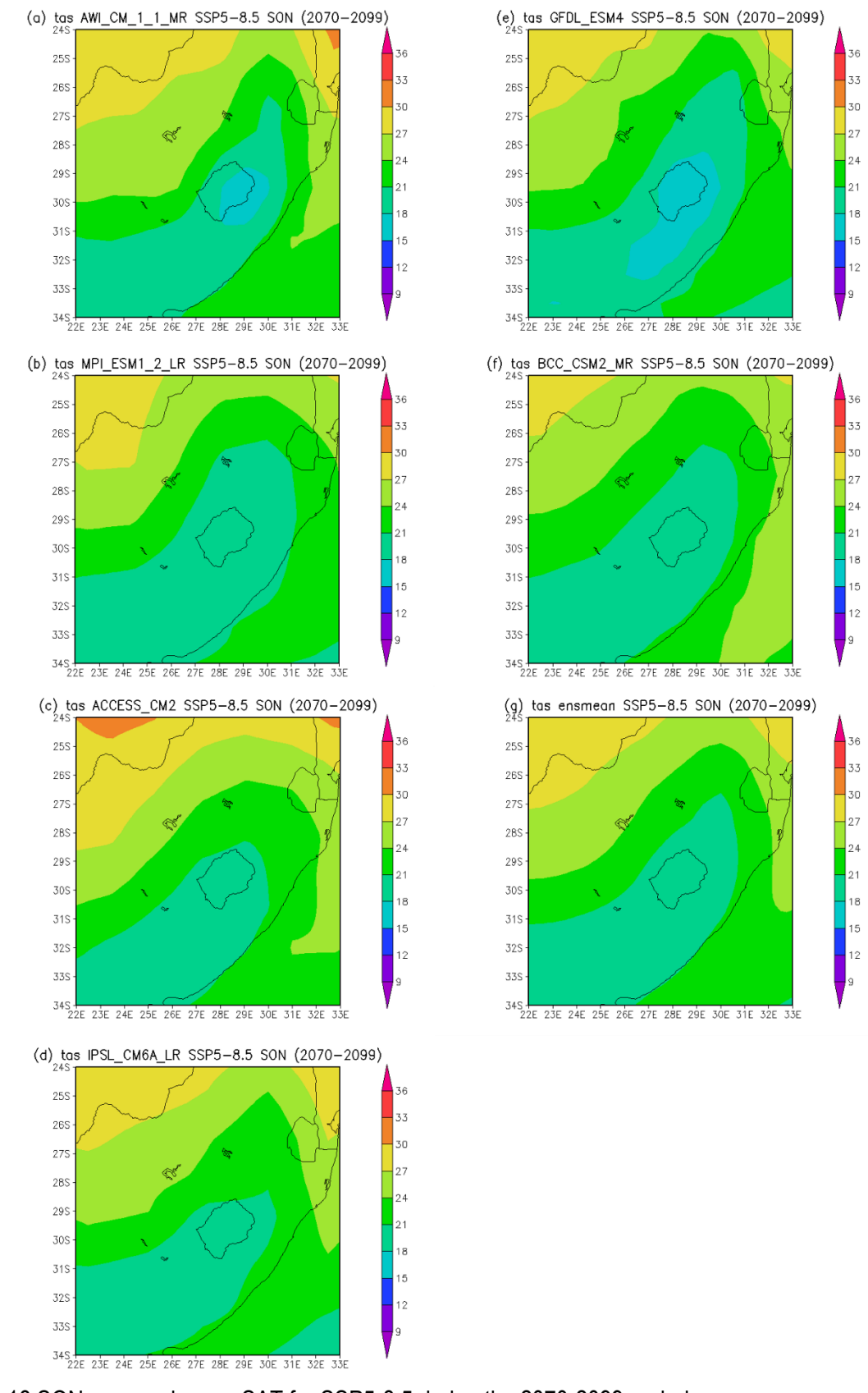


Figure 5.18 SON seasonal mean SAT for SSP5-8.5 during the 2070-2099 period

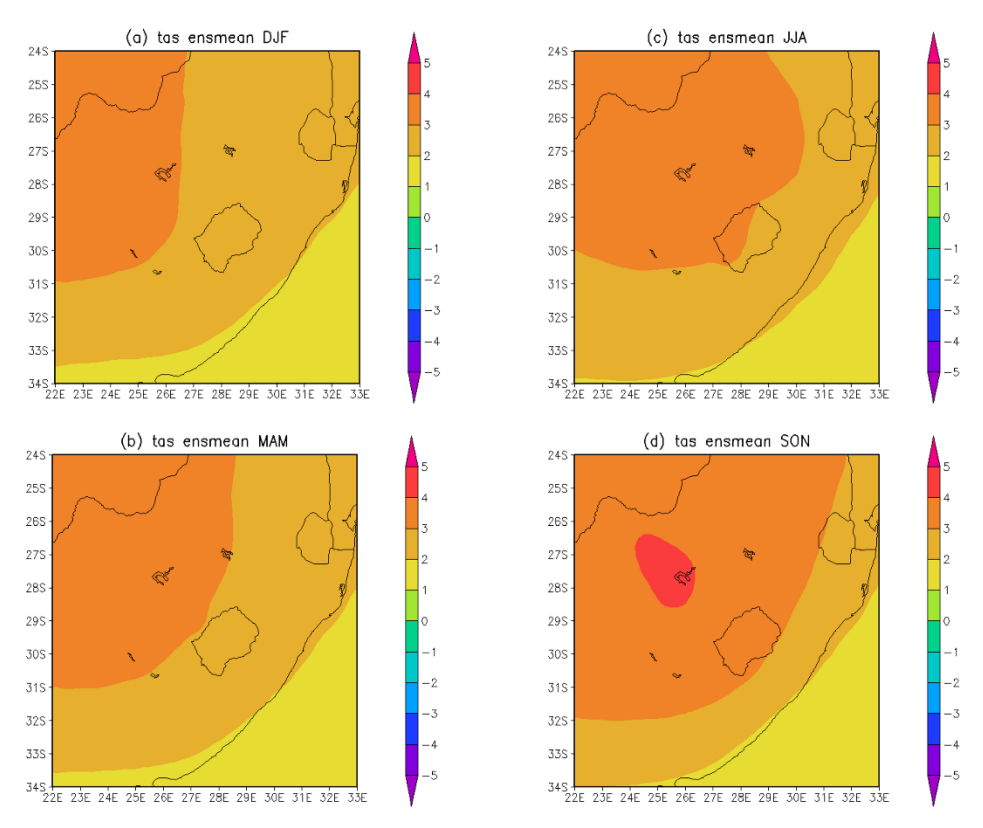


Figure 5.19 Seasonal changes in SAT for SSP2-4.5 between reference climate (1961-1990) and far-future (2070-2099) periods

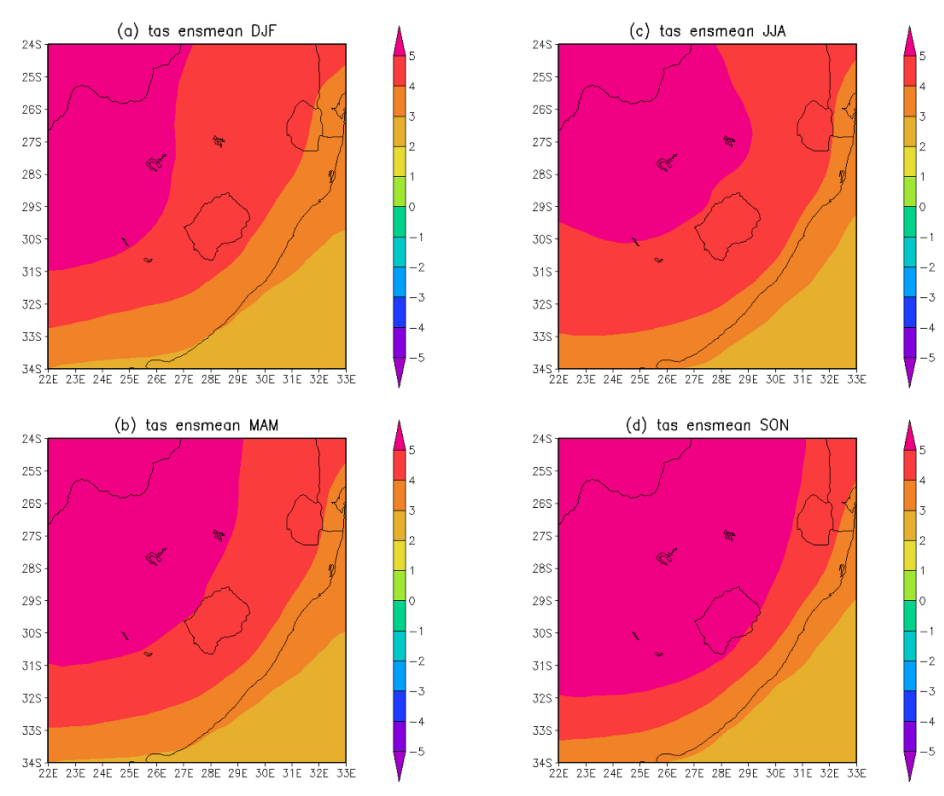


Figure 5.20 Seasonal changes in SAT for SSP5-8.5 between reference climate (1961-1990) and far-future (2070-2099) periods

5.2 Future projections of rainfall over the study area

5.2.1 Near-future (2021-2050)

South Africa's east coast is one of the regions in the country that are affected by heavy rainfall events that usually cause socio-economic impacts (Favre et al. 2013). Future rainfall projections were made for SSP2-4.5 and SSP5-8.5, and the results of the projections are presented using seasonal means. Seasonal changes in rainfall for SSP2-4.5 and SSP5-8.5, are also presented below.

5.2.1.1 Seasonal mean rainfall for SSP2-4.5 and SSP5-8.5

ENSO controls dry and wet events during summer rainfall seasons in South Africa (Archer et al. 2017). DJF seasonal mean rainfall for SSP2-4.5 and SSP5-8.5 are presented below in Figure 5.21 and Figure 5.25 respectively, during the 2021-2050 period. The models projected the highest rainfall over eastern South Africa compared to other parts of the country during the summer season in the near-future under both mitigation scenarios. According to all six models and the ensmean, KZN will experience more summer rainfall than MP (particularly north of the province), and the models ACCESS_CM2, and IPSL_CM6A_LR projected the highest rainfall that ranges from 120 mm/month to 320 mm/month under SSP2-4.5 in KZN. Furthermore, under the low mitigation scenario (SSP5-8.5), IPSL_CM6A_LR projected 320 mm/month to 360 mm/month of summer rainfall in KZN on the tip of the northeast of Lesotho. Model MPI_ESM1_2_LR projected the lowest summer rainfall for both scenarios. This may suggest the severe intensity of rainfall that may lead to floods over the study area in the 2021-2050 period. TCs are likely to occur over the study area during the summer season in the near-future period. According to Chikoore et al. (2021), TCs taking place over SWIO affect the east coast of South Africa during summer, and they cause heavy rainfall that leads to floods.

During the MAM season, the models projected higher rainfall over the study area (particularly KZN, including EC) in the near-future period compared to other regions of the country, however, the autumn rainfall is projected to decrease from the summer rainfall (Figure 5.22 and Figure 5.26). According to Ncube (2019), rainfall usually decreases in the east of South Africa during the transition season compared to DJF season. The autumn rainfall is projected to range from below 40 mm/month to 200 mm/month under both scenarios amongst the models, with the north of MP projected by AWI_CM_1_1_MR to have the lowest rainfall (< 40 mm/month) and the south of KZN projected by IPSL_CM6A_LR to receive the highest rainfall (160 mm/month to 200 mm/month) under the moderate to high mitigation scenario (SSP2-4.5). The autumn season is

associated with COLs that have caused floods in the past that led to damage to infrastructure and the death of people in KZN (Singh et al. 2022; Thambiran et al. 2023). COLs occur throughout the whole year, however, they are at their peak during the autumn season bringing heavy rainfall strongly over the south and east coasts of South Africa (Favre et al. 2012; Favre et al. 2013).

According to Engelbrecht et al. (2009), South Africa experiences the driest weather conditions during the winter season. The model projections for both scenarios show that the east coast of KZN is projected to receive more winter rainfall than the rest of the study area. Models ACCESS_CM2, and IPSL_CM6A_LR projected rainfall that ranges between 40 mm/month to 80 mm/month on the south of MP (Highveld), and ACCESS_CM2 projected the highest rainfall (80 mm/month to 120 mm/month) on the east coast of KZN (Figure 5.23 and Figure 5.27). This may mean that places such as Durban are likely to experience more rainfall compared to other places (such as Nelspruit, MP) in the study area during this driest season in South Africa. All models under both mitigation scenarios projected resilient increases in spring rainfall (40 mm/month to 280 mm/month) from the winter season. Under both scenarios, model ACCESS_CM2 projected the highest rainfall in KZN ranging from 120 mm/month to 280 mm/month, however, under SSP5-8.5 (Figure 5.28), this model projected that the highest projected spring rainfall over the study area will occur on a larger part of KZN.

5.2.1.2 Seasonal change in rainfall for SSP2-4.5 and SSP5-8.5

Variable seasonal changes in rainfall over eastern South Africa are demonstrated in Figure 5.29 and Figure 5.30 for SSP2-4.5 and SSP5-8.5 respectively, for the 2021-2050 period. The projections of seasonal changes over the study area are different for both scenarios. During the summer season, under SSP2-4.5, rainfall is projected to decrease over the Highveld and to increase over the Lowveld in MP. Moreover, regions, where Durban is located, are projected to receive lesser summer rainfall under the moderate to high mitigation scenario. This may mean that the Highveld in MP might experience droughts in the near-future, as the models projected an extreme decline in summer rainfall. Furthermore, agriculture in MP may be affected by below-average rainfall in the future. According to Odongo et al. (2022), one of the extreme weather events that affect the agricultural produce of southern Africa is drought. During the MAM season, in the central interior of MP (<-2 mm/month), the rainfall is projected to decline whereas in the interior going south of KZN the rainfall is projected to extremely increase (> 5 mm/month) compared to the rest of the study area under SSP2-4.5. In winter and spring, the rainfall is projected to decrease to below -5 mm/month over the majority

of the study area but the rainfall in the north of MP is projected to decrease to below -3 mm/month in winter. Under SSP5-8.5, an increase in summer rainfall (> 2 mm/month) is projected over most regions of the study area, particularly the east coast. The models under SSP2-4.5, projected the rainfall over the Highveld in MP to decline (< -1 mm/month) as well under SSP5-8.5, however, the magnitude of change is not the same. Rainfall is projected to increase over KZN under the low mitigation scenario lesser compared to SSP2-4.5 and to decrease less in MP during autumn. During the winter season, the rainfall is projected to occur and decrease unevenly according to different regions over the study area. The KZN province will experience less decrease in winter rainfall compared to MP under SSP5-8.5. The rainfall projection changes during the spring season under both scenarios are the same over MP (< -5 mm/month), however, over the east of KZN, the rainfall is projected to decrease less (< -1 mm/month) under SSP5-8.5 compared to SSP2-4.5 (< -5 mm/month over majority of KZN) and increase in the south of KZN (> 0 mm/month) to EC.

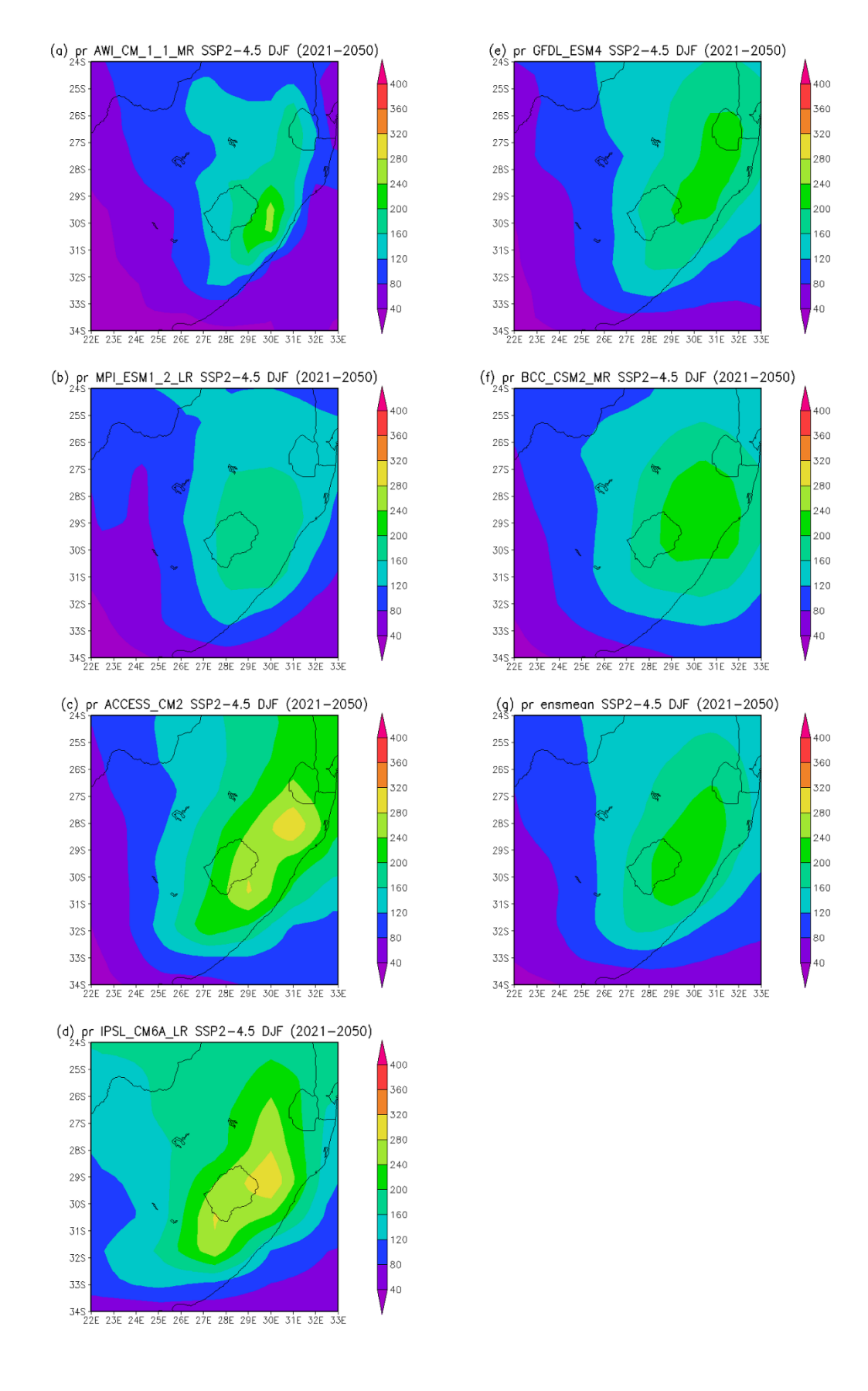


Figure 5.21 DJF seasonal mean rainfall for SSP2-4.5 during the 2021-2050 period

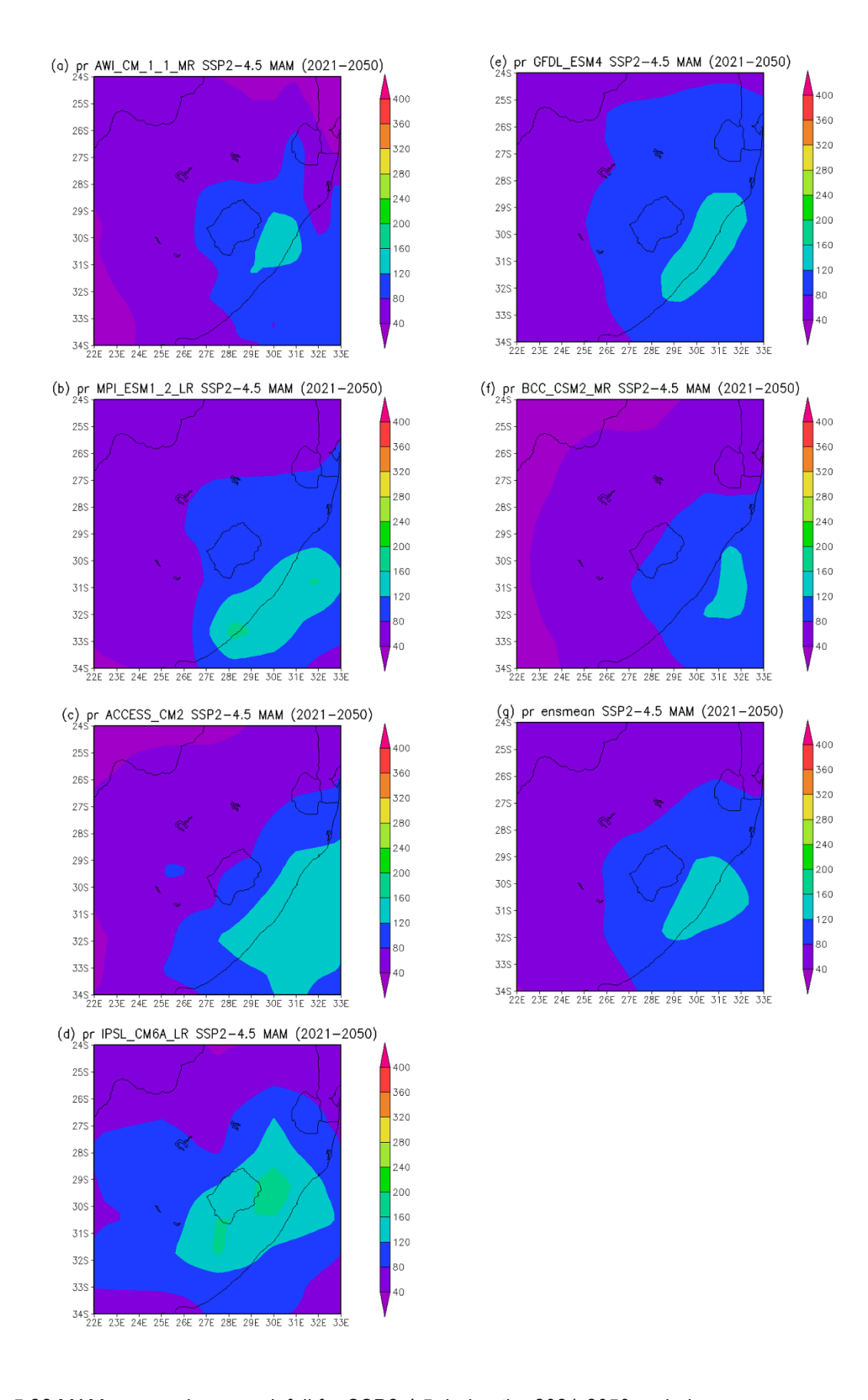


Figure 5.22 MAM seasonal mean rainfall for SSP2-4.5 during the 2021-2050 period

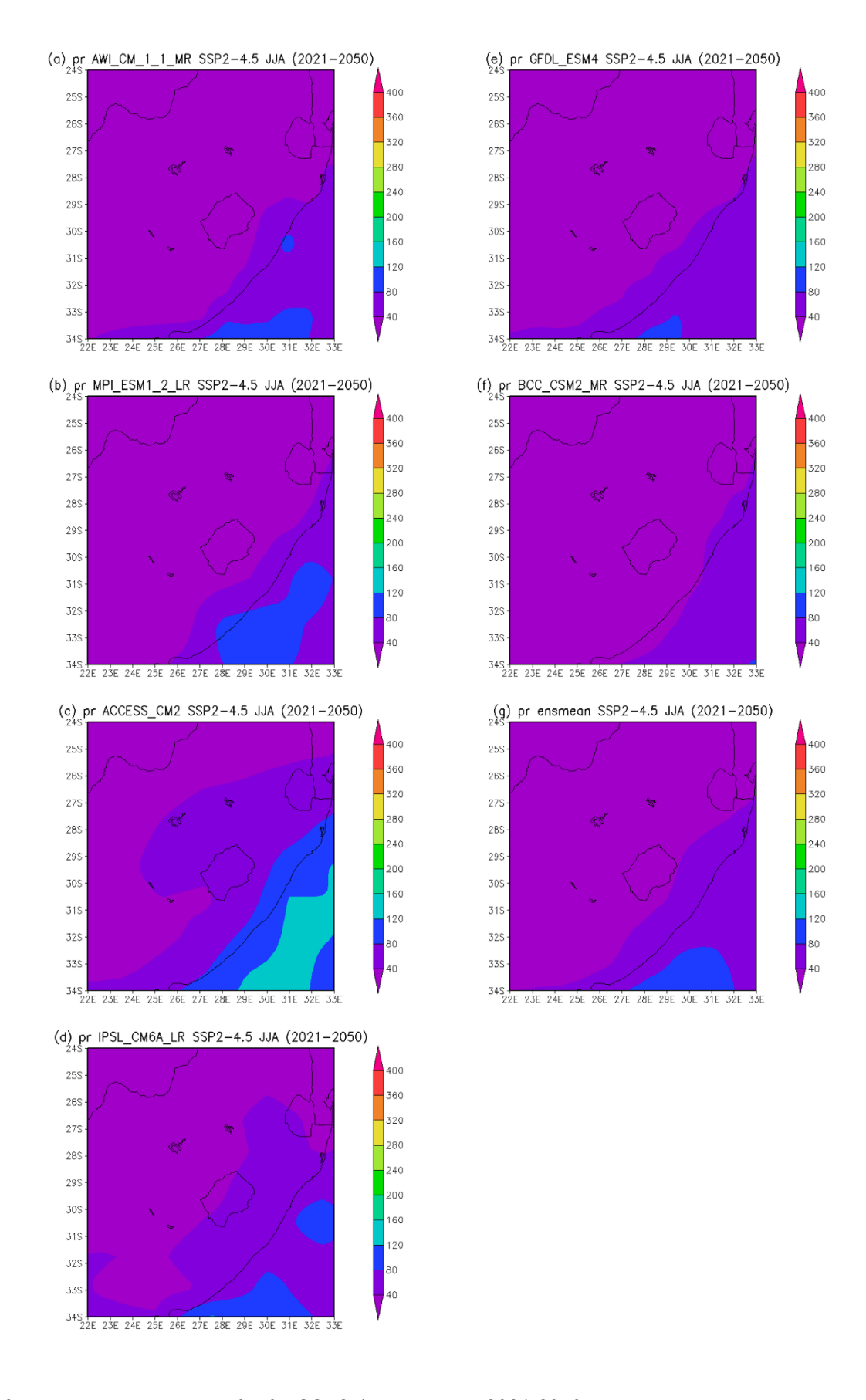


Figure 5.23 JJA seasonal mean rainfall for SSP2-4.5 during the 2021-2050 period

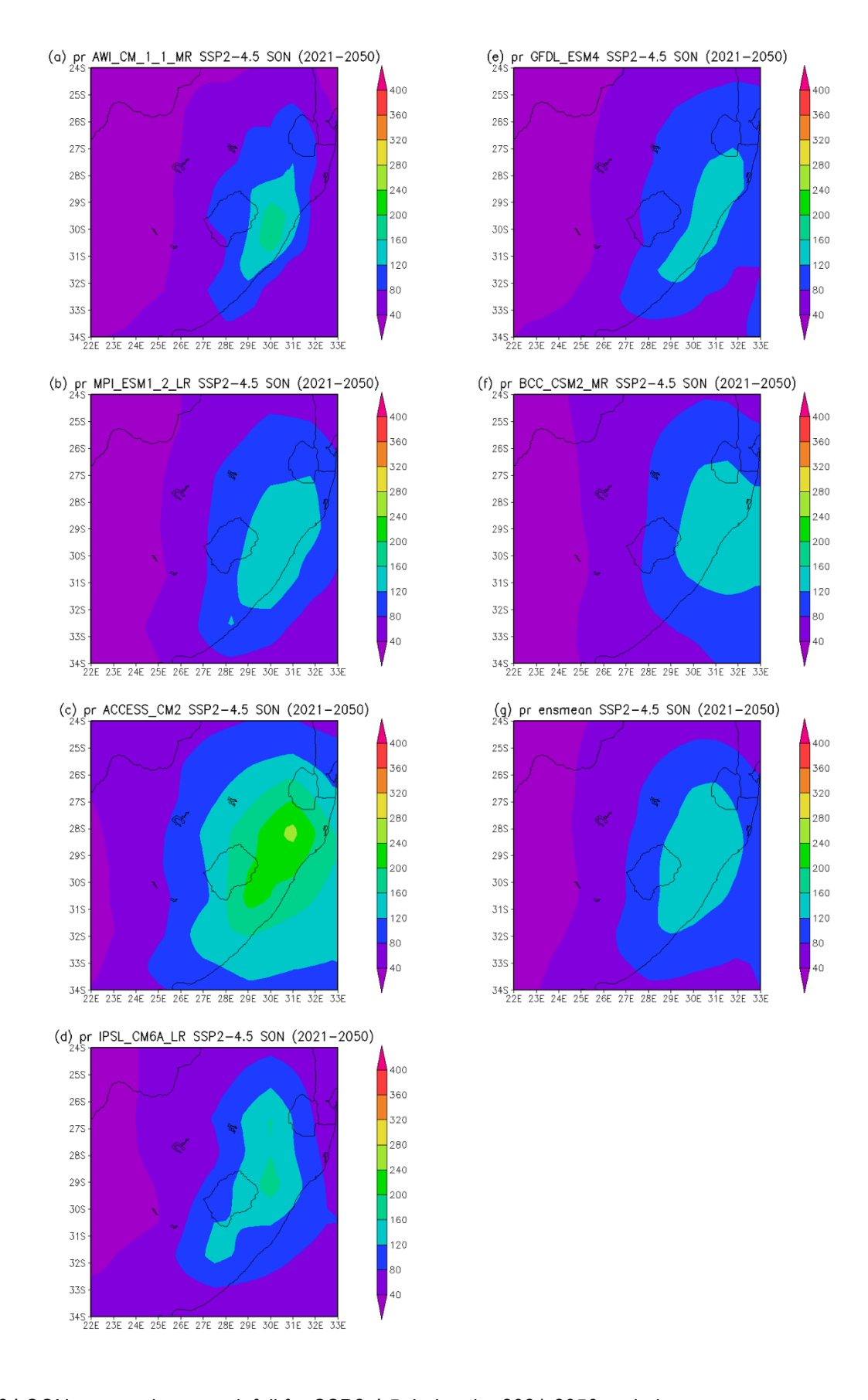


Figure 5.24 SON seasonal mean rainfall for SSP2-4.5 during the 2021-2050 period

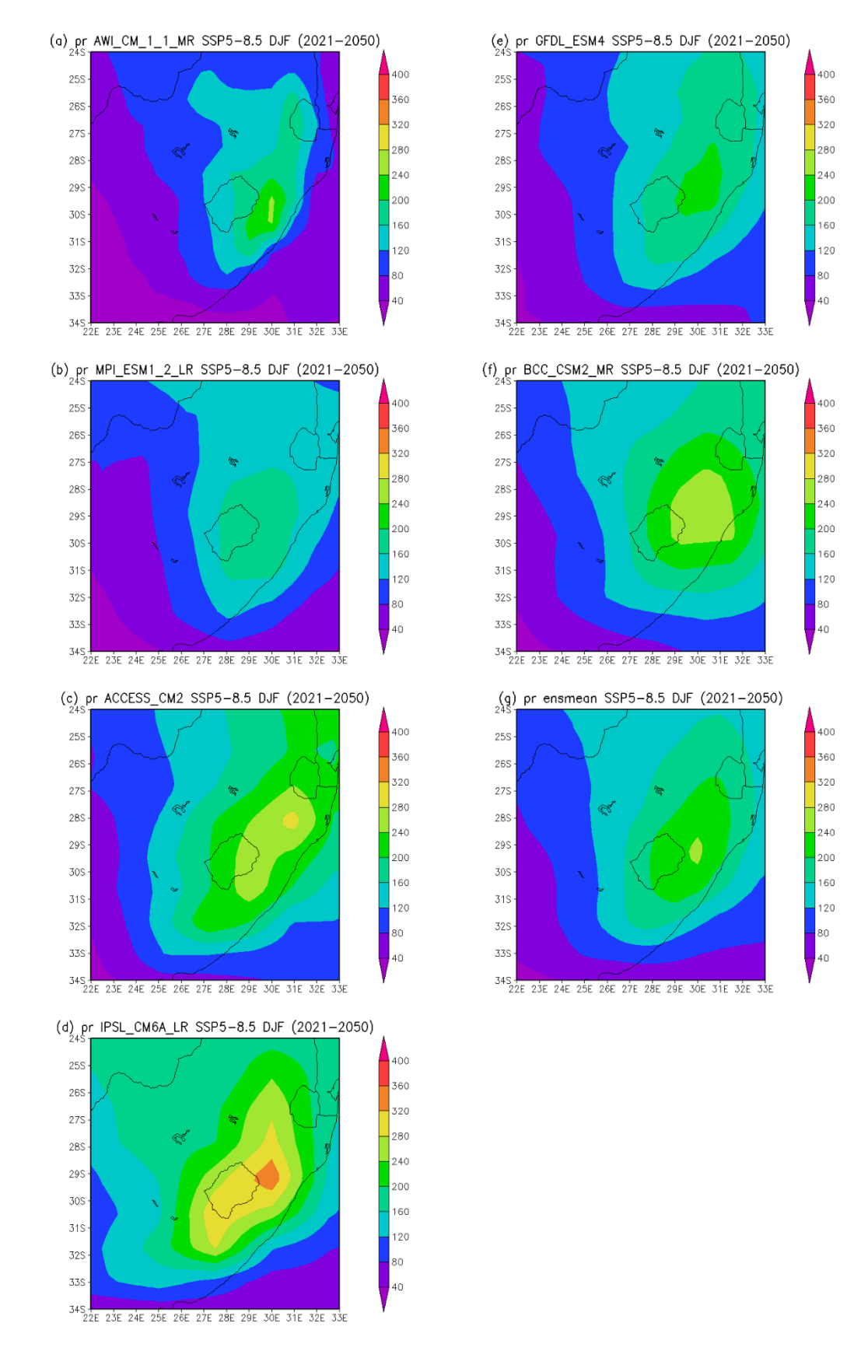


Figure 5.25 DJF seasonal mean rainfall for SSP5-8.5 during the 2021-2050 period

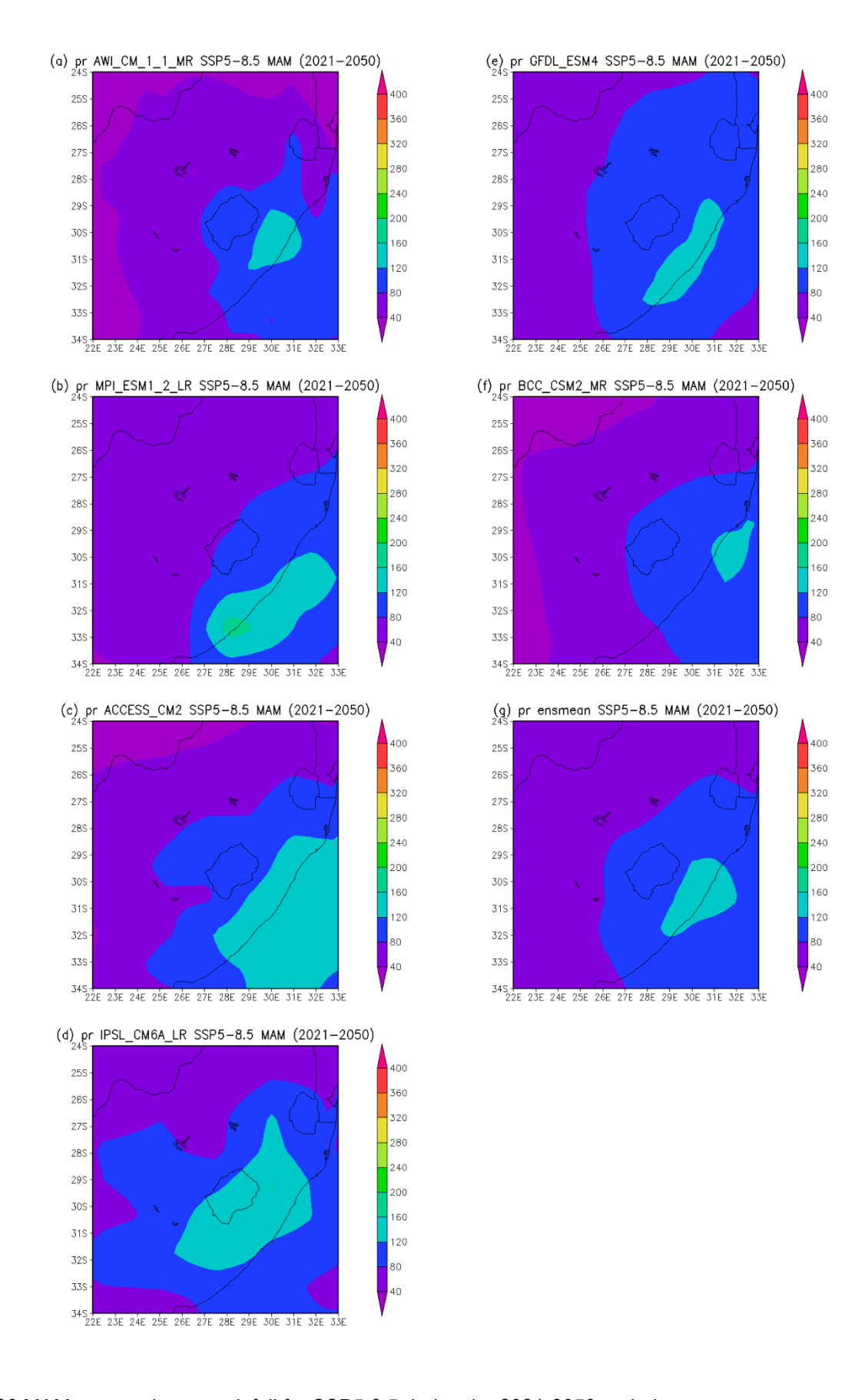


Figure 5.26 MAM seasonal mean rainfall for SSP5-8.5 during the 2021-2050 period

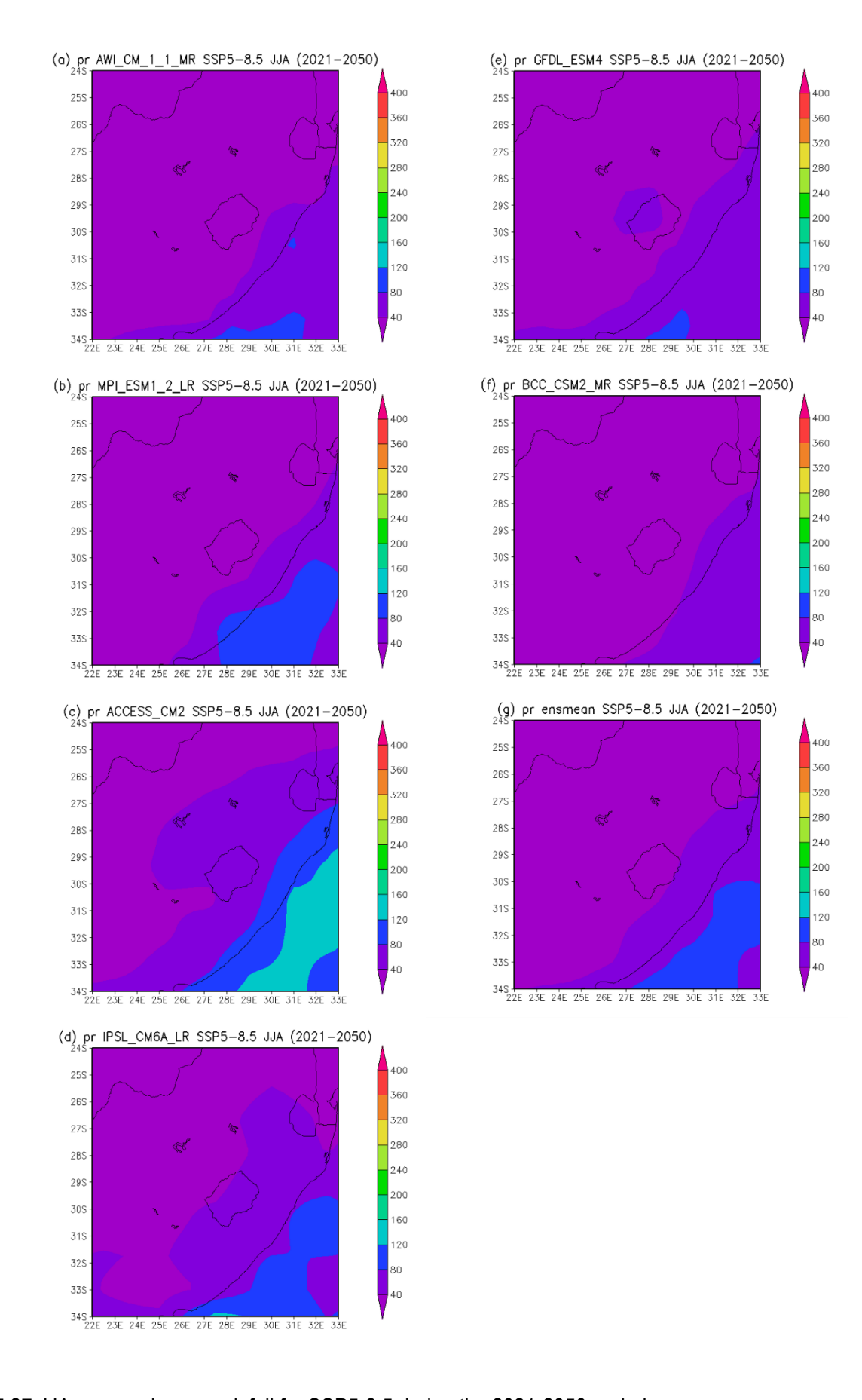


Figure 5.27 JJA seasonal mean rainfall for SSP5-8.5 during the 2021-2050 period

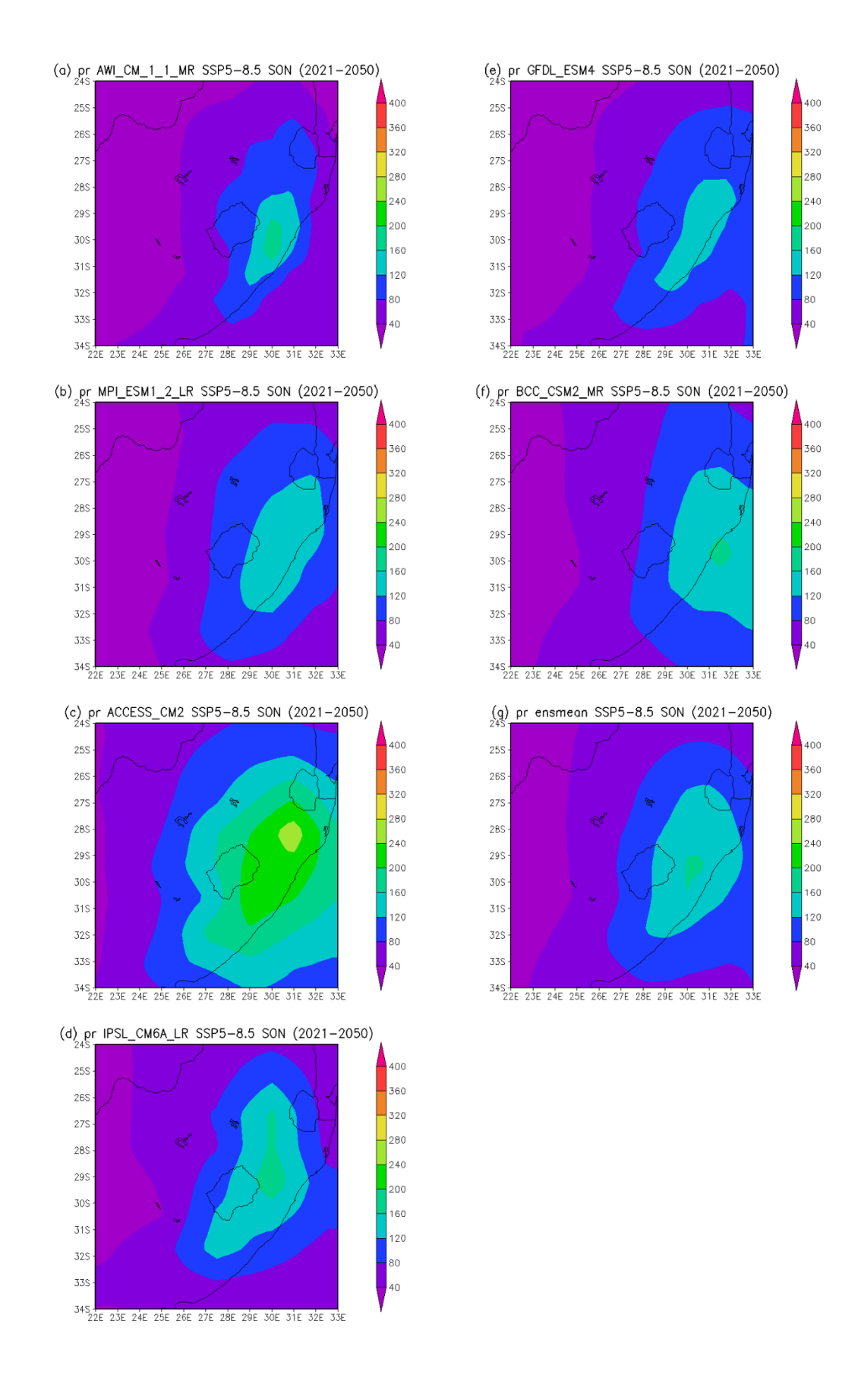


Figure 5.28 SON seasonal mean rainfall for SSP5-8.5 during the 2021-2050 period

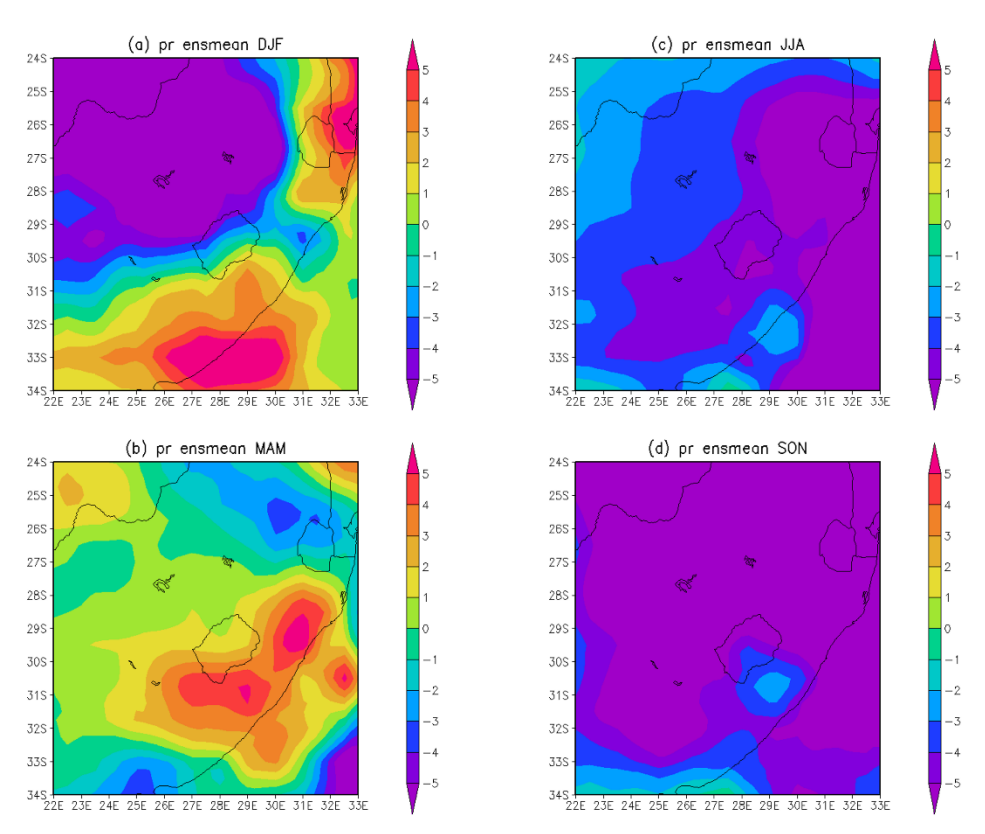


Figure 5.29 Seasonal changes in rainfall for SSP2-4.5 between reference climate (1961-1990) and near-future (2021-2050) periods

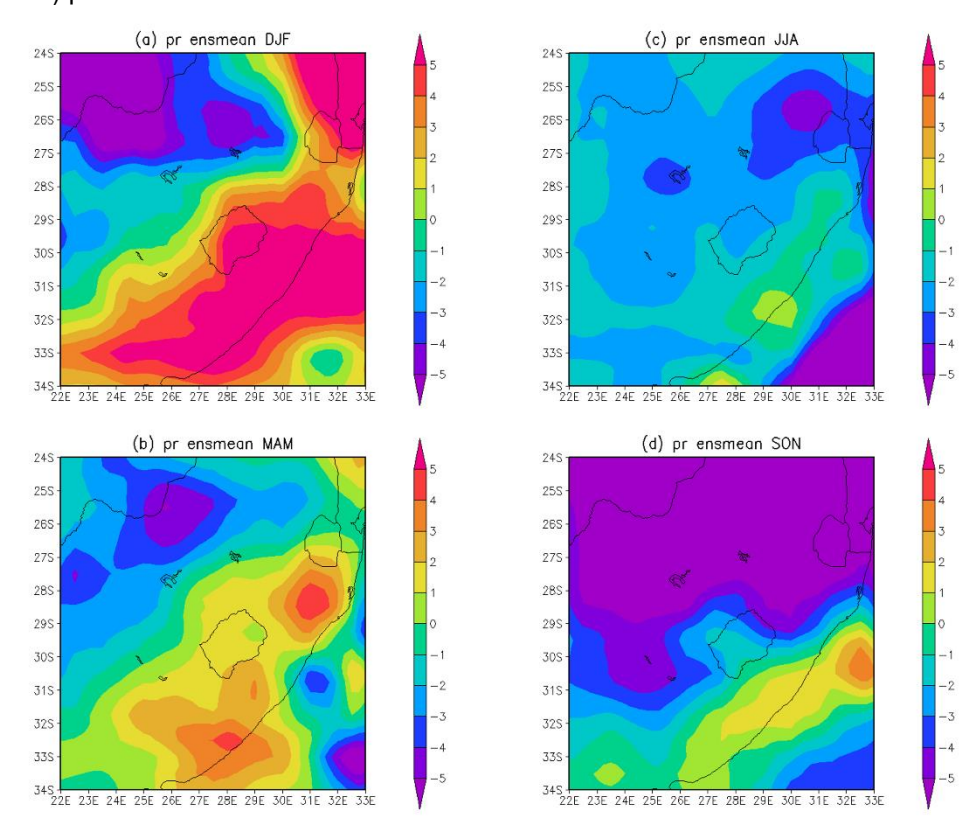


Figure 5.30 Seasonal changes in rainfall for SSP5-8.5 between reference climate (1961-1990) and near-future (2021-2050) periods

5.2.2 Far-future (2070-2099)

According to Jury et al. (2018), research conducted on South African climate trends, did not produce significant results of changes in rainfall between 1980 and 2014, except for a region closer to Cape Town. Due to the highly variable climate, South Africa has different trends of rainfall. Below is the presentation of far-future projections for rainfall using the seasonal means and changes under SSP2-4.5 and SSP5-8.5.

5.2.2.1 Seasonal mean rainfall for SSP2-4.5 and SSP5-8.5

According to Ibebuchi (2023), in South Africa high rainfall is experienced during the summer season compared to other seasons. The projected summer rainfall ranges from 40 mm/month to 360 mm/month over the study area in the far-future period under SSP2-4.5 and AWI_CM_1_1_MR projected the lowest rainfall (40 mm/month to 200 mm/month) over MP. The models ACCESS_CM2, and IPSL_CM6A_LR projected the highest rainfall over the study area followed by BCC_CSM2_MR, under both mitigation scenarios compared to other models (Figure 5.31 and Figure 5.35). However, these models projected higher summer rainfall over the study area to occur over a larger area under SSP5-8.5 compared to SSP2-4.5. This shows that under a low mitigation scenario, heavy rainfall is projected to occur (which may cause floods) and affect a lot of places in the study area, such as Ladysmith, Newcastle, and Pongola.

The KZN province (particularly the east coast) is projected to receive the highest autumn rainfall and MP is projected to receive the lowest rainfall in the study area during this season in the 2070-2099 period under both mitigation scenarios. Some studies (such as Mackellar et al. 2014; Engelbrecht et al. 2013) suggest that the northeastern and majority of South Africa's eastern regions usually experience low rainfall during the autumn season. The rainfall projections for the autumn season are similar under both mitigation scenarios. The highest rainfall is projected by IPSL_CM6A_LR over the south of KZN (160 mm/month to 200 mm/month) and the lowest rainfall is projected by AWI_CM_1_1_MR on the north to the east of MP (< 40 mm/month). The projections of the models suggest that KZN is still likely to be affected by floods in the far-future.

South Africa is one of the countries in southern Africa that receives rainfall every season (Roffe et al. 2019). The winter rainfall projections for the 2070-2099 period under both mitigation scenarios are similar to the near-future projections because rainfall is projected to occur over the study area during the winter season and the region on the east coast of KZN is projected to experience more rainfall compared to other regions in the study area. The models projected winter rainfall over the study area ranging from below 40 mm/month

to 120 mm/month under a moderate to high mitigation scenario. As the model ACCESS_CM2 projected in the near-future period, high winter rainfall (80 mm/month to 120 mm/month) in the far-future period is projected by this model to occur on the east of KZN under both scenarios and this may mean that places such as Port Edward and Durban may experience heavy rainfall compared to other locations in the study area. Eastern South Africa is not the only region that receives rainfall in winter. Southwest South Africa receives more rainfall compared to different parts of the country from the cold fronts that move to the west coast during winter (Odoulami et al. 2021; De Kock et al. 2022).

During the spring season, rainfall is projected to increase compared to winter. Furthermore, the rainfall is projected to range from 40 mm/month to 240 mm/month under SSP2-4.5, with the highest spring rainfall projected by model ACCESS_CM2 (200 mm/month to 240 mm/month). Under SSP5-8.5, ACCESS_CM2 projected the highest rainfall over KZN (240 mm/month to 280 mm/month). COLs are likely to occur over the study area and cause floods. According to Singleton and Reason (2007), COLs in South Africa are at their maximum during autumn and at their secondary peak during spring.

5.2.2.2 Seasonal change in rainfall for SSP2-4.5 and SSP5-8.5

The projections of seasonal changes in rainfall are similar for both scenarios. In the far-future period, during the summer season, rainfall is projected to increase (> 5 mm/month) over the majority of areas particularly the interior and east coast of the study area under both mitigation scenarios. This implies that eastern South Africa in the future may be subjected to more socio-economic impacts resulting from heavy summer rainfall. During the autumn season, rainfall is projected to increase in KZN and over the Highveld, and decrease over the Lowveld in MP. The winter (< -2 mm/month) and spring (< -5 mm/month) rainfall is projected to decrease over the study area under both mitigation scenarios, as shown in Figure 5.39 and Figure 5.40.

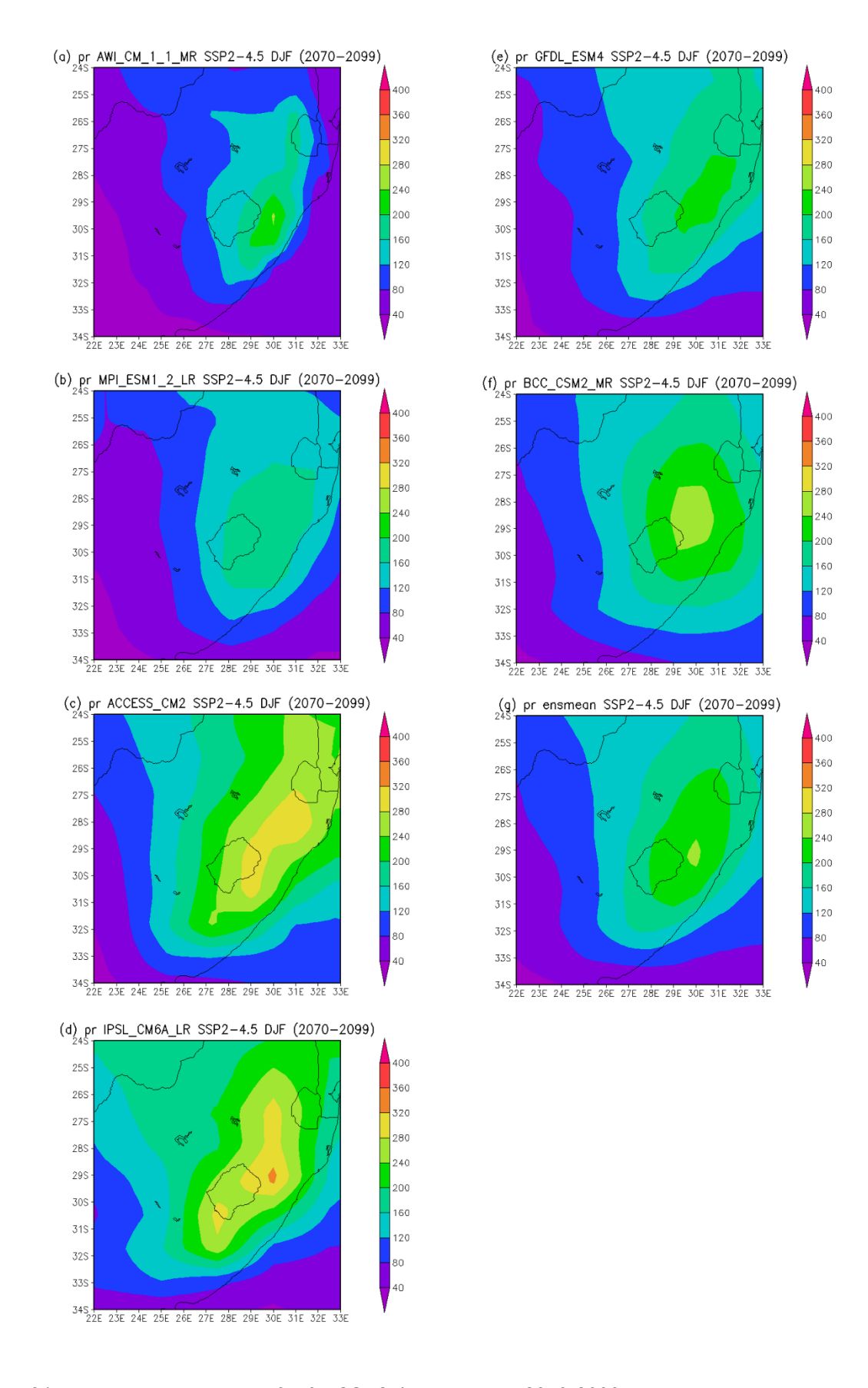


Figure 5.31 DJF seasonal mean rainfall for SSP2-4.5 during the 2070-2099 period

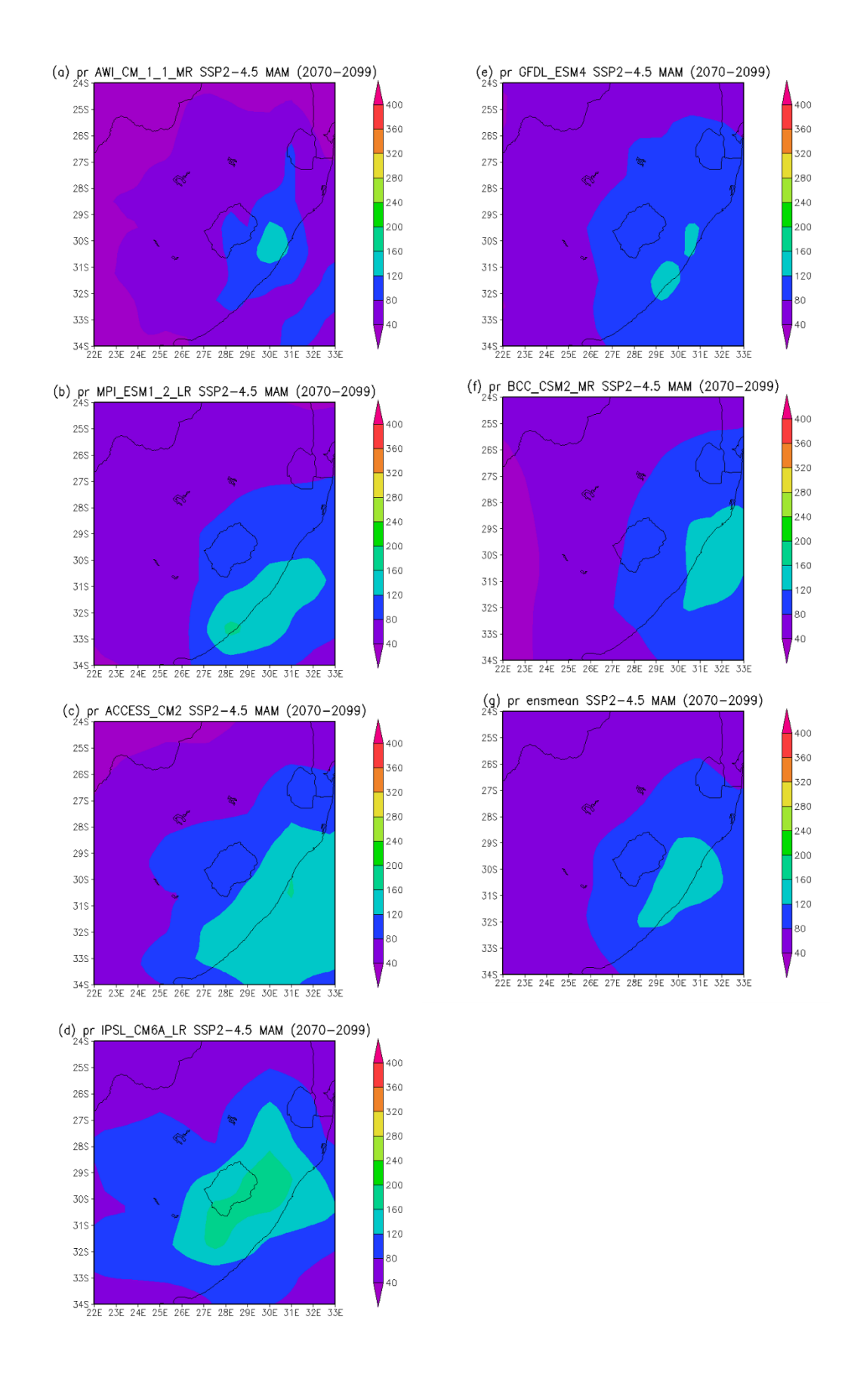


Figure 5.32 MAM seasonal mean rainfall for SSP2-4.5 during the 2070-2099 period

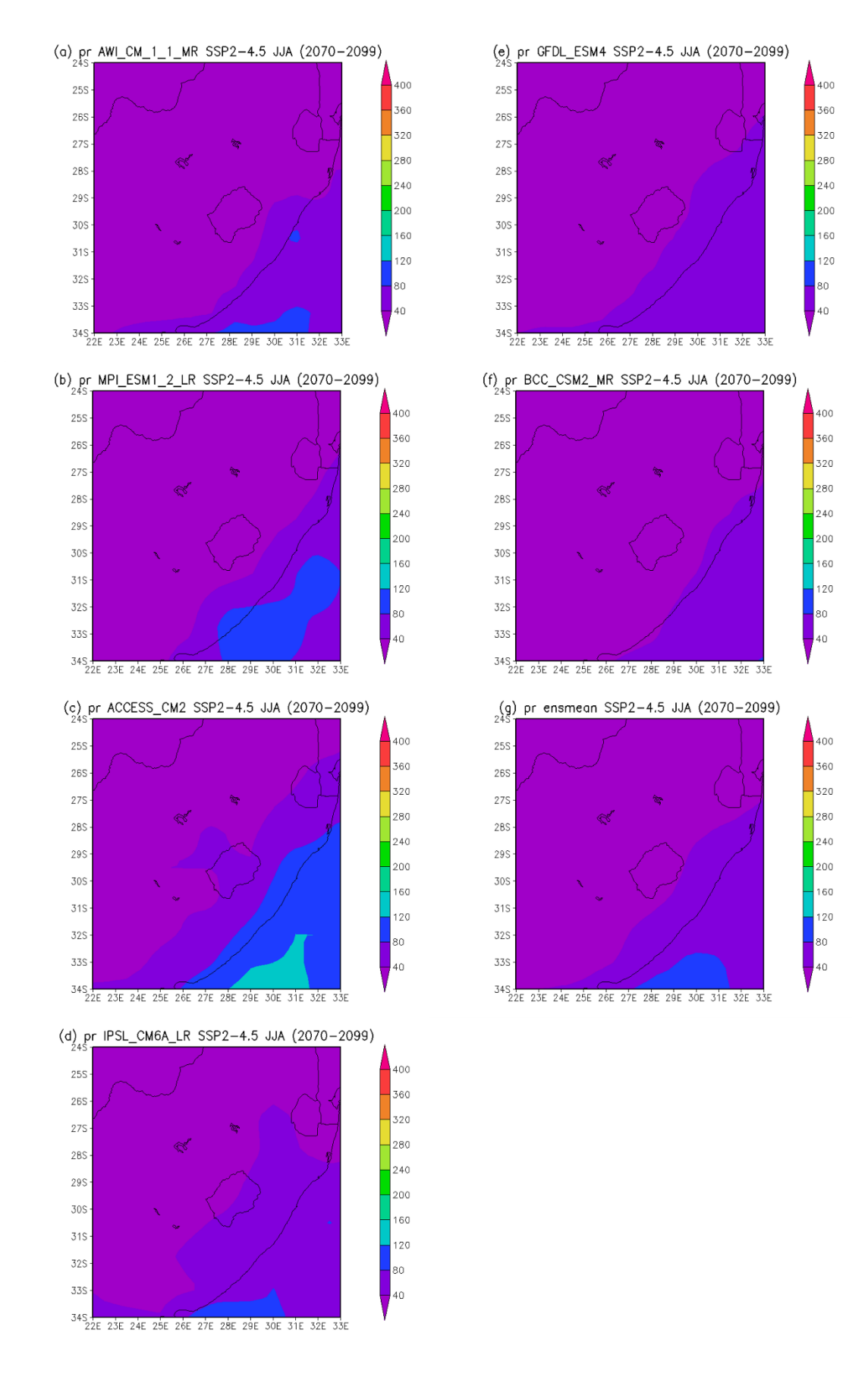


Figure 5.33 JJA seasonal mean rainfall for SSP2-4.5 during the 2070-2099 period

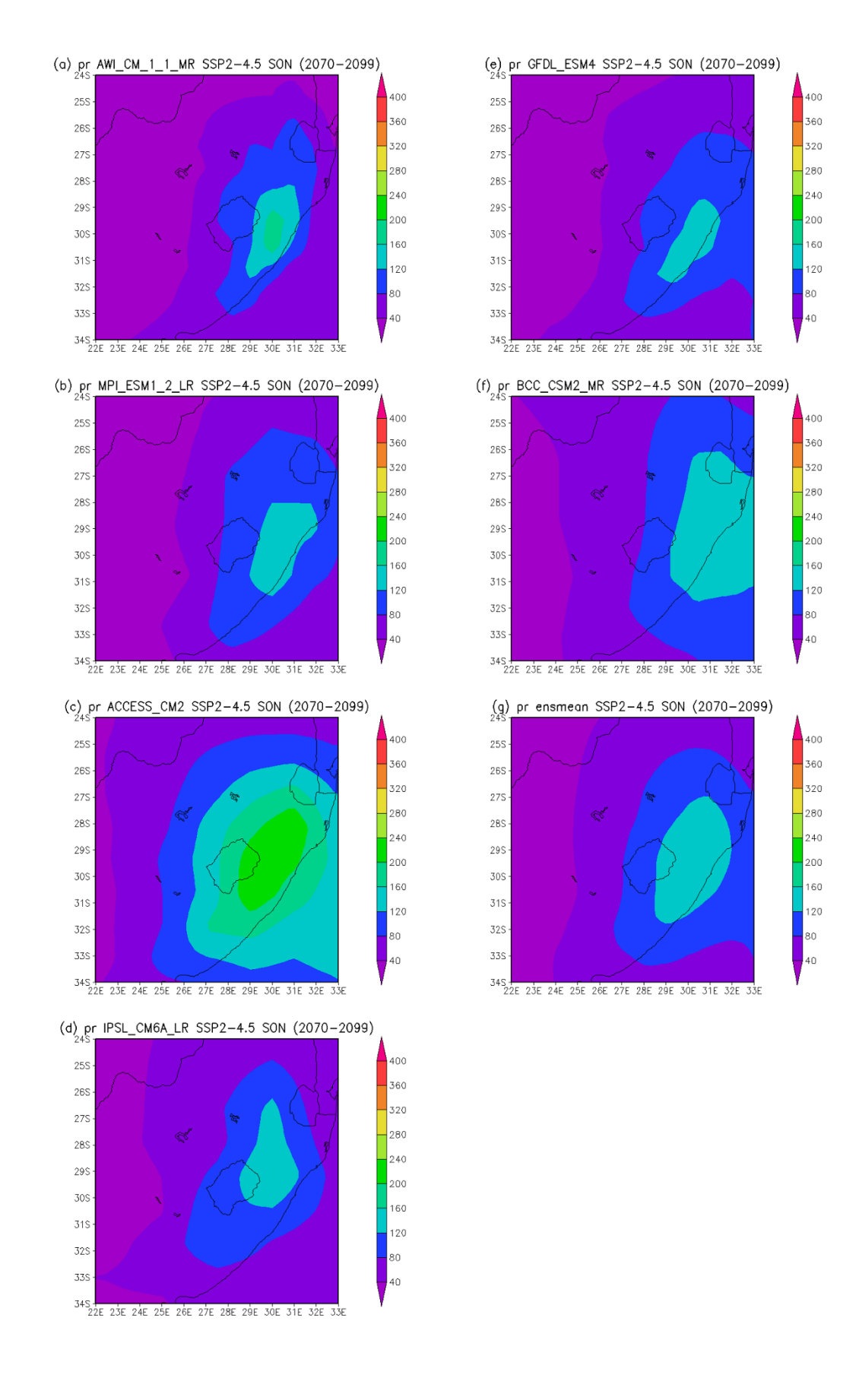


Figure 5.34 SON seasonal mean rainfall for SSP2-4.5 during the 2070-2099 period

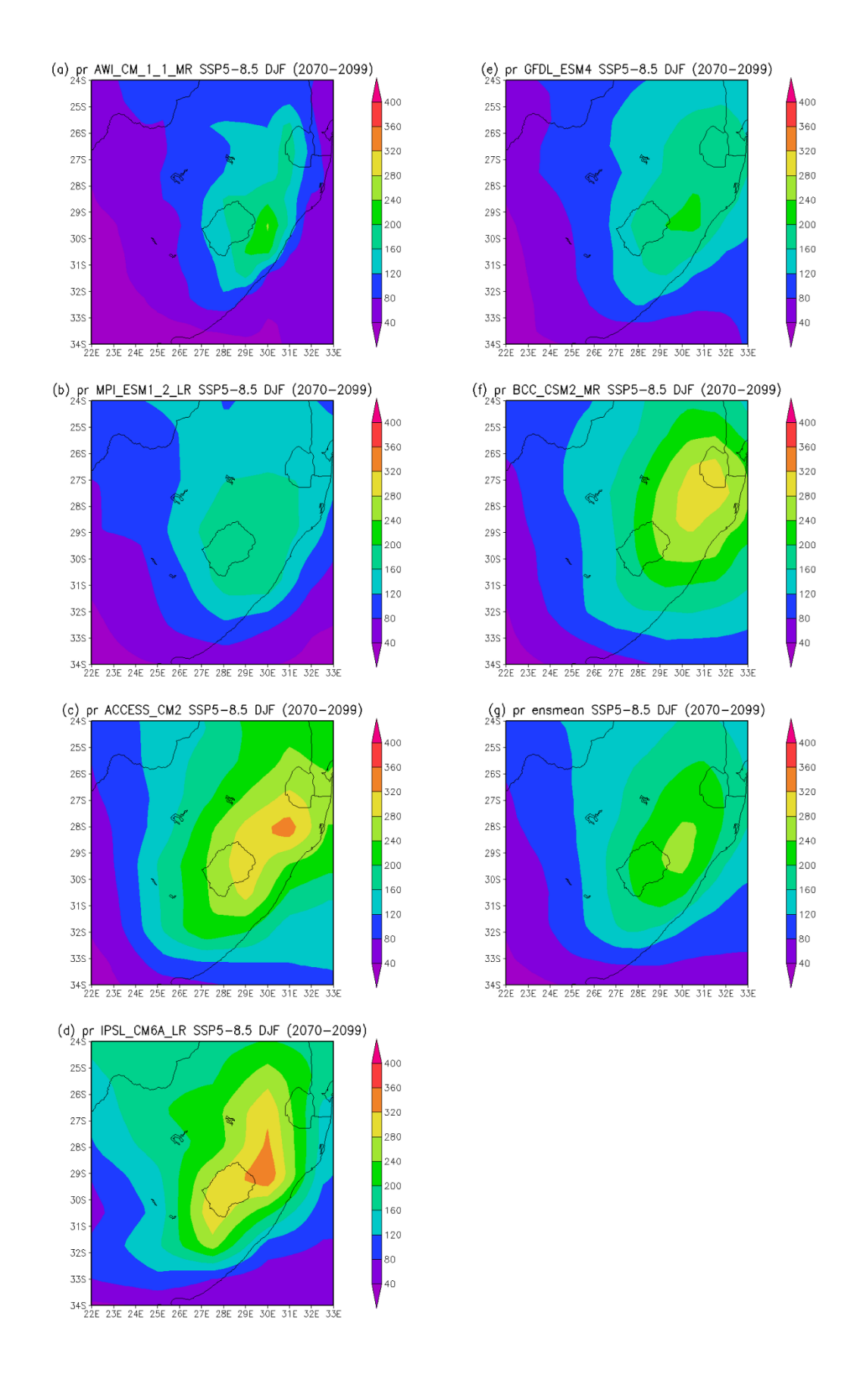


Figure 5.35 DJF seasonal mean rainfall for SSP5-8.5 during the 2070-2099 period

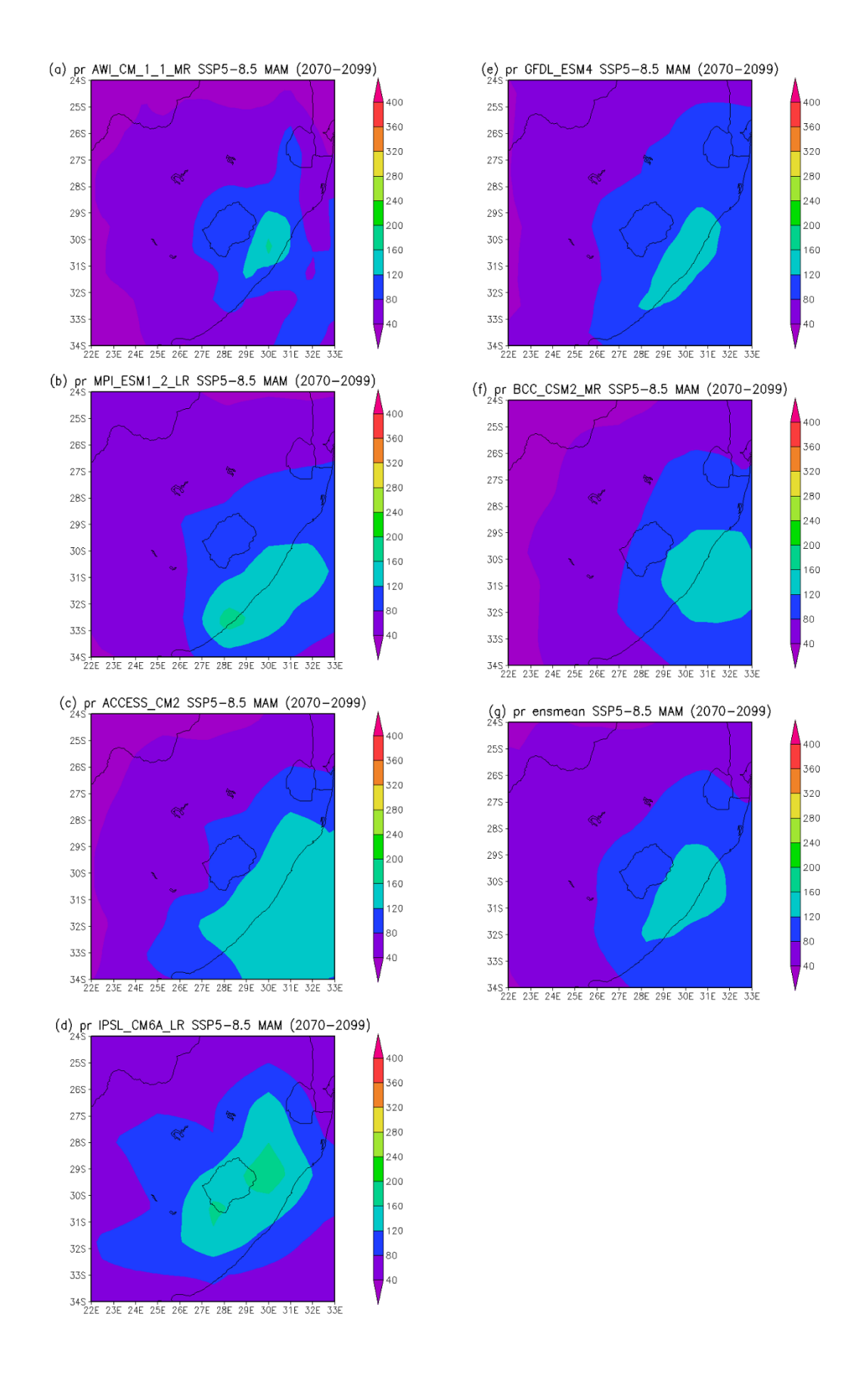


Figure 5.36 MAM seasonal mean rainfall for SSP5.8-5 during the 2070-2099 period

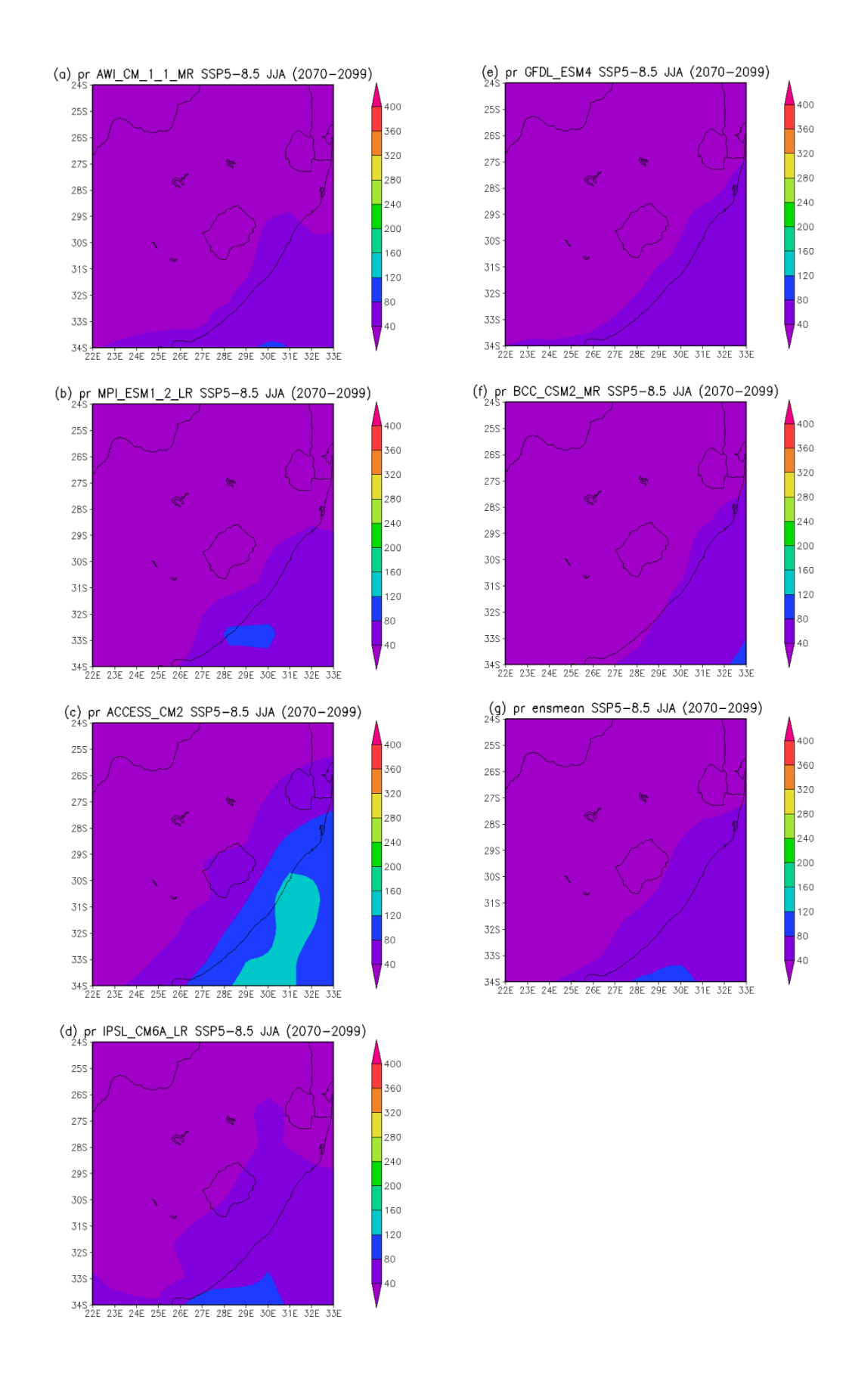


Figure 5.37 JJA seasonal mean rainfall for SSP5-8.5 during the 2070-2099 period

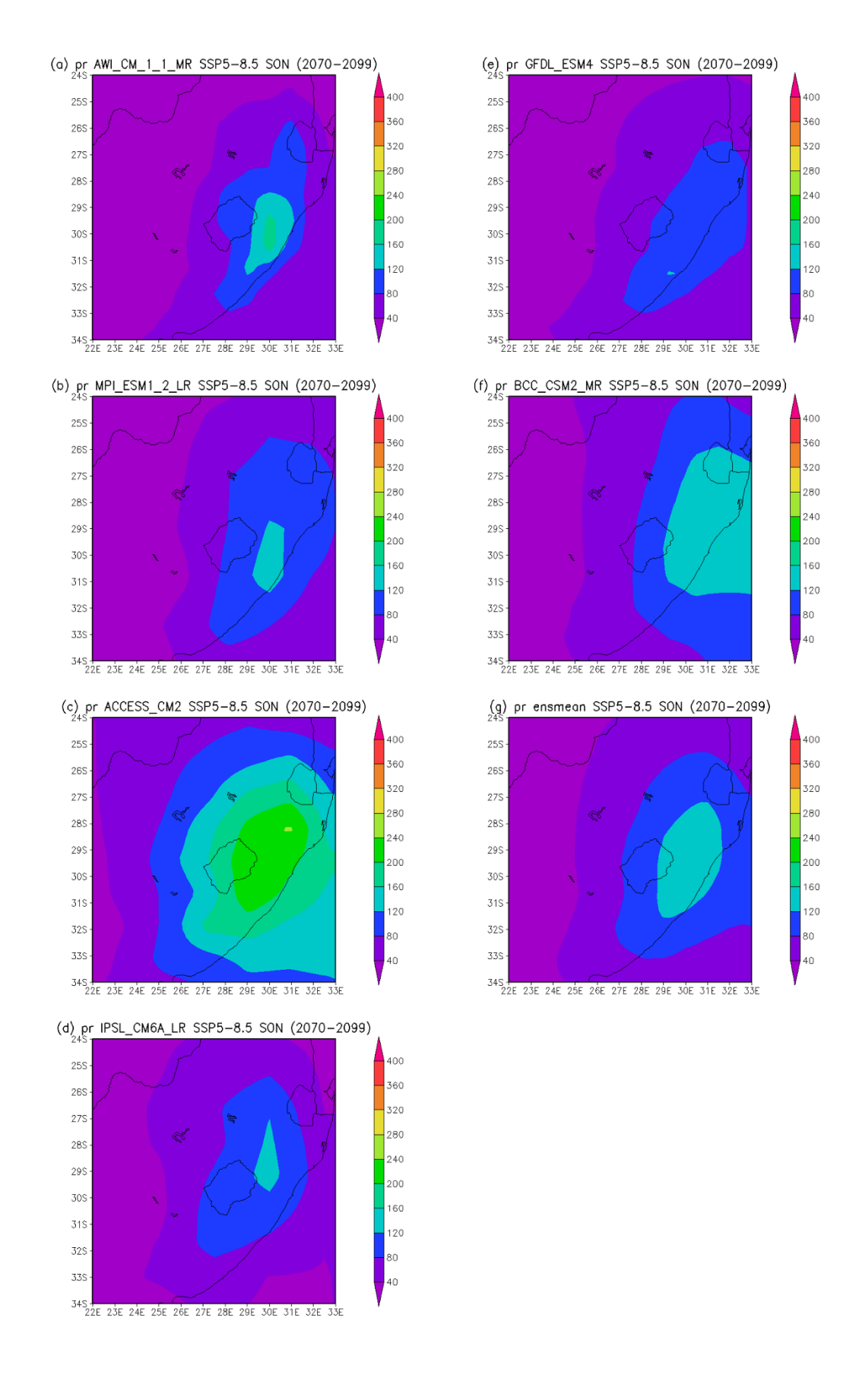


Figure 5.38 SON seasonal mean rainfall for SSP5-8.5 during the 2070-2099 period

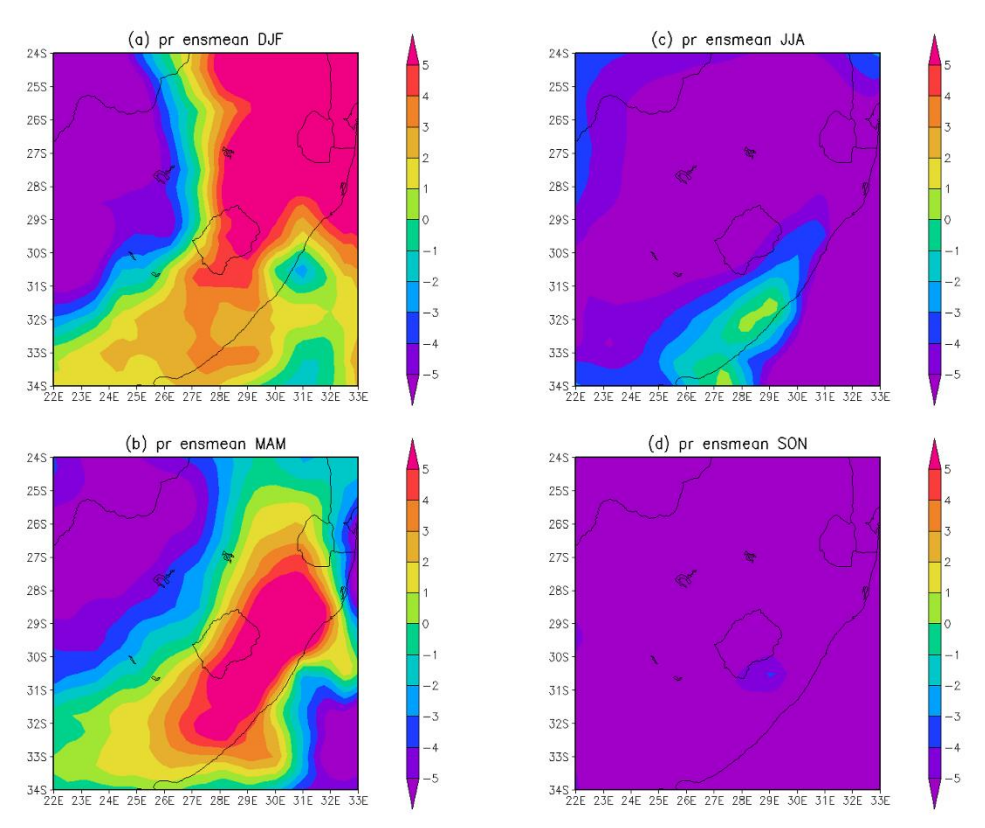


Figure 5.39 Seasonal changes in rainfall for SSP2-4.5 between reference climate (1961-1990) and far-future (2070-2099) periods

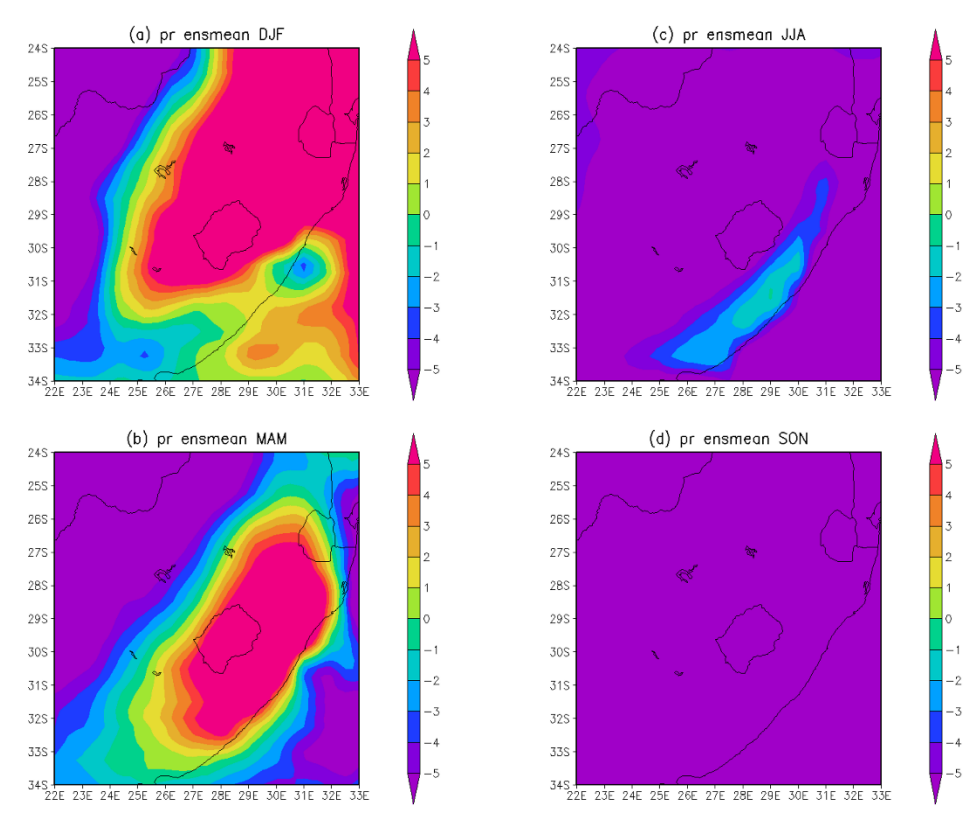


Figure 5.40 Seasonal changes in rainfall for SSP5-8.5 between reference climate (1961-1990) and far-future (2070-2099) periods

5.3 Summary

This chapter focussed on future projections of two periods, near-future (2021-2050) and far-future (2070-2099) periods under SSP2-4.5 and SSP5-8.5. Furthermore, it has outlined how SATs and rainfall are projected to increase and decrease over the study area using seasonal means. The projections show that KZN may be affected by high temperatures and extreme weather events that lead to floods in the future more than MP. Furthermore, these results highlight the importance of preparing for floods and heatwave adaptation strategies. Low SATs are projected on the eastern interior of South Africa which covers the Highveld in MP and west of KZN, and high SATs are projected to dominate the east coast of the country. Models ACCESS_CM2, and IPSL_CM6A_LR projected the highest summer rainfall over KZN in the near-future and far-future periods under both mitigation scenarios. In this chapter seasonal changes were projected using the reference climate (1961-1990) and the future periods (2021-2099). Seasonal changes in SAT for SSP2.4-5 and SSP5.8-5 between reference climate (1961-1990) and near-future (2021-2050) periods across all the seasons the models projected an increase in SATs that range between 1°C and 2°C over the study area under both scenarios. The seasonal changes in SAT for SSP5-8.5 between reference climate (1961-1990) and far-future (2070-2099) periods showed more increase in the model's projections (during all seasons) over the study area compared to seasonal changes in SAT for SSP2.4-5. Seasonal changes in rainfall for both scenarios between reference climate (1961-1990) and near-future (2021-2050) periods and between reference climate (1961-1990) and far-future (2070-2099) periods in summer and autumn showed various rainfall projections (both increase and decrease of rainfall) of the models over the study area. Furthermore, the models projected seasonal changes in rainfall for SSP2-4.5 and SSP5.8-5 during the winter and spring seasons to only a decrease in rainfall over the study area.

CHAPTER 6: CONCLUSION AND RECOMMENDATIONS

6.0 Introduction

This is the final chapter of the study and it discusses the key findings of the research for both the present day (1961-2020) and future climate change projections (2021-2099) from chapters 4 and 5. Furthermore, it discusses the implications and recommendations of this work and provides the conclusion of the study. The study aimed to investigate historical (1961 to 2020) and projected variability and change of climate over eastern South Africa under high and low mitigation focusing on the near-future (2021 to 2050) and the far-future (2070 to 2099) periods. SAT and rainfall were the key variables of the study.

6.1 Discussions of key findings

6.1.1 Historical trends

The study focussed on analysing the historical trends in SATs and rainfall characteristics using relevant indices during the historical baseline of the study, the 1961-2020 period. The indices used for historical trends in SATs were the cool days' index (TX10P) and hot days' index (TX90P). South Africa has experienced cold events in the recent past decades (Davis and Vincent, 2017). The cool days' index indicates that during the 1961-2020 period in MP at the Kruger Mpumalanga International Airport, the highest number of cool days occurred in 1968 for 29 days. Furthermore, the least number of cool days at this airport occurred in 1962 for 5 days. Durban also experienced its highest number of cool days in 1968 for over 35 days and its lowest peak of cool days in 1999 and 2014 for 5 days. Furthermore, these results could imply that there might have been a cold wave during this period on the east side of South Africa affecting the coastal regions. According to van Der Walt and Fitchett (2021), cold wave trends in 1960 to 2016 were observed increasing for stations in the provinces of KZN, Eastern Cape, Gauteng and Northern Cape at a rate of 0,01 events/day-1. The lowtemperature persistent days can be detrimental to the environment, animals, and human beings because in KZN the cold days led to the death of people, livestock, and damage to infrastructure in 2002 during winter and 1996 as stated by Van der Walt (2020). The cool days' indices in Kruger Mpumalanga International Airport and Durban indicate no statistically significant and statistically significant trends respectively, in the number of cool days during the 1961-2020 period. This suggests that the east of the study area experienced a high number of cool days and a low number of cool days at the beginning and towards the end of the 1961-2020 period respectively.

The hot days' index in Kruger Mpumalanga International Airport showed the highest number of hot days in 1992 and 2015 for more than 25 days during the 1961-2020 period. In 1992, large regions in South Africa were affected by droughts that were associated with El Niño (Ibebuchi, 2021). The year 2015 was one of the hottest years in the history of South Africa (McBride et al. 2022b) and heatwaves and droughts were experienced during 2015/16 (Monyela, 2017). The least number of hot days occurred in 1967 and 2000 for less than 5 days at the airport in Mbombela, MP. The highest number of hot days in Durban occurred for more than 20 days in 1991/92 and the lowest number of hot days occurred in 1968 and 1975 (for < 5 days). The findings show that the Mbombela where the Kruger Mpumalanga International Airport is located, is exposed to more heat conditions compared to Durban. Furthermore, this is because the hot days' index in Durban showed less high peaks of hot days compared to Kruger Mpumalanga International Airport. However, the hot days' indices for both locations showed increasing and statistically significant trends in the number of hot days during the historical baseline of the study. These trends suggest a warming climate at both locations.

Southern Africa is often affected by heavy rainfall that leads to floods and that causes loss of lives, damage to infrastructure, and huge financial losses (Dyson, 2000). The indices employed for the historical analysis of trends in rainfall were R10mm (heavy rainfall) and R50mm (frequency rainfall exceeding 50mm/day). The heavy rainfall indices in Kruger Mpumalanga International Airport and Durban showed more high peaks than low peaks of heavy rainfall days. Kruger Mpumalanga International Airport received its highest peak of heavy rainfall in 2000 for more than 40 days. Furthermore, some of the years where it received low peaks of heavy rainfall days (between 10-15 days) were 1965, between 2003 and 2004, and from 2015 to 2016. Durban experienced heavy rainfall days in 1986 for 40 days and one of the years where it received less heavy rainfall days was in 1980 (between 15 to 20 days). The findings showed that Durban recorded more heavy rainfall days compared to Kruger Mpumalanga International Airport during the 1961-2020 period. The heavy rainfall indices for Kruger Mpumalanga International Airport and Durban showed no significant trends at either location.

The findings showed that Kruger Mpumalanga International Airport had less events of rainfall days exceeding 50mm/day than Durban. In 2000, Kruger Mpumalanga International Airport experienced rainfall exceeding 50mm/day for more than 4 days. The northeast of South Africa was affected by heavy rainfall linked to a TC which caused floods in 2000 (Chikoore et al. 2021). Several years of 0 days of rainfall exceeding 50mm/day were recorded in Kruger Mpumalanga International Airport and some of those years include 1961 to 1963,

1965 to 1968, and 1970 to 1971. For more than 3 days in 1985, 1987, and 1989, Durban had its highest peak of rainfall exceeding 50mm/day which led to floods (Molekwa, 2013). In 1961, 1963, 1992, 2005, 2010, and 2015, Durban did not have rainfall exceeding 50mm/day. The index for frequency of rainfall exceeding 50mm/day in Kruger Mpumalanga International Airport showed a constant and no statistically significant trend throughout the historical baseline of the study and Durban showed an increasing but no statistically significant trend. The trend in Kruger Mpumalanga International Airport suggests no change in the number of rainfall days exceeding 50mm/day.

6.1.2 Model verification

The study used six CMIP6 models, the ensemble of the models, and the ERA5 observations to verify the models from 1961-1990. The Taylor diagrams were employed to evaluate the performance of the models against ERA5 observation. Statistical tools featured in a Taylor diagram include standard deviation, correlation coefficient, and RMSE. For this climate variability and change study, key variables employed for model verification include SAT and rainfall. SAT model verification showed that models IPSL_CM6A_LR, and MPI_ESM1_2_LR underestimated the observed variability, and models AWI_CM_1_1_MR, BCC_CSM2_MR, GFDL_ESM4, and ACCESS_CM2, overestimated the observed variability. All models obtained a correlation greater than 0,9 and ACCESS_CM2 showed a high skill. Furthermore, all models had the least RSME with IPSL_CM6A_LR having a high skill. According to the rainfall model verification, all models obtained a moderate correlation and least RMSE (< 50mm).

The models performed well against ERA5 observation in simulating seasonal mean SAT for the 1961-1990 period. The models simulated the highest SATs on the east of the study area and the lowest on the west of KZN and south of MP during all the seasons. Models AWI_CM_1_1_MR, IPSL_CM6A_LR, MPI_ESM1_2_LR, and GFDL_ESM4 constantly showed cooler temperatures on the Highveld among all the seasons. Rainfall visual verification showed that models simulated more seasonal rainfall over the interior of KZN than MP. Furthermore, model IPSL_CM6A_LR and ACCESS_CM2 overestimated summer and spring rainfall respectively, during the 1961-1990 period.

6.1.3 Future climate change projections (2021-2099)

In the near-future period, the models projected high seasonal mean SATs in the east of the study area (Lowveld of MP and northeast of KZN), and models AWI_CM_1_1_MR, MPI_ESM1_2_LR, and GFDL_ESM4 projected the lowest SATs on the west of KZN and Highveld in MP under both mitigation scenarios. Warmer conditions over the study area are projected to remain and increase in the near-future period of the study. Some studies (such as Archer et al. 2018 and Kapuka et al. 2022) suggest that under low mitigation, conditions are going to be drier however, under moderate to high mitigation there will be more room for adaptation. Future projections showed that under SSP2-4.5, the effects of climate change will be lesser over the study area. In the far-future, the models projected higher SATs to dominate the larger parts of eastern South Africa across all seasons under SSP5-8.5 compared to SSP2-4.5. Low-pressure systems are likely to be triggered during warm conditions (Engelbrecht et al. 2013). The Highveld is projected to have lower SATs in the 2070-2099 period. According to seasonal changes made using the ensmeans, the SATs are projected to increase more over the study area in the far-future period and to be higher under SSP5-8.5 than SSP2-4.5.

The model rainfall seasonal mean projections in the near-future showed more rainfall in KZN than in MP, particularly in summer and spring. Furthermore, these are seasons where KZN is affected by extreme weather systems such as TCs and COLs (Mpungose, 2022; Favre et al. 2012). The model IPSL_CM6A_LR projected the highest rainfall in KZN under SSP5-8.5 during summer compared to other models. Drought is most likely to affect the Highveld in MP in the near-future period during summer and spring because of the projected decrease in rainfall. Furthermore, below-average rainfall may affect agriculture (Ogundeji, 2022; Mpungose, 2022). Extreme rainfall events will likely continue to affect KZN in summer and autumn (particularly southeast of the province) due to the projected increase in rainfall. The rainfall projections in the far-future period are similar to those of the near-future. The models IPSL_CM6A_LR and ACCESS_CM2 projected the highest rainfall in summer and spring under both mitigation scenarios respectively, compared to other models. The far-future rainfall is projected to increase in summer and decrease in winter and spring over the study area. Furthermore, the autumn rainfall is projected to vary in the study area, as it is projected to decrease in the Lowveld and increase in KZN under both mitigation scenarios.

6.2 Implications and recommendations

The study employed relevant indices to demonstrate the historical trends in SATs and rainfall at Kruger Mpumalanga International Airport and Durban during the 1961-2020 period. More high peaks of hot days and heavy rainfall days were recorded in Kruger Mpumalanga International Airport and Durban respectively. Indices used were for the days, for both trends in SATs and rainfall. Therefore, for a future study, indices for the nights would give a different perspective on the trends in SATs and rainfall at the two selected locations. The present study used SSPs (SSP2-4.5 and SSP5-8.5) for future climate change projections in order to inform adaptation strategies. Comparing SSPs and RCPs that belong to CMIP5 (Eyring et al. 2016) for future climate change projections would provide different input and perspectives about the performances of CMIP6 and CMIP5 models. The study provided historical simulations of SATs and rainfall, and that has given an insight on the changes of climate over the study area in the past. Furthermore, comparing the historical simulations of CMIP6 and CMIP5 models would also show how well they perform against ERA5 observation and the improvement in CMIP6 from CMIP5. Analysing the future climate projections using percentiles would distinguish the climate variabilities of future rainfall in the study area. According to Singo et al. 2023, in climate change projections, percentiles are used frequently to show the distribution of uncertainty related to future projections for each variable. The research has significant implications for climate adaptation and policy planning in eastern South Africa. The findings highlight the need for enhanced climate monitoring, continued high-resolution modelling, and improved climate projections at regional scales. The increasing frequency of extreme heat events necessitates adaptation measures in agriculture, water resource management, and urban planning. The projected variability in rainfall underscores the importance of flood preparedness and drought mitigation strategies.

6.3 Conclusion

The study of projecting future climate change in the regions that are vulnerable to rising temperatures and floods is important in contributing to awareness of extreme weather events affecting those particular regions. The study aimed to investigate historical and projected variability and change of climate over eastern South Africa under high and low mitigation focusing on the near-future and far-future periods. The aim was achieved by executing the objectives. The future climate change projections for the near-future (2021-2050) and far-future (2070-2099) periods are presented in the present study. The CMIP6 models were utilized together with

their ensemble. According to Giorgi (2019), models provide knowledge about potential changes in the climate. Models were validated to evaluate their performance against the ERA5 observation through statistical and visual verification methods, and they performed well against ERA5 observation during the reference climate (1961-1990). The study highlights significant warming trends in temperature indices at Kruger Mpumalanga International Airport and Durban, with a more pronounced decrease in cool days and an increase in hot days at both locations. The stability in heavy rainfall indices suggests that changes in temperature are not accompanied by significant changes in heavy rainfall patterns. Furthermore, the frequency of rainfall exceeding 50mm/day trends varied by location. This analysis provides valuable insights into the long-term climatic changes in these regions, which can inform future climate adaptation and mitigation strategies. The findings of this study are consistent with other previous studies, projecting increases in temperatures, rainfall, and dry conditions in the future over South Africa (Engelbrecht and Monteiro, 2021; Chikoore et al. 2021). Furthermore, the findings have shown that under moderate to high mitigation scenario there is more room for adaptation compared to low mitigation scenario.

REFERENCES

Abba, O.S., 2020. *Understanding the characteristics of cut-off lows over the Western Cape, South Africa.* (Doctoral dissertation, University of Cape Town). http://hdl.handle.net/11427/32478

Abdolalizadeh, F., Mohammad Khorshiddoust, A. and Jahanbakhsh, S., 2022. Assessment of the performance of CMIP6 model for analysis of temperature and precipitation in Urmia Lake basin. *Climate Change Research*, 3(11), pp.17-30.

Aderinto, N., 2023. Tropical cyclone Freddy exposes major health risks in the hardest-hit southern African countries: lessons for climate change adaptation. *IJS Global Health*, 6(3), pp.152.

Agbor, M.E., Udo, S.O., Ewona, I.O., Nwokolo, S.C., Ogbulezie, J.C. and Amadi, S.O., 2023. Potential impacts of climate change on global solar radiation and PV output using the CMIP6 model in west Africa. *Cleaner Engineering and Technology*, *13*, pp.100-630.

Agostoni, C., Baglioni, M., La Vecchia, A., Molari, G. and Berti, C., 2023. Interlinkages between climate change and food systems: the impact on child malnutrition—Narrative Review. *Nutrients*, *15*(2), pp.416.

Ali, M.E. and Medhat, T., 2021. Correlation coefficient via statistical and rough set concepts. *Inf. Sci. Lett*, 10(3), pp.6.

Anwana, E.O. and Owojori, O.M., 2023. Analysis of flooding vulnerability in informal settlements literature: mapping and research agenda. *Social Sciences*, *12*(1), pp.40.

Archer, E.R., Engelbrecht, F.A., Hänsler, A., Landman, W., Tadross, M. and Helmschrot, J., 2018. Seasonal prediction and regional climate projections for southern Africa. In: Climate change and adaptive land management in southern Africa – assessments, changes, challenges, and solutions, pp. 14-21, Biodiversity & Ecology, 6, Klaus Hess Publishers, Göttingen & Windhoek.

Archer, E.R.M., Landman, W.A., Malherbe, J., Maluleke, P. and Weepener, H., 2021. Managing climate risk in livestock production in South Africa: how might improved tailored forecasting contribute? *Climate Risk Management*, 32, pp.100-312.

Archer, E.R.M., Landman, W.A., Tadross, M.A., Malherbe, J., Weepener, H., Maluleke, P. and Marumbwa, F.M., 2017. Understanding the evolution of the 2014–2016 summer rainfall seasons in southern Africa: key lessons. *Climate Risk Management*, *16*, pp.22-28.

Azran, N.I., Jeofry, H., Chung, J.X., Juneng, L., Ali, S.A.S., Griffiths, A., Ramli, M.Z., Ariffin, E.H., Miskon, M.F., Mohamed, J. and Yunus, K., 2023. Southern South China Sea Dynamics: sea level change from Coupled Model Intercomparison Project Phase 6 (CMIP6) in the 21st Century. *Journal of Marine Science and Engineering*, 11(2), pp.458.

Baker, J., Bradley, B. and Stafford, P., 2021. Seismic hazard and risk analysis. Cambridge University Press.

Barnes, M.A., Ndarana, T. and Landman, W.A., 2021. Cut-off lows in the southern hemisphere and their extension to the surface. *Climate Dynamics*, *56*(11-12), pp.3709-3732.

Barnes, M.A., Turner, K., Ndarana, T. and Landman, W.A., 2021. Cape storm: a dynamical study of a cut-off low and its impact on South Africa. *Atmospheric Research*, 249, pp.105-290.

Baudoin, M.A., Nortje, K., Naik, M., Rouault, M. and Vogel, C., 2022. South Africa: El Niño impacts and management in South Africa: lessons learned for an 'El Niño Ready'Nation. In *El Niño ready nations and disaster risk reduction:* 19 Countries in perspective (pp. 271-305). Cham: Springer International Publishing.

Beermann, S., Dobler, G., Faber, M., Frank, C., Habedank, B., Hagedorn, P., Kampen, H., Kuhn, C., Nygren, T., Schmidt-Chanasit, J. and Schmolz, E., 2023. Impact of climate change on vector-and rodent-borne infectious diseases. *Journal of Health Monitoring*, 8(3), pp.33.

Bhadauriya, S., 2018. *Analysis and visualization of numerical weather prediction forecast using geospatial techniques* (Master's thesis, Symbiosis International University).

Bhatti, U.A., Bhatti, M.A., Tang, H., Syam, M.S., Awwad, E.M., Sharaf, M. and Ghadi, Y.Y., 2024. Global production patterns: understanding the relationship between greenhouse gas emissions, agriculture greening and climate variability. *Environmental Research*, 245, pp.118049.

Bi, D., Dix, M., Marsland, S., O'farrell, S., Sullivan, A., Bodman, R., Law, R., Harman, I., Srbinovsky, J., Rashid, H.A. and Dobrohotoff, P., 2020. Configuration and spin-up of ACCESS-CM2, the new generation Australian community climate and earth system simulator coupled model. *Journal of Southern Hemisphere Earth Systems Science*, 70(1), pp.225-251.

Bi, D., Dix, M., Marsland, S., O'Farrell, S., Rashid, H., Uotila, P., Hirst, A., Kowalczyk, E., Golebiewski, M., Sullivan, A. and Yan, H., 2013. The ACCESS coupled model: description, control climate, and evaluation. *Australian Meteorological and Oceanographic Journal*, 63(1), pp.41-64.

Bi, D., Wang, G., Cai, W., Santoso, A., Sullivan, A., Ng, B. and Jia, F., 2022. Improved simulation of ENSO variability through feedback from the equatorial Atlantic in a pacemaker experiment. *Geophysical Research Letters*, *49*(2), pp.e2021GL096887.

Blunden, J. and Arndt, D.S., 2016. State of the climate in 2015. *Bulletin of the American Meteorological Society*, 97(8), pp.Si-S275.

Bouchard, J.P., Pretorius, T.B., Kramers-Olen, A.L., Padmanabhanunni, A. and Stiegler, N., 2023. Global warming and psychotraumatology of natural disasters: the case of the deadly rains and floods of April 2022 in South Africa. In *Annales Médico-psychologiques, revue psychiatrique* (Vol. 181, No. 3, pp. 234-239). Elsevier Masson.

Boucher, O., Servonnat, J., Albright, A.L., Aumont, O., Balkanski, Y., Bastrikov, V., Bekki, S., Bonnet, R., Bony, S., Bopp, L. and Braconnot, P., 2020. Presentation and evaluation of the IPSL-CM6A-LR climate model. *Journal of Advances in Modeling Earth Systems*, *12*(7), pp.e2019MS002010.

Bouramdane, A.A., 2022. Assessment of CMIP6 multi-model projections worldwide: which regions are getting warmer and are going through a drought in Africa and Morocco? What Changes from CMIP5 to CMIP6? Sustainability, 15(1), pp.690.

Bradshaw, C.D., Pope, E., Kay, G., Davie, J.C., Cottrell, A., Bacon, J., Cosse, A., Dunstone, N., Jennings, S., Challinor, A. and Chapman, S., 2022. Unprecedented climate extremes in South Africa and implications for maize production. *Environmental Research Letters*, 17(8), pp.084028.

Budhidarma, V., 2023. Coherent risk measurement. In *Proceeding of International Conference on Entrepreneurship (IConEnt)* (Vol. 2, pp. 93-98).

Calverley, C.M. and Walther, S.C., 2022. Drought, water management, and social equity: analyzing Cape Town, South Africa's water crisis. *Frontiers in Water*, *4*.

Celik, S., 2020. The effects of climate change on human behaviors. Environment, climate, plant and vegetation growth, Springer Cham, pp.577-589. https://doi.org/10.1007/978-3-030-49732-3_22

Chang, M. and Smith, R.K., 2021. Genesis of Typhoon Hagupit (2008) as revealed by ERA5 reanalyses and satellite observations. *Quarterly Journal of the Royal Meteorological Society*, 8, pp.1-8.

Chen, H., He, Z., Xie, Q. and Zhuang, W., 2023. Performance of CMIP6 models in simulating the dynamic sea level: mean and interannual variance. *Atmospheric and Oceanic Science Letters*, *16*(1), pp.100-288.

Cheung, K.K., Ji, F., Nishant, N., Herold, N. and Cook, K., 2023. Evaluation of convective environments in the NARCliM Regional Climate Modelling System for Australia. *Atmosphere*, *14*(4), pp.690.

Chevuru, S., de Wit, A., Supit, I. and Hutjes, R., 2023. Copernicus global crop productivity indicators: an evaluation based on regionally reported yields. *Climate Services*, *30*, pp.100-374.

Chikoore, H., Bopape, M.J.M., Ndarana, T., Muofhe, T.P., Gijben, M., Munyai, R.B., Manyanya, T.C. and Maisha, R., 2021. Synoptic structure of sub-daily extreme precipitation and flood event in Thohoyandou, north-eastern South Africa. *Weather and Climate Extremes*, 33, pp.100-327.

Chikoore, H., Mbokodo, I.L., Singo, M.V., Mohomi, T., Munyai, R.B., Havenga, H., Mahlobo, D.D., Engelbrecht, F.A., Bopape, M.J.M. and Ndarana, T., 2024. Dynamics of an extreme low temperature event over South Africa amid a warming climate. *Weather and Climate Extremes*, *44*, pp.100-668.

Chikoore, H. and Jury, M.R., 2021. South African drought, deconstructed. *Weather and Climate Extremes*, 33, pp.100-334.

Chimoto, K., Yamanaka, H., Tsuno, S. and Matsushima, S., 2023. Predicted results of the velocity structure at the target site of the blind prediction exercise from microtremors and surface wave method as Step-1, report for the experiments for the 6th international symposium on effects of surface geology on seismic motion. *Earth, Planets and Space*, 75(1), pp.79.

Christensen, J.H., Hewitson, B., Busuioc, A., Chen, A., Gao, X., Held, I., Jones, R., Kolli, R.K., Kwon, W-T., Laprise, R., Magana Rueda, V., Mearns, L., Menendez, C.G., Raisanen, J., Rinke, A., Sarr, A. and Whetton, P., 2007. Regional climate projections. Climate change 2007: the physical science basis (ed. by S. Solomon, D. Qin, M. Manning, Z. Chen, M. Marquis, A.B. Averyt, M. Tignor and H.L. Miller). Contribution of working group I to the fourth Assessment Report of the Intergovernmental Panel on Climate Change. Cambridge University Press, Cambridge, UK.

Clarke, B., Otto, F., Stuart-Smith, R. and Harrington, L., 2022. Extreme weather impacts of climate change: an attribution perspective. *Environmental Research: Climate*, *1*(1), pp.012001.

Coetzee, C., Khoza, S., Nemakonde, L.D., Shoroma, L.B., Wentink, G.W., Nyirenda, M., Chikuse, S., Kamanga, T., Maripe, K., Rankopo, M.J. and Mwansa, L.K., 2023. Financing disaster risk reduction: exploring the opportunities, challenges, and threats within the southern African development community region. *International Journal of Disaster Risk Science*, pp.1-15.

Collins, J.M., 2011. Temperature variability over Africa. *Journal of Climate*, 24(14), pp.3649-3666.

Danilov, S., Kivman, G. and Schröter, J., 2004. A finite-element ocean model: principles and evaluation. *Ocean Modelling*, 6(2), pp.125-150.

David, T.H., 2022. The contribution of wool production to the sustainability of crop/pasture production systems in the Southern Cape (Master's thesis, Faculty of AgriSciences).

Davis, C.L. and Vincent, K., 2017. Climate risk and vulnerability: A handbook for Southern Africa (2nd ed). CSIR. Pretoria. South Africa.

De Coning, E., Forbes, G.S. and Poolman, E., 1998. Heavy precipitation and flooding on 12-14 February 1996 over the summer rainfall regions of South Africa: Synoptic and isentropic analyses. *Natl. Wea. Dig*, 22(3), pp.25-36.

Dedekind, Z., Engelbrecht, F.A. and Van der Merwe, J., 2016. Model simulations of rainfall over southern Africa and its eastern escarpment. *Water SA*, *42*(1), pp.129-143.

De Kock, W.M., Blamey, R.C. and Reason, C.J.C., 2022. Large-scale mechanisms linked to anomalously wet summers over the southwestern Cape, South Africa. *Climate Dynamics*, 59(11-12), pp.3503-3517.

Demessie, S.F., Dile, Y.T., Bedadi, B., Gashaw, T. and Tefera, G.W., 2023. Evaluations of regional climate models for simulating precipitation and temperature over the Guder sub-basin of Upper Blue Nile Basin, Ethiopia. *Modelling Earth Systems and Environment*, pp.1-22.

Dembedza, V.P., Chopera, P., Mapara, J., Mpofu-Hamadziripi, N., Kembo, G. and Macheka, L., 2023. The relationship between climate change induced natural disasters and selected nutrition outcomes: a case of cyclone Idai, Zimbabwe. *BMC nutrition*, 9(1), pp.19.

Dessai, S., Hulme, M., Lempert, R. and Pielke Jr, R., 2009. Climate prediction: a limit to adaptation. *Adapting to climate change: thresholds, values, governance*, *64*, pp.78.

Do, C. and Kuleshov, Y., 2023. Tropical cyclone multi-hazard risk mapping for Queensland, Australia. *Natural Hazards*, *116*(3), pp.3725-3746.

Doury, A., Somot, S., Gadat, S., Ribes, A. and Corre, L., 2023. Regional Climate Model emulator based on deep learning: concept and first evaluation of a novel hybrid downscaling approach. *Climate Dynamics*, *60*(5-6), pp.1751-1779.

Driga, A.M. and Drigas, A.S., 2019. Climate change 101: how everyday activities contribute to the ever-growing issue. *Int. J. Recent Contributions Eng. Sci. IT*, 7(1), pp.22-31.

Dube, K., 2022. EXPERT Opinion: Flooding events in Kwazulu Natal and Eastern Cape and implications for disaster management in South Africa—Vaal University of Technology. Available online: https://www.vut.ac.za/expert-opinion-flooding-events-in-kwazulu-natal-and-eastern-cape-and-implications-for-disaster-management-in-south-africa/ (accessed on 14 September 2022).

Dube, K., Nhamo, G. and Chikodzi, D., 2022a. Climate change-induced droughts and tourism: impacts and responses of Western Cape province, South Africa. *Journal of Outdoor Recreation and Tourism*, 39, pp.100-319.

Dube, K., Nhamo, G. and Chikodzi, D., 2022b. Flooding trends and their impacts on coastal communities of Western Cape province, South Africa. *GeoJournal*, 87(4), pp.453-468.

Dunne, J.P., Horowitz, L.W., Adcroft, A.J., Ginoux, P., Held, I.M., John, J.G., Krasting, J.P., Malyshev, S., Naik, V., Paulot, F. and Shevliakova, E., 2020. The GFDL Earth System Model version 4.1 (GFDL-ESM 4.1): overall coupled model description and simulation characteristics. *Journal of Advances in Modeling Earth Systems*, *12*(11), pp.e2019MS002015.

Du Plessis, J.A. and Schloms, B., 2017. An investigation into the evidence of seasonal rainfall pattern shifts in the Western Cape, South Africa. *Journal of the South African Institution of Civil Engineering*, 59(4), pp.47-55.

Dyson, L.L., 2000. A dynamical forecasting perspective on synoptic scale weather systems over southern Africa. University of Pretoria (South Africa).

Dyson, L.L. and Van Heerden, J., 2001. The heavy rainfall and floods over the northeastern interior of South Africa during February 2000. *South African Journal of Science*, *97*(3), pp.80-86.

Ebert, E.E., 2001. Verification of precipitation areas. In *Proceedings of the 1st WWRP/WMO Workshop on the Verification of Quantitative Precipitation Forecasts* (pp. 14-16).

Engdaw, M.M., Steiner, A.K., Hegerl, G.C. and Ballinger, A.P., 2023. Attribution of observed changes in extreme temperatures to anthropogenic forcing using CMIP6 models. *Weather and Climate Extremes*, 39, pp.100-548.

Engelbrecht, F., Adegoke, J., Bopape, M.J., Naidoo, M., Garland, R., Thatcher, M., McGregor, J., Katzfey, J., Werner, M., Ichoku, C. and Gatebe, C., 2015. Projections of rapidly rising surface temperatures over Africa under low mitigation. *Environmental Research Letters*, *10*(8), pp.085004.

Engelbrecht, F.A. and Monteiro, P., 2021. The IPCC assessment report six working group 1 report and southern Africa: reasons to take action. *South African Journal of Science*, *117*(11-12), pp.1-7.

Engelbrecht, F.A., McGregor, J.L. and Engelbrecht, C.J., 2009. Dynamics of the conformal-cubic atmospheric model projected climate-change signal over southern Africa. *International Journal of Climatology: A Journal of the Royal Meteorological Society*, 29(7), pp.1013-1033.

Engelbrecht, C.J., Engelbrecht, F.A. and Dyson, L.L., 2013. High-resolution model-projected changes in mid-tropospheric closed-lows and extreme rainfall events over southern Africa. *International Journal of Climatology*, 33(1), pp.173-187.

Erasmus, M., 2019. Formation and development of tropical temperate troughs across southern Africa as simulated by a state-of-the-art coupled model (Master's thesis, University of Pretoria).

Eriksen, S., Schipper, E.L.F., Scoville-Simonds, M., Vincent, K., Adam, H.N., Brooks, N., Harding, B., Lenaerts, L., Liverman, D., Mills-Novoa, M. and Mosberg, M., 2021. Adaptation interventions and their effect on vulnerability in developing countries: help, hindrance or irrelevance? *World Development*, *141*, pp.105-383.

Eyring, V., Bony, S., Meehl, G.A., Senior, C.A., Stevens, B., Stouffer, R.J. and Taylor, K.E., 2016. Overview of the Coupled Model Intercomparison Project Phase 6 (CMIP6) experimental design and organization. *Geoscientific Model Development*, 9(5), pp.1937-1958.

Fan, F., Bradley, R.S. and Rawlins, M.A., 2014. Climate change in the northeastern US: regional climate model validation and climate change projections. *Climate dynamics*, *43*, pp.145-161.

Fan, X., Duan, Q., Shen, C., Wu, Y. and Xing, C., 2020. Global surface air temperatures in CMIP6: historical performance and future changes. *Environmental Research Letters*, *15*(10), pp.104056.

Fang, G., Wei, M., Zhao, L., Xu, K., Cao, S. and Ge, Y., 2022. Site-and-building height-dependent design extreme wind speed vertical profile of tropical cyclone. *Journal of Building Engineering*, 62, pp.105322.

Favre, A., Hewitson, B., Lennard, C., Cerezo-Mota, R. and Tadross, M., 2013. Cut-off lows in the South Africa region and their contribution to precipitation. *Climate dynamics*, *41*, pp.2331-2351.

Favre, A., Hewitson, B., Tadross, M., Lennard, C. and Cerezo-Mota, R., 2012. Relationships between cut-off lows and the semi-annual and southern oscillations. *Climate dynamics*, *38*, pp.1473-1487.

Feng, T., Zhu, X. and Dong, W., 2023. Historical assessment and future projection of extreme precipitation in CMIP6 models: global and continental. *International Journal of Climatology*, *43*(9), pp 4119-4135.

Field, C.B. ed., 2012. Managing the risks of extreme events and disasters to advance climate change adaptation: special report of the intergovernmental panel on climate change. Cambridge University Press.

Flamant, C., Gaetani, M., Chaboureau, J.P., Chazette, P., Cuesta, J., Piketh, S.J. and Formenti, P., 2022. Smoke in the river: an Aerosols, Radiation and Clouds in southern Africa (AEROCLO-SA) case study. *Atmospheric Chemistry and Physics*, 22(8), pp.5701-5724.

Fouotsa Manfouo, N.C., Potgieter, L., Watson, A. and Nel, J.H., 2023. A comparison of the statistical downscaling and long-short-term-memory artificial neural network models for long-term temperature and precipitation forecasting. *Atmosphere*, *14*(4), pp.708.

Fu, T., Tang, X., Cai, Z., Zuo, Y., Tang, Y. and Zhao, X., 2020. Correlation research of phase angle variation and coating performance by means of Pearson's correlation coefficient. *Progress in Organic Coatings*, 139, pp.105-459.

Gadedjisso-Tossou, A., Adjegan, K.I. and Kablan, A.K.M., 2021. Rainfall and temperature trend analysis by Mann–Kendall test and significance for Rainfed Cereal Yields in Northern Togo. *Sci*, *3*(1), pp.17.

Gates, W.L., Rowntree, P.R. and Zeng, Q.C., 1990. Validation of climate models. In *Climate change: the IPCC scientific assessment* (pp. 93-130). Cambridge University Press.

Ge, F., Zhu, S., Luo, H., Zhi, X. and Wang, H., 2021. Future changes in precipitation extremes over Southeast Asia: insights from CMIP6 multi-model ensemble. *Environmental Research Letters*, *16*(2), pp.024013.

Gbetibouo, G.A., 2009. Understanding farmers' perceptions and adaptations to climate change and variability: The case of the Limpopo Basin, South Africa (Vol. 849). Intl Food Policy Res Inst.

Ginis, I., 2021. Tropical cyclones. *From hurricanes to epidemics: The ocean's evolving impact on human health-perspectives from the US*, Springer Cham, pp.121-128. https://doi.org/10.1007/978-3-030-55012-7

Giorgi, F., 2019. Thirty years of regional climate modelling: where are we and where are we going next? *Journal of Geophysical Research: Atmospheres*, 124(11), pp.5696-5723.

Girvetz, E., Ramirez-Villegas, J., Claessens, L., Lamanna, C., Navarro-Racines, C., Nowak, A., Thornton, P. and Rosenstock, T.S., 2019. Future climate projections in Africa: where are we headed? *The climate-smart agriculture papers: Investigating the business of a productive, resilient and low emission future*, pp.15-27.

Goddard, L. and Gershunov, A., 2020. Impact of El Niño on weather and climate extremes. *El Niño Southern* Oscillation in a changing climate, pp.361-375.

Grose, M.R., Narsey, S., Delage, F.P., Dowdy, A.J., Bador, M., Boschat, G., Chung, C., Kajtar, J.B., Rauniyar, S., Freund, M.B. and Lyu, K., 2020. Insights from CMIP6 for Australia's future climate. *Earth's Future*, *8*(5), pp.e2019EF001469.

Guo, J., Wang, X., Xiao, C., Liu, L., Wang, T. and Shen, C., 2022. Evaluation of the temperature downscaling performance of PRECIS to the BCC-CSM2-MR model over China. *Climate Dynamics*, *59*(3-4), pp.1143-1159.

Haensler, A., Hagemann, S. and Jacob, D., 2011. The role of the simulation setup in a long-term high-resolution climate change projection for the southern African region. *Theoretical and applied climatology*, *106*, pp.153-169.

Hair Jr, J.F., Hult, G.T.M., Ringle, C.M., Sarstedt, M., Danks, N.P., Ray, S., Hair, J.F., Hult, G.T.M., Ringle, C.M., Sarstedt, M. and Danks, N.P., 2021. Overview of R and RStudio. *Partial Least Squares Structural Equation Modelling (PLS-SEM) Using R*, pp.31.

Haile, G.G., Tang, Q., Hosseini-Moghari, S.M., Liu, X., Gebremicael, T.G., Leng, G., Kebede, A., Xu, X. and Yun, X., 2020. Projected impacts of climate change on drought patterns over East Africa. *Earth's Future*, *8*(7), pp.e2020EF001502. https://doi.org/10.1029/2020EF001502

Hamed, M.M., Nashwan, M.S., Shahid, S., bin Ismail, T., Wang, X.J., Dewan, A. and Asaduzzaman, M., 2022. Inconsistency in historical simulations and future projections of temperature and rainfall: a comparison of CMIP5 and CMIP6 models over Southeast Asia. *Atmospheric Research*, 265, pp.105-927.

Harrison, M.S.J., 1984. A generalized classification of South African summer rain-bearing synoptic systems. *Journal of Climatology*, *4*(5), pp.547-560.

Hart, N.C., Reason, C.J. and Fauchereau, N., 2013. Cloud bands over southern Africa: seasonality, contribution to rainfall variability and modulation by the MJO. *Climate dynamics*, *41*, pp.1199-1212.

Hartmann, D.L., Tank, A.M.K., Rusticucci, M., Alexander, L.V., Brönnimann, S., Charabi, Y.A.R., Dentener, F.J., Dlugokencky, E.J., Easterling, D.R., Kaplan, A. and Soden, B.J., 2013. Observations: atmosphere and surface. In *Climate change 2013 the physical science basis: Working group I contribution to the fifth assessment report of the intergovernmental panel on climate change* (pp. 159-254). Cambridge University Press.

Hausfather, Z., Marvel, K., Schmidt, G.A., Nielsen-Gammon, J.W. and Zelinka, M., 2022. Climate simulations: recognize the 'hot model' problem. *Nature*, *605*(7908), pp.26-29.

Hersbach, H., Bell, B., Berrisford, P., Hirahara, S., Horányi, A., Muñoz-Sabater, J., Nicolas, J., Peubey, C., Radu, R., Schepers, D. and Simmons, A., 2020. The ERA5 global reanalysis. *Quarterly Journal of the Royal Meteorological Society*, *146*(730), pp.1999-2049.

Hersbach, H., Bell, B., Berrisford, P., Biavati, G., Horányi, A., Muñoz Sabater, J., Nicolas, J., Peubey, C., Radu, R., Rozum, I. and Schepers, D., 2023. ERA5 hourly data on pressure levels from 1940 to the present. *Copernicus Climate Change Service (C3S) Climate Data Store (CDS) [data set]*, 10.

Hoell, A., Funk, C., Zinke, J. and Harrison, L., 2017. Modulation of the southern Africa precipitation response to the El Niño Southern Oscillation by the subtropical Indian Ocean dipole. *Climate Dynamics*, 48, pp.2529-2540.

Hook, M., 2011. Fuelling future emissions—examining fossil fuel production outlooks used in climate models. *Climate change-research and technology for adaptation and mitigation*.

Hook, M. and Tang, X., 2013. Depletion of fossil fuels and anthropogenic climate change—A review. *Energy policy*, 52, pp.797-809.

Hourdin, F., Rio, C., Grandpeix, J.Y., Madeleine, J.B., Cheruy, F., Rochetin, N., Jam, A., Musat, I., Idelkadi, A., Fairhead, L. and Foujols, M.A., 2020. LMDZ6A: The atmospheric component of the IPSL climate model with improved and better-tuned physics. *Journal of Advances in Modeling Earth Systems*, *12*(7), pp.e2019MS001892.

Hove, L. and Kambanje, C., 2019. Lessons from the El Niño –induced 2015/16 drought in the southern Africa region. In *Current directions in water scarcity research* (Vol. 2, pp. 33-54). Elsevier.

Howard, E., Washington, R. and Hodges, K.I., 2019. Tropical lows in southern Africa: tracks, rainfall contributions, and the role of ENSO. *Journal of Geophysical Research: Atmospheres*, 124(21), pp.11009-11032.

Ibebuchi, C.C., 2021. Revisiting the 1992 severe drought episode in South Africa: the role of El Niño in the anomalies of atmospheric circulation types in Africa south of the equator. *Theoretical and Applied Climatology*, 146(1), pp.723-740.

Ibebuchi, C.C., 2023. Patterns of atmospheric circulation linking the positive tropical Indian Ocean dipole and southern African rainfall during summer. *Journal of Earth System Science*, *132*(1), pp.13.

IPCC, I., 2007. IPCC fourth assessment report: climate change 2007. *Intergovernmental panel on climate change. Cambridge University Press, Cambridge*, pp.213-252.

Jury, M.R., 2018. Climate trends across South Africa since 1980. Water SA, 44(2), pp.297-307.

Jury, M.R. and Pathack, B., 1991. A study of climate and weather variability over the tropical South-West Indian Ocean. *Meteorology and Atmospheric Physics*, *47*(1), pp.37-48.

Kapuka, A., Hlásny, T. and Helmschrot, J., 2022. Climate change research in southern Africa in recent two decades: progress, needs, and policy implications. *Regional Environmental Change*, 22(1), pp.18.

Karl, T.R. and Trenberth, K.E., 2003. Modern global climate change. science, 302(5651), pp.1719-1723.

Kaspar, F., Schulzweida, U. and Müller, R., 2010. September. Climate data operators" as a user-friendly processing tool for CM SAF's satellite-derived climate monitoring products. In *Conference: EUMETSAT Meteorological Satellite Conference* 2010 (pp. 20-24).

Kaur, S., Kaushal, S., Adhikari, D., Raj, K., Rao, K.S., Tandon, R., Goel, S., Barik, S.K. and Baishya, R., 2023. Different GCMs yet similar outcome: predicting the habitat distribution of Shorea robusta CF Gaertn. in the Indian Himalayas using CMIP5 and CMIP6 climate models. *Environmental Monitoring and Assessment*, 195(6), pp.715.

Keriwala, N. and Patel, A., 2022. Impact assessment of tropical cyclone Tauktae on coastal region of Gujarat, India. *ECS Transactions*, 107(1), pp.6185.

Khine, M.M. and Langkulsen, U., 2023. The implications of climate change on health among vulnerable populations in South Africa: a systematic review. *International Journal of Environmental Research and Public Health*, 20(4), pp.3425.

Klopper, E., Landman, W.A. and Van Heerden, J., 1998. The predictability of seasonal maximum temperature in South Africa. *International Journal of Climatology: A Journal of the Royal Meteorological Society*, *18*(7), pp.741-758.

Krotov, V., 2017. A Quick Introduction to R and RStudio (pp. 1-15). Technical Report.

Kruger, A.C. and Sekele, S.S., 2013. Trends in extreme temperature indices in South Africa: 1962-2009. *International Journal of Climatology*, 33(3).

Kruger, A.C. and Shongwe, S., 2004. Temperature trends in South Africa: 1960-2003. *International journal of Climatology*, *24*(15), pp.1929-1945.

Kumar, P. and Sarthi, P.P., 2019. Surface temperature evaluation and future projections over India using CMIP5 models. *Pure and Applied Geophysics*, *176*(11), pp.5177-5201.

Kumari, S., Aggarwal, S.P., Thakur, P. and Patel, P., 2015. Hydrometeorological data assimilation in the weather forecasting model using open source tools.

Lamers, A., Sharma, M., Berg, R., Gálvez, J.M., Yu, Z., Kriat, T., Cardos, S., Grant, D. and Moron, L.A., 2023. Forecasting tropical cyclone rainfall and flooding hazards and impacts. *Tropical Cyclone Research and Review*, *12*(2), pp.100-112.

Landman, W.A., Malherbe, J. and Engelbrecht, F., 2017. South Africa's present-day climate. *Understanding the social and environmental implications of global change*, pp.7-12.

Lazenby, M.J., Todd, M.C., Chadwick, R. and Wang, Y., 2018. Future precipitation projections over central and southern Africa and the adjacent Indian Ocean: what causes the changes and the uncertainty? *Journal of Climate*, 31(12), pp.4807-4826.

Li, X., Fang, G., Wei, J., Arnault, J., Laux, P., Wen, X. and Kunstmann, H., 2023. Evaluation and projection of precipitation and temperature in a coastal climatic transitional zone in China based on CMIP6 GCMs. *Climate Dynamics*, pp.1-23.

Li, Y., Ruan, S., Zhou, A., Xie, P., Azam, S.R. and Ma, H., 2022. Ultrasonic modification on fermentation characteristics of Bacillus varieties: impact on protease activity, peptide content and its correlation coefficient. *LWT*, 154, pp.112-852.

Lin, I.I., Camargo, S.J., Patricola, C.M., Boucharel, J., Chand, S., Klotzbach, P., Chan, J.C., Wang, B., Chang, P., Li, T. and Jin, F.F., 2020. ENSO and tropical cyclones. *El Niño Southern Oscillation in a changing climate*, pp.377-408.

Liu, Z., Eden, J.M., Dieppois, B., Conradie, W.S. and Blackett, M., 2023. The April 2021 Cape Town wildfire: has anthropogenic climate change altered the likelihood of extreme fire weather? *Bulletin of the American Meteorological Society*, *104*(1), pp.298-304.

Liu, J., Meucci, A. and Young, I.R., 2023. Projected 21st century wind-wave climate of Bass Strait and southeast Australia: comparison of EC-Earth3 and ACCESS-CM2 climate model forcing. *Journal of Geophysical Research:* Oceans, 128(4) pp. e2022JC018996.

Longobardi, A. and Villani, P., 2010. Trend analysis of annual and seasonal rainfall time series in the Mediterranean area. *International Journal of Climatology*, *30*(10), pp.1538-1546.

Lu, Y., Wu, T., Li, Y. and Yang, B., 2021. Mitigation of the double ITCZ syndrome in BCC-CSM2-MR through improving parameterizations of boundary-layer turbulence and shallow convection. *Geoscientific Model Development*, *14*(8), pp.5183-5204.

Mabhaudhi, T., Mpandeli, S., Nhamo, L., Senzanje, A., Chimonyo, V.G.P. and Modi, A.T., 2019. Options for improving agricultural water productivity under increasing water scarcity in South Africa. In *3rd World Irrigation Forum (WIF3) on development for water, food and nutrition security in a competitive environment, Bali, Indonesia* (pp. 1-7).

MacKellar, N., New, M. and Jack, C., 2014. Observed and modelled trends in rainfall and temperature for South Africa: 1960-2010. *South African Journal of Science*, *110*(7-8), pp.1-13.

Mahlalela, P.T., Blamey, R.C., Hart, N.C.G. and Reason, C.J.C., 2020. Drought in the Eastern Cape region of South Africa and trends in rainfall characteristics. *Climate Dynamics*, *55*, pp.2743-2759.

Mahlalela, P.T., Blamey, R.C. and Reason, C.J.C., 2019. Mechanisms behind early winter rainfall variability in the southwestern Cape, South Africa. *Climate Dynamics*, 53, pp.21-39.

Mahlobo, D.D., 2013. The verification of different model configurations of the unified atmospheric model over South Africa (Master's thesis, University of Pretoria).

Mahlobo, D.D., Ndarana, T., Grab, S. and Engelbrecht, F., 2019. Integrated climatology and trends in the subtropical hadley cell, sunshine duration, and cloud cover over South Africa. *International Journal of Climatology*, 39(4), pp.1805-1821.

Makungo, R. and Mashinye, M.D., 2022. Long-term trends and changes in rainfall magnitude and duration in a semi-arid catchment, South Africa. *Journal of Water and Climate Change*, *13*(6), pp.2319-2336.

Martinez, A. and Iglesias, G., 2023. Climate-change impacts on offshore wind resources in the Mediterranean Sea. *Energy Conversion and Management*, 291, pp.117-231.

Mashao, F.M., Mothapo, M.C., Munyai, R.B., Letsoalo, J.M., Mbokodo, I.L., Muofhe, T.P., Matsane, W. and Chikoore, H., 2023. Extreme rainfall and flood risk prediction over the east coast of South Africa. *Water*, *15*(1), pp.50.

Matthews, B., McIlwrath, B., Giaretta, D. and Conway, E., 2008. The significant properties of software: A study. *JISC report, March*.

Maule, C.F., Mendlik, T. and Christensen, O.B., 2017. The effect of the pathway to a two degrees' warmer world on the regional temperature change of Europe. *Climate Services*, 7, pp.3-11.

Mauritsen, T., Bader, J., Becker, T., Behrens, J., Bittner, M., Brokopf, R., Brovkin, V., Claussen, M., Crueger, T., Esch, M. and Fast, I., 2019. Developments in the MPI-M Earth System Model version 1.2 (MPI-ESM1. 2) and its response to increasing CO2. *Journal of Advances in Modelling Earth Systems*, *11*(4), pp.998-1038.

Malherbe, J., Engelbrecht, F.A. and Landman, W.A., 2013. Projected changes in tropical cyclone climatology and landfall in the South-West Indian Ocean region under enhanced anthropogenic forcing. *Climate dynamics*, *40*, pp.2867-2886.

Mbokodo, I., Bopape, M.J., Chikoore, H., Engelbrecht, F. and Nethengwe, N., 2020. Heatwaves in the future warmer climate of South Africa. *Atmosphere*, *11*(7), pp.712.

Mbokodo, I.L., Bopape, M.J.M., Ndarana, T., Mbatha, S.M., Muofhe, T.P., Singo, M.V., Xulu, N.G., Mohomi, T., Ayisi, K.K. and Chikoore, H., 2023. Heatwave Variability and Structure in South Africa during Summer Drought. *Climate*, *11*(2), pp.38.

McBride, C.M., Kruger, A.C. and Dyson, L., 2022a. Changes in extreme daily rainfall characteristics in South Africa: 1921–2020. *Weather and Climate Extremes*, 38, pp.100-517.

McBride, C.M., Kruger, A.C. and Dyson, L.L., 2022b. Trends in probabilities of temperature records in the non-stationary climate of South Africa.

Meinshausen, M., Nicholls, Z.R., Lewis, J., Gidden, M.J., Vogel, E., Freund, M., Beyerle, U., Gessner, C., Nauels, A., Bauer, N. and Canadell, J.G., 2020. The shared socio-economic pathway (SSP) greenhouse gas concentrations and their extensions to 2500. *Geoscientific Model Development*, *13*(8), pp.3571-3605.

Mengistu, A.G., Woyessa, Y.E., Tesfuhuney, W.A., Steyn, A.S. and Lee, S.S., 2024. Assessing the impact of climate change on future extreme temperature events in major South African cities. *Theoretical and Applied Climatology*, 155(3), pp.1807-1819.

Meque, A., Pinto, I., Maúre, G. and Beleza, A., 2022. Understanding the variability of heatwave characteristics in southern Africa. *Weather and Climate Extremes*, *38*, pp.100-498.

Mertz, O., Halsnæs, K., Olesen, J.E. and Rasmussen, K., 2009. Adaptation to climate change in developing countries. *Environmental management*, *43*, pp.743-752.

Meyiwa, S., 2019. *Numerical modelling of Tropical Cyclone Dineo and its rainfall impacts over north-eastern South Africa*. Faculty of Science, Department of Oceanography. (Master's thesis, Faculty of Science). http://hdl.handle.net/11427/31174

Min, J., Yan, G., Abed, A.M., Elattar, S., Khadimallah, M.A., Jan, A. and Ali, H.E., 2022. The effect of carbon dioxide emissions on building energy efficiency. *Fuel*, *326*, pp.124-842.

Mignot, J., Hourdin, F., Deshayes, J., Boucher, O., Gastineau, G., Musat, I., Vancoppenolle, M., Servonnat, J., Caubel, A., Chéruy, F. and Denvil, S., 2021. The tuning strategy of IPSL-CM6A-LR. *Journal of Advances in Modeling Earth Systems*, *13*(5), pp.e2020MS002340.

Moeletsi, M.E., Tongwane, M. and Tsubo, M., 2016. The study of frost occurrence in Free State province of South Africa. *Advances in Meteorology*, 2016(1), pp.9586150.

Molekwa, S., 2013. *Cut-off lows over South Africa and their contribution to the total rainfall of the Eastern Cape province*. University of Pretoria (South Africa).

Monyela, B. M., 2017. *A two-year long drought in summer 2014/2015 and 2015/2016 over South Africa*. University of Cape Town, Faculty of Science, Department of Oceanography. (Thesis). http://hdl.handle.net/11427/27111

Morishima, W. and Akasaka, I., 2010. Seasonal trends of rainfall and surface temperature over southern Africa. *African study monographs. Supplementary issue.*, 40, pp.67-76.

Moseki, C., Lekalakala, G. and Petja, B., 2022. The current policy situation as an enabler for water sector climate change response to increase resilience. *Climate Change Impacts on Water Resources: Implications and Practical Responses in Selected South African Systems*, pp.186.

Moses, O., Blamey, R.C. and Reason, C.J.C., 2023. Extreme rainfall events over the Okavango River basin, southern Africa. *Weather and Climate Extremes*, 41, pp.100-589.

Mpandeli, S., Naidoo, D., Mabhaudhi, T., Nhemachena, C., Nhamo, L., Liphadzi, S., Hlahla, S. and Modi, A.T., 2018. Climate change adaptation through the water-energy-food nexus in southern Africa. *International Journal of Environmental Research and Public Health*, *15*(10), pp.2306.

Mpungose, N., Thoithi, W., Blamey, R.C. and Reason, C.J.C., 2022. Extreme rainfall events in southeastern Africa during the summer. *Theoretical and Applied Climatology*, *150*(1-2), pp.185-201.

Mpungose, N.B., 2022. Extreme rainfall events over the Pongola-Mtamvuna Water Management Area of South Africa (Master's thesis, Faculty of Science).

Mthembu, A. and Hlophe, S., 2020. Building resilience to climate change in vulnerable communities: a case study of uMkhanyakude district municipality. *Town and Regional Planning*, 77, pp.42-56.

Mudefi, E., 2023. Disaster management 'deeds' in the context of April 2022 KwaZulu-Natal floods: a scoping review. *International Journal of Disaster Risk Reduction*, 98, pp.104122.

Munday, C. and Washington, R., 2017. Circulation controls on southern African precipitation in coupled models: the role of the Angola low. *Journal of Geophysical Research: Atmospheres*, 122(2), pp.861-877.

Munyai, R.B., Chikoore, H., Musyoki, A., Chakwizira, J., Muofhe, T.P., Xulu, N.G. and Manyanya, T.C., 2021. Vulnerability and adaptation to flood hazards in rural settlements of Limpopo province, South Africa. *Water*, *13*(24), pp.34-90.

Mutengwa, C.S., Mnkeni, P. and Kondwakwenda, A., 2023. Climate-smart agriculture and food security in southern Africa: a review of the vulnerability of smallholder agriculture and food security to climate change. Sustainability, 15(4), pp.2882.

Muyambo, F., Belle, J., Nyam, Y.S. and Orimoloye, I.R., 2023. Climate-change-induced weather events and implications for urban water resource management in the Free State province of South Africa. *Environmental Management*, 71(1), pp.40-54.

Muofhe, T.P., Chikoore, H., Bopape, M.J.M., Nethengwe, N.S., Ndarana, T. and Rambuwani, G.T., 2020. Forecasting intense cut-off lows in South Africa using the 4.4 km Unified Model. *Climate*, *8*(11), pp.129.

Naher, N., 2016. Analysis of low-level moisture transport over South Asia. http://lib.buet.ac.bd:8080/xmlui/handle/123456789/4547

Nakicenovic, N., Alcamo, J., Davis, G., Vries, B.D., Fenhann, J., Gaffin, S., Gregory, K., Grubler, A., Jung, T.Y., Kram, T. and La Rovere, E.L., 2000. Special report on emissions scenarios.

Nanda, V.P., 2021. Global climate change and international law and institutions. In *World climate change* (pp. 227-239). Routledge.

Neelin, J.D., 2010. Climate change and climate modelling. Cambridge University Press.

Nembilwi, N., Chikoore, H., Kori, E., Munyai, R.B. and Manyanya, T.C., 2021. The occurrence of drought in Mopani district municipality, South Africa: impacts, vulnerability, and adaptation. *Climate*, *9*(4), pp.61. Ncoyini, Z., Savage, M.J. and Strydom, S., 2022. Limited access and use of climate information by small-scale sugarcane farmers in South Africa: a case study. *Climate Services*, *26*, pp.100-285.

Ncube, T.M., 2019. Rainfall variability and change in South Africa (1976-2065) (Master's thesis).

Ndarana, T., Rammopo, T.S., Chikoore, H., Barnes, M.A. and Bopape, M.J., 2020. A quasi-geostrophic diagnosis of the zonal flow associated with cut-off lows over South Africa and surrounding oceans. *Climate Dynamics*, 55, pp.2631-2644.

Ndarana, T., Mpati, S., Bopape, M.J.M., Engelbrecht, F.A. and Chikoore, H., 2021. The flow and moisture fluxes associated with ridging South Atlantic Ocean anticyclones during the subtropical southern African summer.

Ndlovu, M., Clulow, A.D., Savage, M.J., Nhamo, L., Magidi, J. and Mabhaudhi, T., 2021. An assessment of the impacts of climate variability and change in KwaZulu-Natal province, South Africa. *Atmosphere*, *12*(4), pp.427.

Ngcamu, B., 2022. Climate change and disaster preparedness issues in Eastern Cape and Kwazulu-Natal, South Africa. *Town and regional planning*, *81*, pp.53-66.

Nguyen, P.L., Bador, M., Alexander, L.V. and Lane, T.P., 2023. Selecting regional climate models based on their skill could give more credible precipitation projections over the complex Southeast Asia region. *Climate Dynamics*, pp.1-22.

Nhamo, L., Matchaya, G., Mabhaudhi, T., Nhlengethwa, S., Nhemachena, C. and Mpandeli, S., 2019. Cereal production trends under climate change: impacts and adaptation strategies in southern Africa. *Agriculture*, *9*(2), pp.30.

Nhemachena, C., Nhamo, L., Matchaya, G., Nhemachena, C.R., Muchara, B., Karuaihe, S.T. and Mpandeli, S., 2020. Climate change impacts on water and agriculture sectors in southern Africa: threats and opportunities for sustainable development. *Water*, *12*(10), pp.2673.

Odoulami, R.C., Wolski, P. and New, M., 2021. A SOM-based analysis of the drivers of the 2015–2017 Western Cape drought in South Africa. *International Journal of Climatology*, *41*(1), pp.1518-1530.

Odongo, M.T., Misati, R.N., Kamau, A.W. and Kisingu, K.N., 2022. Climate change and inflation in Eastern and southern Africa. *Sustainability*, *14*(22), pp.14764.

Ogundeji, A.A., 2022. Adaptation to climate change and impact on smallholder farmers' food security in South Africa. *Agriculture*, *12*(5), pp.589.

Ohde, T., 2018. Coastal sulphur plumes off Peru during El Niño, La Niña, and neutral phases. *Geophysical Research Letters*, *45*(14), pp.7075-7083.

Olanrewaju, C.C. and Reddy, M., 2022. Assessment and prediction of flood hazards using standardized precipitation index—A case study of eThekwini metropolitan area. *Journal of Flood Risk Management*, 15(2), pp. e12788.

Olorunfemi, F.B., 2011, May. Managing flood disasters under a changing climate: lessons from Nigeria and South Africa. In *NISER Research Seminar Series*, *NISER*, *Ibadan* (Vol. 3, pp. 1-44).

O'Neill, B.C., Kriegler, E., Riahi, K., Ebi, K.L., Hallegatte, S., Carter, T.R., Mathur, R. and Van Vuuren, D.P., 2014. A new scenario framework for climate change research: the concept of shared socioeconomic pathways. *Climatic change*, 122, pp.387-400.

O'Neill, B.C., Kriegler, E., Ebi, K.L., Kemp-Benedict, E., Riahi, K., Rothman, D.S., Van Ruijven, B.J., Van Vuuren, D.P., Birkmann, J., Kok, K. and Levy, M., 2017. The roads ahead: narratives for shared socioeconomic pathways describing world futures in the 21st century. *Global environmental change*, 42, pp.169-180.

Ouma, J.O., Wakjira, D., Amdihun, A., Nyaga, E., Opijah, F., Muthama, J., Otieno, V., Kayijamahe, E., Munywa, S. and Artan, G., 2022. Forage monitoring and prediction model for early warning application over the east of Africa region. *Journal of Atmospheric Science Research*, *5*(4), pp.1-9.

Pandy, W.R. and Rogerson, C.M., 2021. Climate change risks and tourism in South Africa: projections and policy. *Geo Journal of Tourism and Geosites*, 35(2), pp.445-455.

Parker, E.R., Mo, J. and Goodman, R.S., 2022. The dermatological manifestations of extreme weather events: a comprehensive review of skin disease and vulnerability. *The Journal of Climate Change and Health*, *8*, pp.100-162.

Petja, B., Nhamo, L., Mpandeli, S., Zvimba, J., Adams, S. and Naidoo, D., 2021. Reflecting on the projected impacts of climate change on water security in South Africa and the need to increase the resilience.

Philippon, N., Rouault, M., Richard, Y. and Favre, A., 2012. The influence of ENSO on winter rainfall in South Africa. *International Journal of Climatology*, 32(15), pp.2333-2347.

Pillay, M.T. and Fitchett, J.M., 2019. Tropical cyclone landfalls south of the Tropic of Capricorn, South-West Indian Ocean. *Climate Research*, 79(1), pp.23-37.

Pourali, M., Kavianpour, M.R., Kamranzad, B. and Alizadeh, M.J., 2023. Future variability of wave energy in the Gulf of Oman using a high-resolution CMIP6 climate model. *Energy*, 262, pp.125-552.

Quiroz, N.F., Gibson, L., Conradie, W.S., Ryan, P., Heydenrych, R., Moran, A., van Straten, A. and Walls, R., 2023. Analysis of the 2017 knysna fires disaster with emphasis on fire spread, home losses and the influence of vegetation and weather conditions: a South African case study. *International Journal of Disaster Risk Reduction*, 88, pp.103-618.

Racine, J.S., 2012. RStudio: a platform-independent IDE for R and Sweave. *Journal of Applied Econometrics*, 27(1), pp.167-172.

Rankoana, S.A., 2022. Small-scale farmers' vulnerability to the impacts of climate change in Limpopo province, South Africa: a review. *International Journal of Development and Sustainability*, 11(7), pp.236-248.

Rapolaki, R.S., Blamey, R.C., Hermes, J.C. and Reason, C.J., 2019. A classification of synoptic weather patterns linked to extreme rainfall over the Limpopo River Basin in southern Africa. *Climate Dynamics*, 53, pp.2265-2279.

Ratna, S.B., Behera, S., Ratnam, J.V., Takahashi, K. and Yamagata, T., 2013. An index for tropical temperate troughs over southern Africa. *Climate dynamics*, *41*, pp.421-441.

Ravi, L., 2018. AVISTED: Analysis and visualization toolset for environmental data (Doctoral dissertation, University of Nevada, Reno).

Ray, D.K., West, P.C., Clark, M., Gerber, J.S., Prishchepov, A.V. and Chatterjee, S., 2019. Climate change has likely already affected global food production. *PloS one*, *14*(5), pp.0217148.

Reason, C.J.C., 2017. Climate of southern Africa. In Oxford research encyclopedia of climate science.

Reason, C.J.C. and Keibel, A., 2004. Tropical cyclone Eline and its unusual penetration and impacts over the southern African mainland. *Weather and forecasting*, *19*(5), pp.789-805.

Reid, K.J., Simmonds, I., Vincent, C.L. and King, A.D., 2019. The Australian northwest cloud band: climatology, mechanisms, and association with precipitation. *Journal of Climate*, 32(20), pp.6665-6684.

Riahi, K., Van Vuuren, D.P., Kriegler, E., Edmonds, J., O'neill, B.C., Fujimori, S., Bauer, N., Calvin, K., Dellink, R., Fricko, O. and Lutz, W., 2017. The Shared Socioeconomic Pathways and their energy, land use, and greenhouse gas emissions implications: an overview. *Global environmental change*, *42*, pp.153-168.

Roffe, S.J., Fitchett, J.M. and Curtis, C.J., 2019. Classifying and mapping rainfall seasonality in South Africa: a review. *South African Geographical Journal= Suid-Afrikaanse Geografiese Tydskrif*, *101*(2), pp.158-174. Rohli, R.V. and Li, C., 2021. Tropical cyclones. *Meteorology for Coastal Scientists*, pp.291-308.

Rouault, M., Dieppois, B., Tim, N., Hünicke, B. and Zorita, E., 2024. Southern Africa Climate Over the Recent Decades: Description, Variability and Trends. In *Sustainability of Southern African Ecosystems under Global Change: Science for Management and Policy Interventions* (pp. 149-168). Cham: Springer International Publishing.

Rouault, M., Florenchie, P., Fauchereau, N. and Reason, C.J., 2003. South East tropical Atlantic warm events and southern African rainfall. *Geophysical Research Letters*, 30(5).

Salarieh, B., Ugwu, I.A. and Salman, A.M., 2023. Impact of changes in sea surface temperature due to climate change on hurricane wind and storm surge hazards across US Atlantic and Gulf coast regions. *SN Applied Sciences*, *5*(8), pp.205.

Sazib, N., Mladenova, L.E. and Bolten, J.D., 2020. Assessing the impact of ENSO on agriculture over Africa using earth observation data. *Frontiers in Sustainable Food Systems*, *4*, pp.509-914.

Scholes, R. and Engelbrecht, F., 2021. Climate impacts in southern Africa during the 21st Century. Report for Earth Justice and the Centre for Environmental Rights. Global Change Institute, University of Witwatersrand.

Semmler, T., Danilov, S., Gierz, P., Goessling, H.F., Hegewald, J., Hinrichs, C., Koldunov, N., Khosravi, N., Mu, L., Rackow, T. and Sein, D.V., 2020. Simulations for CMIP6 with the AWI climate model AWI-CM-1-1. *Journal of Advances in Modeling Earth Systems*, *12*(9), pp.e2019MS002009.

Semmler, T., Danilov, S., Rackow, T., Sidorenko, D., Barbi, D., Hegewald, J., Pradhan, H.K., Sein, D., Wang, Q. and Jung, T., 2019. AWI-CM-1.1-MR model output prepared for CMIP6 Scenario MIP: links to SSP126, SSP370, and SSP585 scenarios. *Earth System Grid Federation*.

Shikwambana, L., Mhangara, P. and Mbatha, N., 2020. Trend analysis and first-time observations of sulphur dioxide and nitrogen dioxide in South Africa using TROPOMI/Sentinel-5 P data. *International Journal of Applied Earth Observation and Geoinformation*, 91, pp.102-130.

Shikwambana, L., Xongo, K., Mashalane, M. and Mhangara, P., 2023. Climatic and vegetation response patterns over South Africa during the 2010/2011 and 2015/2016 strong ENSO phases. *Atmosphere*, *14*(2), pp.416.

Shikwambana, S. and Malaza, N., 2022. Enhancing the resilience and adaptive capacity of smallholder farmers to drought in the Limpopo province, South Africa. *Conservation*, 2(3), pp.435-449.

Shisanya, S. and Mafongoya, P., 2016. Adaptation to climate change and the impacts on household food security among rural farmers in uMzinyathi District of Kwazulu-Natal, South Africa. *Food security*, *8*, pp.597-608.

Siabi, E.K., Awafo, E.A., Kabo-bah, A.T., Derkyi, N.S.A., Akpoti, K., Mortey, E.M. and Yazdanie, M., 2023. Assessment of Shared Socioeconomic Pathway (SSP) climate scenarios and its impacts on the Greater Accra region. *Urban Climate*, *49*, pp.101-432.

Singh, J.A., Thalheimer, L., van Aalst, M., Li, S., Sun, J., Vecchi, G., Yang, W., Tradowsky, J., Otto, F.E. and Dipura, R., 2022. Climate change exacerbated rainfall causing devastating flooding in Eastern South Africa. *World weather attribution KZN floods scientific report*.

Singleton, A.T. and Reason, C.J.C., 2007. Variability in the characteristics of cut-off low-pressure systems over subtropical southern Africa. *International Journal of Climatology: A Journal of the Royal Meteorological Society*, 27(3), pp.295-310.

Singo, M.V., Chikoore, H., Engelbrecht, F.A., Ndarana, T., Muofhe, T.P., Mbokodo, I.L., Murungweni, F.M. and Bopape, M.J.M., 2023. Projections of future fire risk under climate change over the South African savanna. *Stochastic Environmental Research and Risk Assessment*, 37, pp.1-15.

Slangen, A.B., Palmer, M.D., Camargo, C.M., Church, J.A., Edwards, T.L., Hermans, T.H., Hewitt, H.T., Garner, G.G., Gregory, J.M., Kopp, R.E. and Santos, V.M., 2023. The evolution of 21st-century sea-level projections from IPCC AR5 to AR6 and beyond. *Cambridge Prisms: Coastal Futures*, *1*, pp.7.

Smithers, J.C., Schulze, R.E., Pike, A. and Jewitt, G.P.W., 2001. A hydrological perspective of the February 2000 floods: a case study in the Sabie River catchment. *Water Sa*, 27(3), pp.325-332.

Sohrabi, M.M., Marofi, S. and Ababaei, B., 2009, August. Investigation of temperature and precipitation indices by using RClimDex and R software in Semnan province. In *International conference on water Resources* (pp. 16-18).

Stander, J.H., Dyson, L. and Engelbrecht, C.J., 2016. A snow forecasting decision tree for significant snowfall over the interior of South Africa. *South African Journal of Science*, *112*(9-10), pp.1-10.

Steiner, A., Aguilar, G., Bomba, K., Bonilla, J.P., Campbell, A., Echeverría, R.G., Gandhi, R., Hedegaard, C., Holdorf, D., Ishii, N. and Quinn, K.M., 2020. Actions to transform food systems under climate change.

Stock, C.A., Dunne, J.P., Fan, S., Ginoux, P., John, J., Krasting, J.P., Laufkötter, C., Paulot, F. and Zadeh, N., 2020. Ocean biogeochemistry in GFDL's Earth System Model 4.1 and its response to increasing atmospheric CO2. *Journal of Advances in Modeling Earth Systems*, *12*(10), pp.e2019MS002043.

Sun, Y., Zhang, X., Ding, Y., Chen, D., Qin, D. and Zhai, P., 2022. Understanding human influence on climate change in China. *National science review*, *9*(3), pp.113.

Taljaard, J.J., 1985. *Cut-off lows in the South African region* (No. 14). Weather Bureau, Department of Transport.

Tangang, F., Supari, S., Chung, J.X., Cruz, F., Salimun, E., Ngai, S.T., Juneng, L., Santisirisomboon, J., Santisirisomboon, J., Ngo-Duc, T. and Phan-Van, T., 2018. Future changes in annual precipitation extremes over Southeast Asia under global warming of 2 C. *APN Science Bulletin*, 8(1).

Tapiador, F.J., Navarro, A., Levizzani, V., García-Ortega, E., Huffman, G.J., Kidd, C., Kucera, P.A., Kummerow, C.D., Masunaga, H., Petersen, W.A. and Roca, R., 2017. Global precipitation measurements for validating climate models. *Atmospheric Research*, *197*, pp.1-20.

Tapiador, F.J., Navarro, A., Moreno, R., Sánchez, J.L. and García-Ortega, E., 2020. Regional climate models: 30 years of dynamical downscaling. *Atmospheric Research*, 235, pp.104785.

Taylor, K.E., 2001. Summarizing multiple aspects of model performance in a single diagram. *Journal of Geophysical Research: Atmospheres*, 106(7), pp.7183-7192.

Taylor, K.E., 2005. Taylor diagram primer. Work. Pap, pp.1-4.

Taylor, K.E., Stouffer, R.J. and Meehl, G.A., 2012. An overview of CMIP5 and the experiment design. *Bulletin of the American Meteorological Society*, 93(4), pp.485-498.

Tayyebi, M., Sharafati, A., Nazif, S. and Raziei, T., 2023. Assessment of adaptation scenarios for agriculture water allocation under climate change impact. *Stochastic Environmental Research and Risk Assessment*, pp.1-23.

Tehrani, M.J., Bozorg-Haddad, O., Pingale, S.M., Achite, M. and Singh, V.P., 2022. Introduction to key features of climate models. In *Climate change in sustainable water resources management* (pp. 153-177). Singapore: Springer Nature Singapore.

Thambiran, T., Naidoo, S., Lötter, D., John, J., Padayachi, Y. and Area, H.C.C.I., 2023. Initiative for climate action transparency-ICAT first set of refined tools and methodologies based on lessons learned in pilot testing: multi-hazard early warning systems monitoring and evaluation framework for South Africa.

Theron, S.N., Archer, E.R.M., Midgley, S.J.E. and Walker, S., 2022. Exploring farmers' perceptions and lessons learned from the 2015–2018 drought in the Western Cape, South Africa. *Journal of Rural Studies*, 95, pp.208-222.

Thoithi, W., Blamey, R.C. and Reason, C.J., 2022. April 2022 Floods over East Coast South Africa: interactions between a mesoscale convective system and a coastal meso-low. *Atmosphere*, *14*(1), pp.78.

Tongwane, M.I., Ramotubei, T.S. and Moeletsi, M.E., 2022. Influence of climate on conflicts and migrations in southern Africa in the 19th and early 20th centuries. *Climate*, *10*(8), pp.119.

Trenberth, K.E., 2011. Changes in precipitation with climate change. *Climate research*, 47(1-2), pp.123-138.

Van der Merwe, J.P., Germishuizen, I., Clarke, C. and Mansfield, S.D., 2022. The impact of soil, altitude, and climate on tree form and wood properties of plantation grown Pinus patula in Mpumalanga, South Africa. *Holzforschung*.

Van der Merwe, J.P., Wang, T., Clarke, C. and Mansfield, S.D., 2023. Predicting temperature and rainfall for plantation forestry in Mpumalanga, South Africa, using locally developed climate models. *Agricultural and Forest Meteorology*, 329, pp.109-275.

Van der Walt, A.J., 2020. *An analysis of extreme temperature events in South Africa:* 1960-2015 (Doctoral dissertation).

Van Der Walt, A.J. and Fitchett, J.M., 2020. Statistical classification of South African seasonal divisions on the basis of daily temperature data. *South African Journal of Science*, *116*(9-10), pp.1-15.

Van Der Walt, A.J. and Fitchett, J.M., 2021. Trend analysis of cold extremes in South Africa: 1960–2016. *International Journal of Climatology*, *41*(3), pp.2060-2081.

Van Der Walt, A.J. and Fitchett, J.M., 2022. Extreme temperature events (ETEs) in South Africa: a review. *South African Geographical Journal*, 104(1), pp.70-88.

Van Vuuren, D.P., Kriegler, E., O'Neill, B.C., Ebi, K.L., Riahi, K., Carter, T.R., Edmonds, J., Hallegatte, S., Kram, T., Mathur, R. and Winkler, H., 2014. A new scenario framework for climate change research: scenario matrix architecture. *Climatic change*, *122*, pp.373-386.

Vetter, T.R., 2017. Descriptive statistics: reporting the answers to the 5 basic questions of who, what, why, when, where, and a sixth, so what?. *Anesthesia & Analgesia*, 125(5), pp.1797-1802.

Vincent, K., 2007. Uncertainty in adaptive capacity and the importance of scale. *Global Environmental Change*, 17(1), pp.12-24.

Volgraff, R. and Cele, S., 2022. South Africa declares floods a disaster as deaths pass 300. Available online: https://www.bloomberg.com/news/articles/2022-04-14/south-africa-declares-floods-a-disaster-after-more-than-300-die?leadSource=uverify%20wal (accessed on 13 September 2022).

Volodin, E. and Gritsun, A., 2018. Simulation of observed climate changes in 1850–2014 with climate model INM-CM5. *Earth System Dynamics*, *9*(4), pp.1235-1242.

Wada, I.M., Usman, H.S., Nwankwegu, A.S., Usman, M.N. and Gebresellase, S.H., 2023. Selection and downscaling of CMIP6 climate models in Northern Nigeria. *Theoretical and Applied Climatology*, 153, pp.1-19.

Wang, J. and Zhao, A., 2022. Spatio-temporal variation of extreme climates and its relationship with teleconnection patterns in Beijing-Tianjin-Hebei from 1980 to 2019. *Atmosphere*, *13*(12), pp.1979.

Wang, J., Xu, C., Hu, M., Li, Q., Yan, Z. and Jones, P., 2018. Global land surface air temperature dynamics since 1880. *International Journal of Climatology*, *38*(S1), pp.e466-e474.

Wang, Y. and Matyas, C.J., 2022. Simulating the effects of land surface characteristics on planetary boundary layer parameters for a modeled land falling tropical cyclone. *Atmosphere*, *13*(1), pp.138.

Wang, Y.Q., 2019. An open-source software suite for multi-dimensional meteorological data computation and visualisation. *Journal of Open Research Software*, 7(1), pp 21.

Watanabe, M., Suzuki, T., O'ishi, R., Komuro, Y., Watanabe, S., Emori, S., Takemura, T., Chikira, M., Ogura, T., Sekiguchi, M. and Takata, K., 2010. Improved climate simulation by MIROC5: mean states, variability, and climate sensitivity. *Journal of Climate*, *23*(23), pp.6312-6335.

Wen, Y., Yang, A., Fan, Y., Wang, B. and Scott, D., 2023. Stepwise cluster ensemble downscaling for drought projection under climate change. *International Journal of Climatology*, *43*(5), pp.2318-2338.

Wu, T., Lu, Y., Fang, Y., Xin, X., Li, L., Li, W., Jie, W., Zhang, J., Liu, Y., Zhang, L. and Zhang, F., 2019. The Beijing Climate Center climate system model (BCC-CSM): the main progress from CMIP5 to CMIP6. *Geoscientific Model Development*, *12*(4), pp.1573-1600.

Xin, X., 2019, January. Performance of BCC-CSM2-MR in simulating summer climate changes in East Asia. In *Geophysical Research Abstracts* (Vol. 21).

Xulu, N.G., 2017. *Impact of spatio-temporal variability of the Mascarene High on weather and climate over southern Africa* (Master's thesis, University of Venda).

Xulu, N.G., Chikoore, H., Bopape, M.J.M. and Nethengwe, N.S., 2020. Climatology of the Mascarene high and its influence on weather and climate over southern Africa. *Climate*, 8(7), pp.86.

Xulu, N.G., Chikoore, H., Bopape, M.J.M., Ndarana, T., Muofhe, T.P., Mbokodo, I.L., Munyai, R.B., Singo, M.V., Mohomi, T., Mbatha, S.M. and Mdoka, M.L., 2023. Cut-Off Lows over South Africa: a review. *Climate*, *11*(3), pp.59.

Yan, Q., Wan, Z. and Yang, C., 2023. Flight load calculation using neural network residual kriging. *Aerospace*, *10*(7), pp.599.

Zandersen, M., Hyytiäinen, K., Meier, H.M., Tomczak, M.T., Bauer, B., Haapasaari, P.E., Olesen, J.E., Gustafsson, B.G., Refsgaard, J.C., Fridell, E. and Pihlainen, S., 2019. Shared socio-economic pathways extended for the Baltic Sea: exploring long-term environmental problems. *Regional Environmental Change*, *19*, pp.1073-1086.

Zhang, J., Wu, T., Li, L., Furtado, K., Xin, X., Xie, C., Zheng, M., Zhao, H. and Zhou, Y., 2023. Constraint on regional land surface air temperature projections in CMIP6 multi-model ensemble. *npj Climate and Atmospheric Science*, *6*(1), pp.85.

Zhang, Q., Liu, B., Li, S. and Zhou, T., 2023. Understanding models' global sea surface temperature bias in mean state: from CMIP5 to CMIP6. *Geophysical Research Letters*, *50*(4), pp.e2022GL100888.

Zhang, Y., Knutson, T.R., Shevliakova, E. and Paynter, D., 2023. The long-term trends of global land precipitation in GFDL's CM4 and ESM4 climate models. *Journal of Climate*, 36(18), pp.1-55.

Zhang, X. and Yang, F., 2004. RClimDex (1.0): Manual. Environment Canada, Ontario, Canada.

Zhou, Q., Chen, D., Hu, Z. and Chen, X., 2021. Decompositions of Taylor diagram and DISO performance criteria. *International Journal of Climatology*, *41*(12), pp.5726-5732.

Zhou, L., Kori, D.S., Sibanda, M. and Nhundu, K., 2022. An analysis of the differences in vulnerability to climate change: a review of rural and urban areas in South Africa. *Climate*, *10*(8), pp.118.

Zhou, S., Yu, B. and Zhang, Y., 2023. Global concurrent climate extremes are exacerbated by anthropogenic climate change. *Science Advances*, *9*(10), pp16-38.

Ziervogel, G., New, M., Archer van Garderen, E., Midgley, G., Taylor, A., Hamann, R., Stuart-Hill, S., Myers, J. and Warburton, M., 2014. Climate change impacts and adaptation in South Africa. *Wiley Interdisciplinary Reviews: Climate Change*, *5*(5), pp.605-620.

Zimba, S.K., Houane, M.J. and Chikova, A.M., 2020, August. Impact of tropical cyclone Idai on the southern African electric power grid. In 2020 IEEE PES/IAS PowerAfrica (pp. 1-5). IEEE.

Zittis, G., Almazroui, M., Alpert, P., Ciais, P., Cramer, W., Dahdal, Y., Fnais, M., Francis, D., Hadjinicolaou, P., Howari, F. and Jrrar, A., 2022. Climate change and weather extremes in the Eastern Mediterranean and Middle East. *Reviews of Geophysics*, *60*(3), pp.e2021RG000762.